

Solutions to Addendum C

Cylindrical Waveguides

C.1 Frequency range of the dominant mode.

(a) The cutoff frequency of the dominant TE_{10} mode in an air-filled hollow WR-10 rectangular waveguide with $a = 0.254$ cm and $b = 0.127$ cm is given by

$$f_{c_{10}} = \frac{c}{2a} \simeq \frac{3 \times 10^{10}}{2(0.254)} \simeq 59.1 \text{ GHz}$$

(b) Since $a = 2b$, the next higher-order modes are TE_{11} , TE_{20} , and TM_{11} . The cutoff frequency of these three modes is

$$f_{c_{11}} = f_{c_{20}} = 2f_{c_{10}} \simeq 118 \text{ GHz}$$

(c) Therefore, the frequency band over which only the dominant TE_{10} mode can propagate is $f_{c_{10}} - f_{c_{20}} \simeq 59.1$ GHz.

C.2 AM waves through a tunnel?

The minimum tunnel dimension a_{\min} needed for the dominant TE_{10} mode to propagate at 1 MHz can be calculated as

$$f_{c_{10}} \simeq \frac{3 \times 10^8}{2a_{\min}} = 10^6 \quad \rightarrow \quad a_{\min} = 150 \text{ m!}$$

As long as $a > a_{\min} = 150$ m, TE_{10} will propagate regardless of the value of the other dimension b . In practice, since there is no tunnel which has such a large dimension, AM transmission through a tunnel is not feasible.

C.3 Propagation experiment in a road tunnel.

(a) For the rectangular railway tunnel under consideration ($a = 17$ m and $b = 4.9$ m), the cutoff frequencies of the TE_{10} and TE_{01} modes are given by

$$f_{c_{10}} = \frac{c}{2a} \simeq \frac{3 \times 10^8}{2(17)} \simeq 8.82 \text{ MHz}$$

$$f_{c_{01}} = \frac{c}{2b} \simeq \frac{3 \times 10^8}{2(4.9)} \simeq 30.6 \text{ MHz}$$

(b) Using (C.17), the lowest-order modes that do not propagate at the 100 MHz FM frequency are TE_{92} and TM_{92} since the cutoff frequency of these two modes is given by

$$f_{c_{92}} \simeq \frac{3 \times 10^8}{2\pi} \sqrt{\left(\frac{2\pi}{4.9}\right)^2 + \left(\frac{9\pi}{17}\right)^2} \simeq 100.3 \text{ MHz}$$

C.4 Radio-wave propagation in railway tunnels.

For tunnel 1 ($a = 8$ m and $b = 4$ m), the total number of propagating modes at 100 MHz is 26. These modes are TE_{10} , TE_{01} , (TE and TM) $_{02}$, (TE and TM) $_{11}$, (TE and TM) $_{12}$, (TE and TM) $_{20}$, (TE and TM) $_{21}$, (TE and TM) $_{22}$, (TE and TM) $_{30}$, (TE and TM) $_{31}$, (TE and TM) $_{32}$, (TE and TM) $_{40}$, (TE and TM) $_{41}$, and (TE and TM) $_{50}$. For tunnel 2 ($a = 6$ m and $b = 4$ m), the total number of propagating modes at 100 MHz is 18. Unlike tunnel 1, (TE and TM) $_{32}$, (TE and TM) $_{40}$, (TE and TM) $_{41}$, and (TE and TM) $_{50}$ modes do not propagate.

C.5 Rectangular waveguide modes.

(a) For the WR-137 rectangular air waveguide ($a = 3.484$ cm, $b = 1.58$ cm), the cutoff frequencies of the four lowest-order modes TE_{10} , TE_{20} (and TM_{20}), TE_{01} , and TE_{11} (and TM_{11}) are respectively calculated from (C.17) as $f_{c_{10}} \simeq 4.31$ GHz, $f_{c_{20}} \simeq 8.61$ GHz, $f_{c_{01}} \simeq 9.49$ GHz, and $f_{c_{11}} \simeq 10.4$ GHz.

(b) For the dominant TE_{10} mode, the phase velocity \bar{v}_p and the guide wavelength $\bar{\lambda}$ at the two end frequencies (i.e., 5.85 GHz and 8.20 GHz) of the specified frequency range can be calculated using (C.20) and (C.21) as

$$\bar{v}_{p_{10}}|_{f=5.85 \text{ GHz}} \simeq \frac{3 \times 10^8}{\sqrt{1 - \left(\frac{4.31}{5.85}\right)^2}} \simeq 4.43 \times 10^8 \text{ m-s}^{-1}$$

$$\bar{v}_{p_{10}}|_{f=8.20 \text{ GHz}} \simeq \frac{3 \times 10^8}{\sqrt{1 - \left(\frac{4.31}{8.20}\right)^2}} \simeq 3.52 \times 10^8 \text{ m-s}^{-1}$$

$$\bar{\lambda}_{10}|_{f=5.85 \text{ GHz}} \simeq \frac{3 \times 10^8 / (5.85 \times 10^9)}{\sqrt{1 - \left(\frac{4.31}{5.85}\right)^2}} \simeq 7.57 \text{ cm}$$

$$\bar{\lambda}_{10}|_{f=8.20 \text{ GHz}} \simeq \frac{3 \times 10^8 / (8.20 \times 10^9)}{\sqrt{1 - \left(\frac{4.31}{8.20}\right)^2}} \simeq 4.30 \text{ cm}$$

C.6 Dominant mode in a rectangular waveguide.

(a) The cutoff frequency of the dominant TE_{10} mode in the WR-137 rectangular air waveguide ($a = 3.484$ cm, $b = 1.58$ cm) can be calculated from (C.17) as

$$f_{c_{10}} = \frac{c}{2a} \simeq \frac{3 \times 10^{10}}{2(3.484)} \simeq 4.31 \text{ GHz}$$

Using this value, the propagation constant $\bar{\gamma}_{10}$ and wave impedance $Z_{TE_{10}}$ at 3.5 GHz can be found using (C.16) and (C.28) as

$$\bar{\gamma}_{10} = \bar{\alpha}_{10} = \beta \sqrt{\left(\frac{f_{c_{10}}}{f}\right)^2 - 1} \simeq \frac{2\pi(3.5 \times 10^9)}{3 \times 10^8} \sqrt{\left(\frac{4.31}{3.5}\right)^2 - 1} \simeq 52.5 \text{ np-m}^{-1}$$

$$Z_{TE_{10}} = \frac{\eta_{\text{air}}}{\sqrt{1 - (f_{c_{10}}/f)^2}} \simeq \frac{377}{\sqrt{1 - (4.31/3.5)^2}} \simeq j526.3 \Omega$$

Note that the dominant TE_{10} mode is not propagating at 3.5 GHz as expected since $f_{c_{10}} \simeq 4.31 \text{ GHz} > f = 3.5 \text{ GHz}$.

(b) Repeating the same calculations as in part (a) at 7 GHz, we have

$$\bar{\gamma}_{10} = j\beta \sqrt{1 - \left(\frac{f_{c_{10}}}{f}\right)^2} \simeq j \frac{2\pi(7 \times 10^9)}{3 \times 10^8} \sqrt{1 - \left(\frac{4.31}{7}\right)^2} \simeq j115.6 \text{ rad-m}^{-1}$$

$$Z_{TE_{10}} \simeq \frac{377}{\sqrt{1 - (4.31/7)^2}} \simeq 478 \Omega$$

Note that the dominant TE_{10} mode is a propagating mode at 7 GHz since $\sim 4.31 \text{ GHz} < 7 \text{ GHz}$.

C.7 Waveguide wavelength.

(a) Using (C.21), the guide wavelength of the dominant TE_{10} mode propagating in a rectangular air waveguide with $a = 2b = 7.214$ cm can be written as

$$\bar{\lambda}_{10} = \frac{c/f}{\sqrt{1 - (f_{c_{10}}/f)^2}} \simeq \frac{30}{\sqrt{[f(\text{GHz})]^2 - (2.08)^2}} \text{ cm}$$

where $c \simeq 3 \times 10^{10} \text{ cm-s}^{-1}$ and $f_{c_{10}} = c/(2a) \simeq 2.08 \text{ GHz}$ are used. Note that the expression found for $\bar{\lambda}_{10}$ above is only valid for $f > \sim 2.08 \text{ GHz}$ (i.e., propagating case). This expression (i.e., $\bar{\lambda}_{10}$) is plotted as a function of frequency f as shown in Figure C.1.

(b) If the same waveguide is filled with water (assume $\epsilon_r \simeq 81$), then, $f_{c_{10}} \simeq 2.08/\sqrt{81} \simeq 0.231 \text{ GHz}$. Therefore, the guide wavelength for this case is given by

$$\bar{\lambda}_{10} \simeq \frac{30/\sqrt{81}}{\sqrt{[f(\text{GHz})]^2 - (0.231)^2}} \text{ cm}$$

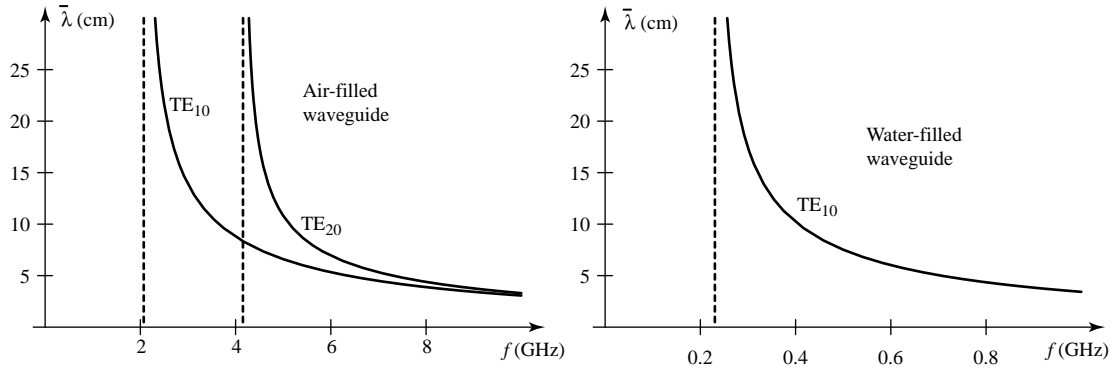


Figure C.1 Figure for Problem C.7. Right panel: $\bar{\lambda}_{10}$ and $\bar{\lambda}_{20}$ versus f for air-filled waveguide. Left panel: $\bar{\lambda}_{10}$ versus f for water-filled waveguide (i.e., $\epsilon_r \simeq 81$).

which is valid for $f > \sim 0.231$ GHz. This expression is plotted in Figure C.1 as a function of the frequency f .

(c) For the propagating TE_{20} mode in the air waveguide of part (a), the $\bar{\lambda}_{20}$ expression is the same as the $\bar{\lambda}_{10}$ expression except 2.08 should be replaced by 4.16 (i.e., $f_{c_{20}} = 2f_{c_{10}}$). This expression is valid for $f > \sim 4.16$ GHz and is plotted as a function of f in Figure C.1. For the propagating TE_{20} mode in the water-filled waveguide of part (b), $\bar{\lambda}_{20}$ expression is the same as the $\bar{\lambda}_{10}$ expression found in part (b) except that 0.231 should be replaced by 0.462. This expression is valid for $f > \sim 0.462$ GHz and is plotted in Figure C.1.

C.8 Rectangular waveguide modes.

(a) For the WR-42 rectangular air waveguide ($a = 1.067$ cm, $b = 0.432$ cm), the cutoff frequencies of the TE_{10} , TE_{01} , TE_{11} , TE_{20} , and TE_{02} modes are given by

$$f_{c_{10}} \simeq \frac{3 \times 10^{10}}{2(1.067)} \simeq 14.06 \text{ GHz} < 40 \text{ GHz}$$

$$f_{c_{01}} \simeq \frac{3 \times 10^{10}}{2(0.432)} \simeq 34.72 \text{ GHz} < 40 \text{ GHz}$$

$$f_{c_{11}} \simeq \frac{3 \times 10^{10}}{2} \sqrt{(1.067)^{-2} + (0.432)^{-2}} \simeq 37.46 \text{ GHz} < 40 \text{ GHz}$$

$$f_{c_{20}} \simeq \frac{3 \times 10^{10}}{(1.067)} \simeq 28.12 \text{ GHz} < 40 \text{ GHz}$$

$$f_{c_{02}} \simeq \frac{3 \times 10^{10}}{(0.432)} \simeq 69.44 \text{ GHz} > 40 \text{ GHz}$$

Note that all these modes except the TE_{02} mode are propagating at 40 GHz. The propagation constants and the wave impedances of these modes can be calculated using (C.18) and (C.19) as

$$\bar{\gamma}_{10} \simeq j \frac{2\pi(4 \times 10^{10})}{3 \times 10^8} \sqrt{1 - \left(\frac{14.06}{40}\right)^2} \simeq j784.3 \text{ rad-m}^{-1}$$

$$Z_{TE_{10}} \simeq \frac{377}{\sqrt{1 - \left(\frac{14.06}{40}\right)^2}} \simeq 402.7\Omega$$

$$\bar{\gamma}_{01} \simeq j \frac{2\pi(4 \times 10^{10})}{3 \times 10^8} \sqrt{1 - \left(\frac{34.72}{40}\right)^2} \simeq j415.9 \text{ rad-m}^{-1}$$

$$Z_{TE_{01}} \simeq \frac{377}{\sqrt{1 - \left(\frac{34.72}{40}\right)^2}} \simeq 759.4\Omega$$

$$\bar{\gamma}_{11} \simeq j \frac{2\pi(4 \times 10^{10})}{3 \times 10^8} \sqrt{1 - \left(\frac{37.46}{40}\right)^2} \simeq j293.8 \text{ rad-m}^{-1}$$

$$Z_{TE_{11}} \simeq \frac{377}{\sqrt{1 - \left(\frac{37.46}{40}\right)^2}} \simeq 1075\Omega$$

$$\bar{\gamma}_{20} \simeq j \frac{2\pi(4 \times 10^{10})}{3 \times 10^8} \sqrt{1 - \left(\frac{28.1}{40}\right)^2} \simeq j595.9 \text{ rad-m}^{-1}$$

$$Z_{TE_{20}} \simeq \frac{377}{\sqrt{1 - \left(\frac{28.1}{40}\right)^2}} \simeq 530\Omega$$

$$\bar{\gamma}_{02} \simeq \frac{2\pi(4 \times 10^{10})}{3 \times 10^8} \sqrt{\left(\frac{69.44}{40}\right)^2 - 1} \simeq 1189 \text{ np-m}^{-1}$$

$$Z_{TE_{02}} \simeq \frac{377}{\sqrt{1 - \left(\frac{69.44}{40}\right)^2}} \simeq j265.65\Omega$$

(b) For the TE_{10} mode, we have from (C.20) and (C.21)

$$\bar{v}_{p_{10}} \simeq \frac{3 \times 10^8}{\sqrt{1 - \left(\frac{14.06}{40}\right)^2}} \simeq 3.20 \times 10^8 \text{ m-s}^{-1}$$

$$\bar{\lambda}_{10} \simeq \frac{\frac{3 \times 10^{10}}{4 \times 10^{10}}}{\sqrt{1 - \left(\frac{14.06}{40}\right)^2}} \simeq 0.801 \text{ cm}$$

Similarly, for the TE_{01} mode, we have

$$\bar{v}_{p_{01}} \simeq \frac{3 \times 10^8}{\sqrt{1 - \left(\frac{34.72}{40}\right)^2}} \simeq 6.04 \times 10^8 \text{ m-s}^{-1}$$

$$\bar{\lambda}_{01} \simeq \frac{\frac{3 \times 10^{10}}{4 \times 10^{10}}}{\sqrt{1 - \left(\frac{34.72}{40}\right)^2}} \simeq 1.51 \text{ cm}$$

In a similar fashion, for the TE_{11} mode, we obtain $\bar{v}_{p_{11}} \simeq 8.56 \times 10^8 \text{ m-s}^{-1}$, $\bar{\lambda}_{11} \simeq 2.14 \text{ cm}$, and for the TE_{20} mode, we obtain $\bar{v}_{p_{20}} \simeq 4.22 \times 10^8 \text{ m-s}^{-1}$, and $\bar{\lambda}_{11} \simeq 1.054 \text{ cm}$ respectively.

C.9 Dielectric-filled waveguide.

(a) For the WR-22 rectangular waveguide ($a = 0.569$ cm, $b = 0.284$ cm) filled with a dielectric material having ϵ_r , the phase shift experienced by the dominant propagating TE₁₀ mode over a length of 1 cm at 13.2 GHz can be written as

$$\bar{\beta}_{10}l = 354.6^\circ \times \frac{\pi}{180^\circ} \rightarrow \bar{\beta}_{10} \simeq 618.9 \text{ rad-m}^{-1}$$

But, from (C.18), we have

$$\bar{\beta}_{10} \simeq \frac{2\pi(13.2 \times 10^9)}{(3 \times 10^8/\sqrt{\epsilon_r})} \sqrt{1 - (f_{c10}(\text{GHz})/13.2)^2} \simeq 618.9$$

where $f_{c10} = 30\sqrt{\epsilon_r}/(2 \times 0.569)$ in GHz. Substituting, we have

$$\bar{\beta}_{10} \simeq 276.5\sqrt{\epsilon_r}\sqrt{1 - 3.99/\epsilon_r} \simeq 618.9$$

from which solving, we find $\epsilon_r \simeq 9$.

(b) Note that $f_{c10} \simeq 8.78$ GHz. Since $a \simeq 2b$, the next higher mode is TE₂₀ (or TE₁₁) which has a cutoff frequency $f_{c20} \simeq 17.6$ GHz $>$ 13.2 GHz. Therefore, no mode other than TE₁₀ propagates at 13.2 GHz.

(c) If the dielectric filling is replaced with air, then, $f_{c10} \simeq 3 \times 10^{10}/(2 \times 0.569) \simeq 26.4$ GHz $>$ 13.2 GHz. Therefore, in this case, no propagation occurs down the guide.

C.10 Rectangular waveguide modes.

(a) For the WR-1500 air waveguide ($a = 2b = 38.1$ cm), the cutoff wavelength of the dominant TE₁₀ mode can be found from (C.19) as $\lambda_{c10} = 2a = 76.2$ cm.

(b) The phase velocity, guide wavelength, and the wave impedance for the dominant TE₁₀ mode at $\lambda_{\text{air}} = 0.8\lambda_{c10}$ can be calculated from (C.20), (C.21) and (C.28) as

$$\bar{v}_p \simeq \frac{3 \times 10^8}{\sqrt{1 - (0.8)^2}} \simeq 5 \times 10^8 \text{ m-s}^{-1}$$

$$\bar{\lambda}_{10} \simeq \frac{0.8 \times 76.2}{\sqrt{1 - (0.8)^2}} \simeq 101.6 \text{ cm} \simeq 1.02 \text{ m}$$

$$Z_{\text{TE}_{10}} \simeq \frac{377}{\sqrt{1 - (0.8)^2}} \simeq 628.3\Omega$$

(c) At $\lambda_{\text{air}} = 40$ cm, only the dominant TE₁₀ mode propagates since the next higher mode TE₂₀ (or TE₁₁) has $\lambda_{c20} = \lambda_{c10}/2 = 38.1$ cm $<$ 40 cm.

(d) At $\lambda_{\text{air}} = 30$ cm, the propagating modes are TE₁₀, TE₂₀ and TM₂₀ ($\lambda_{c20} = 38.1$ cm), TE₀₁ ($\lambda_{c01} = 38.1$ cm), and TE₁₁ and TM₁₁ ($\lambda_{c11} = 2ab/\sqrt{a^2 + b^2} \simeq 34.1$ cm).

C.11 Polyethylene-filled waveguide.

(a) For the WR-1500 polyethylene-filled waveguide ($a = 2b = 38.1$ cm), the cutoff wavelength of the dominant TE_{10} mode can be found from (C.19) as $\lambda_{c10} = 2a = 76.2$ cm.

(b) The phase velocity, guide wavelength, and the wave impedance for the dominant TE_{10} mode at $\lambda_{air} = 0.8\lambda_{c10}$ can be calculated from (C.20), (C.21) and (C.28) as

$$\bar{v}_p \simeq \frac{3 \times 10^8 / \sqrt{2.25}}{\sqrt{1 - (0.8)^2}} \simeq 3.33 \times 10^8 \text{ m-s}^{-1}$$

$$\bar{\lambda}_{10} \simeq \frac{0.8 \times 76.2}{\sqrt{1 - (0.8)^2}} \simeq 101.6 \text{ cm} \simeq 1.02 \text{ m}$$

$$Z_{TE_{10}} \simeq \frac{377 / \sqrt{2.25}}{\sqrt{1 - (0.8)^2}} \simeq 418.9 \Omega$$

(c) At $\lambda_{air} = 40$ cm, only the dominant TE_{10} mode propagates since the next higher mode TE_{20} (or TE_{11}) has $\lambda_{c20} = \lambda_{c10}/2 = 38.1$ cm < 40 cm.

(d) At $\lambda_{air} = 30$ cm, the propagating modes are TE_{10} , TE_{20} and TM_{20} ($\lambda_{c20} = 38.1$ cm), TE_{01} ($\lambda_{c01} = 38.1$ cm), and TE_{11} and TM_{11} ($\lambda_{c11} = 2ab/\sqrt{a^2 + b^2} \simeq 34.1$ cm).

C.12 Unknown rectangular waveguide mode.

(a) Since the y component of the electric field phasor is oriented in the guiding direction of the rectangular waveguide, this mode can neither be TEM or TE_{mn} , therefore, it must be a TM_{mn} mode. Using the waveguide dimensions $a = 4$ cm (in the z direction) and $b = 2$ cm (in the x direction) and comparing the E_y expression given in the problem with the E_z expression given by (C.15), we have

$$\frac{m\pi}{0.04} = 25\pi \rightarrow m = 1$$

$$\frac{n\pi}{0.02} = 50\pi \rightarrow n = 1$$

Therefore, this is a TM_{11} mode. It is an evanescent wave because of the attenuation term $e^{-41\pi y}$.

(b) Using (C.16), the operating frequency can be evaluated from the attenuation constant $\bar{\alpha}_{11}$ as

$$\bar{\gamma}_{11} = \bar{\alpha}_{11} = \beta \sqrt{\left(\frac{f_{c11}}{f}\right)^2 - 1} \simeq \frac{2\pi f(\text{GHz})}{0.3} \sqrt{\left[\frac{8.39}{f(\text{GHz})}\right]^2 - 1} \simeq 41\pi \text{ np-m}^{-1}$$

$$\rightarrow (8.39)^2 - [f(\text{GHz})]^2 = \left(\frac{0.3 \times 41}{2}\right)^2 \rightarrow f \simeq 5.70 \text{ GHz}$$

where we replaced $\beta = 2\pi f/c$, $c \simeq 3 \times 10^8$ m-s⁻¹, and $f_{c11} = 0.5c\sqrt{a^{-2} + b^{-2}} \simeq 8.39$ GHz.

(c) Note that the cutoff frequencies of the two lower-order TE_{10} and TE_{01} modes are $f_{c10} = c/(2a) \simeq 3.75$ GHz $< \sim 5.7$ GHz and $f_{c01} = c/(2b) \simeq 7.5$ GHz $> \sim 5.7$ GHz. Therefore, only TE_{10} mode propagates at ~ 5.7 GHz.

C.13 A large waveguide for deep hyperthermia.

(a) For the large waveguide ($a = 6$ m, $b = 30$ cm) designed to be used for deep hyperthermia, since $a \gg b$, the cutoff frequency of the lower-order modes is determined by the larger dimension a . Assuming the waveguide to be air-filled, the cutoff frequencies of the five lowest-order TE_{m0} are given by

$$f_{c_{m0}} = \frac{mv_p}{2a}$$

(where $v_p = c \simeq 3 \times 10^8$ m·s⁻¹) yielding $f_{c_{TE_{10}}} = 25$ MHz, $f_{c_{TE_{20}}} = 50$ MHz, $f_{c_{TE_{30}}} = 75$ MHz, $f_{c_{TE_{40}}} = 100$ MHz, and $f_{c_{TE_{50}}} = 125$ MHz respectively. Note that the cutoff frequencies of the TM_{m0} modes with $m = 2, 3, 4, 5$ are exactly the same as the cutoff frequencies of their TE_{m0} mode counterparts with $m = 2, 3, 4, 5$.

(b) If the waveguide is filled with water (assume $\epsilon_r \simeq 81$), then $v_p = c/\sqrt{\epsilon_r} = c/9$. Therefore, The cutoff frequencies for the water-filled waveguide are 1/9 times the cutoff frequencies of the air-filled waveguide yielding the cutoff frequencies for the five lowest-order TE_{m0} modes as $f_{c_{TE_{10}}} \simeq 2.78$ MHz, $f_{c_{TE_{20}}} \simeq 5.56$ MHz, $f_{c_{TE_{30}}} \simeq 8.33$ MHz, $f_{c_{TE_{40}}} \simeq 11.1$ MHz, and $f_{c_{TE_{50}}} \simeq 13.9$ MHz respectively.

(c) For the water-filled waveguide with new dimensions $a = 70$ cm and $b = 30$ cm, the cutoff frequencies of the five lowest-order TE_{mn} modes are found to be $f_{c_{TE_{10}}} \simeq 3 \times 10^8 / [2(0.7)(\sqrt{81})] \simeq 23.8$ MHz, $f_{c_{TE_{20}}} = 2f_{c_{TE_{10}}} \simeq 47.6$ MHz, $f_{c_{TE_{30}}} \simeq 71.4$ MHz, $f_{c_{TE_{01}}} \simeq 3 \times 10^8 / [2(0.3)(\sqrt{81})] \simeq 55.6$ MHz, and $f_{c_{TE_{11}}} \simeq 3 \times 10^8 \sqrt{(0.7)^{-2} + (0.3)^{-2}} / (2\sqrt{81}) \simeq 60.4$ MHz respectively. Note that the TM_{20} , TM_{30} , and TM_{11} modes have exactly the same cutoff frequencies as their TE_{mn} counterparts.

C.14 Square waveguide modes.

(a) For the square air waveguide ($a = b = 3$ cm) at 8 GHz, the cutoff frequencies of all the propagating TE_{mn} and TM_{mn} modes at 8 GHz are given by

$$f_{c_{TE_{10}}} = f_{c_{TE_{01}}} = \frac{v_p}{2a} \simeq 5 \text{ GHz}$$

$$f_{c_{TE_{11}}} = f_{c_{TM_{11}}} = \frac{v_p}{a\sqrt{2}} \simeq 7.07 \text{ GHz}$$

where $v_p = c \simeq 3 \times 10^8$ m·s⁻¹ is used. Note that all of these values cutoff frequency values are < 8 GHz and therefore these modes (i.e., TE_{10} , TE_{01} , TE_{11} , and TM_{11}) are the only propagating modes at 8 GHz.

(b) If the same square waveguide is filled with polystyrene ($\epsilon_r \simeq 2.56$), then, we recalculate the cutoff frequencies of the propagating modes as $f_{c_{10}} = f_{c_{01}} = c/(2a\sqrt{\epsilon_r}) \simeq 3.13$ GHz, $f_{c_{11}} = c/(a\sqrt{2\epsilon_r}) \simeq 4.42$ GHz, $f_{c_{20}} = f_{c_{02}} = 2f_{c_{10}} \simeq 6.25$ GHz, $f_{c_{21}} = f_{c_{12}} = [c/(2\sqrt{\epsilon_r})] \sqrt{(2/3)^2 + (1/3)^2} \simeq 6.99$ GHz, and $f_{c_{22}} = [c/(2\sqrt{\epsilon_r})] \sqrt{(2/3)^2 + (2/3)^2} \simeq 8.84$ GHz respectively. Note that the next higher mode (TE_{30} or TE_{03}) has a cutoff frequency which is $f_{c_{30}} = 3f_{c_{10}} \simeq 9.38$ GHz > 8 GHz and so this is not a propagating mode. Therefore, TE_{10} , TE_{01} , TE_{11} , TM_{11} , TE_{20} , TM_{20} , TE_{02} , TM_{02} , TE_{21} , TM_{21} , TE_{12} , and TM_{12} are the only propagating modes on the polystyrene-filled square waveguide at 8 GHz.

C.15 SAR calibration using a rectangular waveguide.

(a) For the specially designed nonstandard air-filled waveguide with dimensions $a = 19$ cm and $b = 14$ cm, the only mode that is excited at 900 MHz is the dominant TE_{10} mode which has a cutoff frequency $f_{c_{10}} \simeq 3 \times 10^{10} / [2(19)] \simeq 789.5$ MHz < 900 MHz.

(b) The cutoff frequency of the next higher mode which is the TE_{01} mode is given by $f_{c_{01}} \simeq 3 \times 10^{10} / [2(14)] \simeq 1.07$ GHz, so, the frequency range over which only the dominant mode can propagate can be found as $f_{c_{01}} - f_{c_{10}} \simeq 282$ MHz.

(c) If the TE_{01} mode does not exist, then, the cutoff frequency of the next higher mode which is the TE_{11} mode (and the TM_{11} mode) is calculated as

$$f_{c_{11}} = \frac{c}{2} \sqrt{a^{-2} + b^{-2}} \simeq \frac{3 \times 10^{10}}{2} \sqrt{(19)^{-2} + (14)^{-2}} \simeq 1.33 \text{ GHz}$$

Therefore, the frequency range in which only the dominant mode propagates (ignoring the existence of the weak TE_{01} mode) is given by $f_{c_{11}} - f_{c_{10}} \simeq 541$ MHz.

C.16 Millimeter-wave rectangular waveguide.

(a) For the W-band rectangular air waveguide with dimensions $a = 2.54$ mm and $b = 0.7$ mm, the cutoff frequencies of the three lowest-order modes are given by

$$f_{c_{TE_{10}}} = \frac{c}{2a} \simeq \frac{3 \times 10^{11} \text{ mm-s}^{-1}}{2(2.54 \text{ mm})} \simeq 59.1 \text{ GHz}$$

$$f_{c_{TE_{20}}} = f_{c_{TM_{20}}} = 2f_{c_{TE_{10}}} \simeq 118 \text{ GHz}$$

$$f_{c_{TE_{30}}} = f_{c_{TM_{30}}} = 3f_{c_{TE_{10}}} \simeq 177 \text{ GHz}$$

(b) The frequency range over which only the dominant TE_{10} mode can propagate is given by

$$f_{c_{TE_{20}}} - f_{c_{TE_{10}}} \simeq 59.1 \text{ GHz}$$

C.17 TE_{10} mode in a rectangular waveguide.

(a) Using (C.25), we have

$$\frac{\pi \text{ rad}}{a} \simeq 29 \text{ rad-m}^{-1} \rightarrow a \simeq 0.1083 \text{ m} = 10.83 \text{ cm}$$

and since $a = 2b$ is given, $b = a/2 \simeq 5.4165$ cm. The operating frequency can be found from $\bar{\beta}_{10} \simeq 42.3 \text{ rad-m}^{-1}$ value as

$$(\bar{\beta})^2 \left(\frac{2\pi}{c} \right)^2 (f^2 - f_{c_{10}}^2) \simeq (42.3)^2$$

where substituting the value of the cutoff frequency $f_{c_{10}} = c/(2a) \simeq 3 \times 10^{10} / (2 \times 10.83) \simeq 1.385$ GHz yields $f \simeq 2.449$ GHz.

(b) Note that the time-average power carried by the dominant TE₁₀ mode along the rectangular waveguide is given by

$$P_{av} = \frac{\bar{\beta}_{10}\omega\mu_0 C^2}{2} \left(\frac{a}{\pi}\right)^2 \frac{ab}{2}$$

where C is the amplitude of the axial magnetic field component H_x given by $C \simeq 26 \text{ A-m}^{-1}$. Substituting $\bar{\beta}_{10} \simeq 42.3 \text{ rad-m}^{-1}$, $\omega = 2\pi(2.449 \times 10^9) \text{ rad-s}^{-1}$, $\mu_0 = 4\pi \times 10^{-7} \text{ H-m}^{-1}$, $a \simeq 0.1083 \text{ m}$, and $b \simeq 0.054165 \text{ m}$ along with the value of C in the above expression, we find $P_{av} \simeq 964.4 \text{ W}$.

C.18 Dominant mode in a rectangular waveguide design.

(a) The three design criteria for the rectangular waveguide under consideration are

$$1.25f_{c_{10}} \leq 15 \text{ GHz}$$

$$1.25 \times 18.5 \text{ GHz} \leq f_{c_{\text{next higher}}}$$

and P_{av} of the dominant TE₁₀ mode is to be maximized. Assuming $a = 2b$ and using $f_{c_{10}} = c/(2a)$ where $c \simeq 3 \times 10^{10} \text{ cm-s}^{-1}$, the first design criteria yields $a_{\min} = 1.25 \text{ cm}$. Next, using $f_{c_{\text{next higher}}} = f_{c_{20}} = 2f_{c_{10}} = c/a$, the second design criteria yields $a_{\max} \simeq 1.2973 \text{ cm}$. Therefore, the longer transverse dimension a must lie in the range $1.25 \leq a \leq \sim 1.2973 \text{ cm}$. However, since the third design criteria is to maximize power transfer, we choose the largest possible value of $a = a_{\max} \simeq 1.2973 \text{ cm}$. For this value of a , the cutoff frequency of the dominant TE₁₀ mode can be calculated as $f_{c_{10}} \simeq 3 \times 10^{10}/(2 \times 1.2973) \simeq 11.56 \text{ GHz}$.

(b) The cutoff frequency of the next higher TE₂₀ (or TE₀₁) mode is $f_{c_{20}} = 2f_{c_{10}} \simeq 23.13 \text{ GHz} > 22 \text{ GHz}$.

(c) Using (C.30) at 15 GHz, the time-average power carried by the dominant TE₁₀ mode with peak electric field value $E_0 = 1.5 \times 10^6 \text{ V-m}^{-1}$ can be calculated as

$$P_{av} \simeq \frac{(1.5 \times 10^6)^2}{377} \frac{(1.297 \times 10^{-2})(0.64865 \times 10^{-2})}{4} \sqrt{1 - \left[\frac{(3 \times 10^{10}/(15 \times 10^9))}{2(1.2973)} \right]^2}$$

$$\simeq 80 \text{ kW}$$

C.19 Rectangular waveguide design.

(a) Using the cutoff frequency of the dominant mode, we have

$$f_{c_{10}} = \frac{c}{2a} = 2.58 \text{ GHz} \rightarrow a \simeq 5.814 \text{ cm}$$

To maximize the frequency range over which no other mode but the dominant TE₁₀ mode can propagate, we choose $b = 0.5a \simeq 2.907 \text{ cm}$ so that $f_{c_{01}} = f_{c_{20}} = 2f_{c_{10}} = 5.16 \text{ GHz}$.

(b) The next higher modes are TE₀₁ and TE₂₀ (and TM₂₀). For these modes, the cutoff frequency is 5.16 GHz.

(c) Using (C.25), the peak electric field value in the air waveguide with $a \simeq 5.814$ cm at 4 GHz can be written as

$$|E_y|_{\max} = \frac{2\pi f \mu_0 a C}{\pi} = 2(4 \times 10^9)(4\pi \times 10^{-7})(0.05814)C = 1.5 \times 10^6$$

from which we can solve for the maximum peak value C of the axial component of the magnetic field corresponding to the breakdown strength of air with a safety factor of 2 at sea level as $C \simeq 2.57$ kA-m⁻¹. Substituting this value, the maximum time-average power carrying capacity of the waveguide can be calculated as

$$P_{\text{av,max}} \simeq \frac{(64.02)(2\pi \times 4 \times 10^9)(4\pi \times 10^{-7})(2,566)^2(0.05814)^3(0.02907)}{4\pi^2} \simeq 1.927 \text{ MW}$$

where

$$\bar{\beta}_{10} \simeq \frac{2\pi(4 \times 10^9)}{3 \times 10^8} \sqrt{1 - \left(\frac{2.58}{4}\right)^2} \simeq 64.02 \text{ rad-m}^{-1}$$

is used.

C.20 Maximum field in a rectangular waveguide.

(a) For the WR-650 rectangular air waveguide ($a = 2b = 16.51$ cm), the cutoff frequency of the dominant TE₁₀ mode is given by

$$f_{c_{10}} = \frac{c}{2a} \simeq \frac{3 \times 10^{10}}{2(16.51)} \simeq 9.085 \times 10^8 \text{ Hz} = 908.5 \text{ MHz}$$

Therefore, since the next higher TE₂₀ mode (or the TE₀₁ mode) has a cutoff frequency of $f_{c_{20}} = 2f_{c_{10}} \simeq 1.82$ GHz > 1.1 GHz, only the dominant TE₁₀ mode propagates on the WR-650 waveguide at 1.1 GHz. For the WR-975 rectangular air waveguide ($a = 2b = 24.765$ cm), the cutoff frequency of the dominant TE₁₀ mode is given by

$$f_{c_{10}} = \frac{c}{2a} \simeq \frac{3 \times 10^{10}}{2(24.765)} \simeq 6.057 \times 10^8 \text{ Hz} = 605.7 \text{ MHz}$$

Therefore, since the next higher TE₂₀ mode (or the TE₀₁ mode) has a cutoff frequency of $f_{c_{20}} = 2f_{c_{10}} \simeq 1.21$ GHz > 1.1 GHz, similar to the case of WR-650 waveguide, only the dominant TE₁₀ mode propagates on the WR-975 waveguide at 1.1 GHz.

(b) For the WR-650 waveguide, the peak electric field corresponding to the peak power of 2 GW can be calculated from

$$P_{\text{peak}} \simeq \frac{E_0^2}{377} \frac{(16.51 \times 10^{-2})(8.255 \times 10^{-2})}{2} \sqrt{1 - \left(\frac{27.27}{2 \times 16.51}\right)^2} \simeq 2 \times 10^9$$

as $E_0 \simeq 14$ MV-m⁻¹ where we used $\lambda = c/f \simeq 3 \times 10^{10}/(1.1 \times 10^9) \simeq 27.27$ cm. Similarly, for the WR-975 waveguide, we have

$$P_{\text{peak}} \simeq \frac{E_0^2}{377} \frac{(24.765 \times 10^{-2})(12.383 \times 10^{-2})}{2} \sqrt{1 - \left(\frac{27.27}{2 \times 24.765}\right)^2} \simeq 2 \times 10^9$$

yielding $E_0 \simeq 7.675$ MV-m⁻¹.

(c) WR-975 waveguide should be chosen for higher power capacity since it has a wider cross-sectional area and as a result can handle more power than the WR-650 waveguide before dielectric breakdown occurs.

C.21 Power capacity of a rectangular waveguide.

(a) For the WR-284 rectangular air waveguide ($a = 7.214$ cm, $b = 3.404$ cm), the cutoff frequency of the dominant TE_{10} mode is given by $f_{c_{10}} = c/(2a) \simeq 2.079$ GHz. From (C.25), the maximum allowable peak electric field can be written as

$$|E_y|_{\max} = \frac{2\pi f \mu_0 a C}{\pi} = 1.5 \times 10^6 \text{ V-m}^{-1}$$

Substituting $f = 2.45$ GHz, $a = 7.214$ cm, and $\mu_0 = 4\pi \times 10^{-7}$ H-m⁻¹, we can solve for the allowable peak value of the axial magnetic field component as $C \simeq 3,377$ A-m⁻¹. The phase constant $\bar{\beta}_{10}$ corresponding to the dominant TE_{10} mode can be found from (C.25) as

$$\bar{\beta}_{10} = \frac{2\pi f}{c} \sqrt{1 - \left(\frac{f_{c_{10}}}{f}\right)^2} \simeq \frac{2\pi(2.45 \times 10^9)}{3 \times 10^8} \sqrt{1 - \left(\frac{2.079}{2.45}\right)^2} \simeq 27.14 \text{ rad-m}^{-1}$$

Using the values of C and $\bar{\beta}_{10}$, we can calculate the maximum time-average power that can be carried by the dominant TE_{10} mode along the WR-284 rectangular air waveguide as

$$P_{\text{avmax}} = \frac{(27.14)(2\pi \times 2.45 \times 10^9)(4\pi \times 10^{-7})(3,377)^2(7.214 \times 10^{-2})^3(3.404 \times 10^{-2})}{4\pi} \simeq 1.938 \text{ MW}$$

(b) Repeating the same calculations in part (a) for the WR-430 rectangular air waveguide ($a = 10.922$ cm, $b = 5.461$ cm), we find $f_{c_{10}} \simeq 1.37$ GHz, $C \simeq 2.23 \times 10^3$ A-m⁻¹, $\bar{\beta}_{10} \simeq 42.49$ rad-m⁻¹, and $P_{\text{avmax}} \simeq 7.37$ MW. Therefore, comparing the maximum power values obtained in parts (a) and (b), one can conclude that the maximum power capacity of the WR-430 waveguide is about 4 times higher than the maximum power capacity of the WR-284 waveguide.

C.22 TE_{11} mode in a rectangular waveguide.

(a) Comparing the given H_z expression for TE_{11} with (C.23), the waveguide dimension can be found as

$$50\pi = \frac{m\pi}{a} = \frac{\pi}{a} \rightarrow a = \frac{1}{50} = 2 \text{ cm} \quad \text{and} \quad 100\pi = \frac{n\pi}{b} = \frac{\pi}{b} \rightarrow b = \frac{1}{100} = 1 \text{ cm}$$

The operating frequency can be obtained using the phase constant given by (C.18) as

$$\begin{aligned} \bar{\beta}_{11} &= \frac{2\pi f}{c} \sqrt{1 - \left(\frac{f_{c_{11}}}{f}\right)^2} = \frac{2\pi}{c} \sqrt{f^2 - f_{c_{11}}^2} = 100\pi \\ \rightarrow f &= \sqrt{\left(\frac{c\bar{\beta}_{11}}{2\pi}\right)^2 + f_{c_{11}}^2} = \sqrt{\left(\frac{3 \times 10^8 \times 100\pi}{2\pi}\right)^2 + (16.7 \times 10^9)^2} \simeq 22.5 \text{ GHz} \end{aligned}$$

where the value of the cutoff frequency $f_{c_{11}}$ is calculated from (C.17) as

$$f_{c_{11}} = \frac{c}{2} \sqrt{\frac{1}{a^2} + \frac{1}{b^2}} \simeq \frac{3 \times 10^{10}}{2} \sqrt{\frac{1}{2^2} + \frac{1}{1^2}} \simeq 16.77 \text{ GHz}$$

(b) Using the field components given in (C.23), the time-average Poynting vector for the TE₁₁ mode can be written as

$$\begin{aligned}\mathbf{S}_{\text{av}} &= \frac{1}{2} \operatorname{Re}\{\mathbf{E} \times \mathbf{H}^*\} = \hat{\mathbf{z}} \frac{1}{2} [E_x H_y^* - E_y H_x^*] \\ &= \hat{\mathbf{z}} \frac{1}{2} \frac{\omega \mu \bar{\beta}_{11} C^2}{h_{11}^4} \left[\left(\frac{\pi}{b}\right)^2 \cos^2\left(\frac{\pi x}{a}\right) \sin^2\left(\frac{\pi y}{b}\right) + \left(\frac{\pi}{a}\right) \sin^2\left(\frac{\pi x}{a}\right) \cos^2\left(\frac{\pi y}{b}\right) \right]\end{aligned}$$

where $h_1 = \pi \sqrt{a^{-2} + b^{-2}}$. The total time-average power carried by the TE₁₁ mode can be found by integrating \mathbf{S}_{av} over the cross-sectional area of the waveguide as

$$P_{\text{av}} = \int_0^b \int_0^a \mathbf{S}_{\text{av}} \cdot (\hat{\mathbf{z}} dx dy) = \frac{\omega \mu \bar{\beta}_{11} C^2}{2h_{11}^2} \frac{ab}{4}$$

Using the given parameter values, $P_{\text{av}} = 10 \text{ kW}$, $\bar{\beta}_{11} = 100\pi \text{ rad-m}^{-1}$, $\omega \simeq 2\pi(22.5 \times 10^9) \text{ rad-s}^{-1}$, and $h_{11} = \pi \sqrt{(0.02)^{-1} + (0.01)^{-2}}$, we can solve for C as

$$10^4 \simeq \frac{2\pi(22.5 \times 10^9)(4\pi \times 10^{-7})(100\pi)C^2(0.02)(0.01)}{8(351.2)^2} \rightarrow C \simeq 940 \text{ A-m}^{-1}$$

(c) The other nonzero components of the TE₁₁ mode can be written from (C.23) as

$$\begin{aligned}H_x &\simeq j 376 \sin(50\pi x) \cos(100\pi y) e^{-j100\pi z} \text{ A-m}^{-1} \\ H_y &\simeq j 752 \cos(50\pi x) \sin(100\pi y) e^{-j100\pi z} \text{ A-m}^{-1} \\ E_x &\simeq j 4.25 \times 10^5 \cos(50\pi x) \sin(100\pi y) e^{-j100\pi z} \text{ V-m}^{-1} \\ E_y &\simeq -j 2.13 \times 10^5 \sin(50\pi x) \cos(100\pi y) e^{-j100\pi z} \text{ V-m}^{-1}\end{aligned}$$

(d) Using the breakdown value of the electric field, we can calculate the new value of C as

$$\frac{\omega \mu}{h_{11}^2} C \frac{\pi}{b} = \frac{2\pi(22.56 \times 10^9)(4\pi^{-7})}{(351.2)^2} C \frac{\pi}{0.01} = E_{\text{BR}} = 1.5 \times 10^6 \rightarrow C \simeq 3,316 \text{ A-m}^{-1}$$

The maximum time-average power corresponding to this new value of C is found to be $P_{\text{av}} \simeq 124 \text{ kW}$.

C.23 No TM₀₁ or TM₁₀ modes in a rectangular waveguide.

To have one of the indices zero means that the field quantity does not vary in the corresponding direction across the cross section of the guide. For a TM mode, the magnetic field lines are by definition entirely transverse, and both components (\mathcal{H}_x and \mathcal{H}_y) must be nonzero since the magnetic field lines must always close on themselves. However, each component must then vary in its own direction (i.e., \mathcal{H}_x must vary in x and \mathcal{H}_y must vary in y) in order to not be perpendicular to the walls as required by the boundary condition. Thus, neither m nor n can be zero.

C.24 No TEM wave in a single-conductor waveguide.

Having a TEM mode would mean that there is neither an \mathcal{E}_z or \mathcal{H}_z component. However, since the magnetic field lines must always close on themselves, \mathcal{H}_x and \mathcal{H}_y must both be nonzero, and their closed loops must then generate (through (7.21c)) displacement current (i.e., $\partial\mathcal{D}/\partial t$) in the z direction, contradicting our original premise of no \mathcal{E}_z component.

C.25 Power capacity of a rectangular waveguide.

(a) Using the time-average power expression of the dominant TE₁₀ mode as

$$P_{\text{av}} = \frac{\bar{\beta}_{10} 2\pi f \mu_0 C^2}{2} \left(\frac{a}{\pi}\right)^2 \frac{ab}{2} = 100 \text{ kW}$$

where $a = 2.591 \text{ cm}$, $b = 1.295 \text{ cm}$, $\mu_0 = 4\pi \times 10^{-7} \text{ H}\cdot\text{m}^{-1}$, $f = 9 \text{ GHz}$, and

$$\bar{\beta}_{10} = \beta \sqrt{1 - \left(\frac{f_{c_{10}}}{f}\right)^2} \simeq \frac{2\pi(9 \times 10^9)}{3 \times 10^8} \sqrt{1 - \left(\frac{5.79}{9}\right)^2} \simeq 144.3 \text{ rad}\cdot\text{m}^{-1}$$

where the cutoff frequency of the dominant mode is replaced by $f_{c_{10}} = c/(2a) \simeq 5.79 \text{ GHz}$, we solve for the amplitude C of the axial magnetic field component to be $C \simeq 1,307 \text{ A}\cdot\text{m}^{-1}$. Therefore, using (C.25), the peak value of the electric field in the waveguide can be calculated as

$$|E_y|_{\text{max}} = \frac{2\pi f \mu_0 a C}{\pi} \simeq \frac{2\pi(9 \times 10^9)(4\pi \times 10^{-7})(0.02591)(1,307)}{\pi} \simeq 766 \text{ kV}\cdot\text{m}^{-1}$$

(b) Since power is proportional to the square of the peak value of the electric field, the maximum time-average power carrying capacity of the TE₁₀ mode under the $|E_y|_{\text{max}} = 1500 \text{ kV}\cdot\text{m}^{-1}$ criteria can be calculated from basic ratio as

$$P_{\text{avmax}} \simeq \frac{(10^5)(1500)^2}{(766)^2} \simeq 3.83 \times 10^5 \text{ W} = 383 \text{ kW}$$

C.26 Cutoff frequency for a circular waveguide.

The cutoff frequency of the dominant TE₁₁ mode in a 7 cm diameter circular air waveguide is given by

$$f_{c_{11}} \simeq \frac{1.8412c}{2\pi a} \simeq \frac{1.8412 \times 3 \times 10^{10}}{2\pi(3.5)} \simeq 2.51 \times 10^9 \text{ Hz}$$

or $\sim 2.51 \text{ GHz}$. Therefore, no waves can be transmitted along this waveguide below $\sim 2.51 \text{ GHz}$.

C.27 TE₁₁ mode in a circular waveguide.

(a) Using the cutoff frequency of the dominant TE₁₁ mode as

$$f_{c_{11\text{max}}} \simeq \frac{1.8412c}{2\pi a_{\text{min}}} = 40 \times 10^6 \text{ Hz}$$

we find the smallest diameter of the circular air waveguide that will allow the propagation of the dominant mode at 40 MHz to be $2a_{\text{min}} \simeq 4.396 \text{ m}$.

(b) Repeating part (a) for 40 GHz yields $2a_{\min} \simeq 4.396$ mm. In other words, when the frequency increases by a factor of 1000, the diameter of the waveguide is reduced by a factor of 1000 for the same mode operation to hold.

C.28 Square-to-circular waveguide.

(a) For the square air waveguide with dimensions $a = b = 2.4$ cm, the cutoff frequency of the dominant TE_{10} and TE_{01} modes is given by

$$f_{c_{10}} = f_{c_{01}} = \frac{c}{2a} \simeq \frac{3 \times 10^{10}}{2 \times 2.4} = 6.25 \times 10^9 \text{ Hz} = 6.25 \text{ GHz}$$

Therefore, only the dominant TE_{10} and TE_{01} modes can propagate at 7 GHz.

(b) Conserving the perimeter, we have $2\pi a = 4 \times 2.4$ cm from which we find the radius a of the circular air waveguide as $a \simeq 1.528$ cm. Using this value, the cutoff frequency of the dominant TE_{11} mode is given by

$$f_{c_{11}} \simeq \frac{1.8412c}{2\pi a} \simeq \frac{1.8412 \times 3 \times 10^{10}}{9.6} \simeq 5.75 \times 10^9 \text{ Hz} = 5.75 \text{ GHz} < 7 \text{ GHz}$$

The cutoff frequency of the next higher TM_{01} mode can be calculated as

$$f_{c_{01}} \simeq \frac{2.4049c}{9.6} \simeq 7.515 \times 10^9 \text{ Hz} = 7.515 \text{ GHz} > 7 \text{ GHz}$$

Therefore, only the dominant TE_{11} mode propagates at 7 GHz.

C.29 Southworth's experiments.

(a) For an air-filled waveguide, the minimum diameter d_{\min} required to allow any propagation at $\lambda_{\text{air}} = 1$ m can be calculated from the cutoff wavelength of the lowest-order TE_{11} mode as

$$\lambda_{c_{TE_{11}}} \simeq \frac{\pi d_{\min}}{1.8412} = \lambda_{\text{air}} = 1 \text{ m} \rightarrow d_{\min} \simeq 58.6 \text{ cm}$$

Similarly, for a water-filled waveguide ($\epsilon_r \simeq 81$), we have

$$\lambda_{c_{TE_{11}}} \simeq \frac{\pi d_{\min}}{1.8412} = \lambda_{\text{water}} = \frac{\lambda_{\text{air}}}{\sqrt{\epsilon_r}} \simeq \frac{1}{9} \text{ m} \rightarrow d_{\min} \simeq 6.51 \text{ cm}$$

(b) Repeating part (a) for an air-filled waveguide at $\lambda_{\text{air}} = 15$ cm, we find $d_{\min} \simeq 8.79$ cm.

(c) Using $2a = 12.7$ cm and $\lambda_{\text{air}} = 15$ cm, the cutoff wavelength is given by

$$\lambda_{c_{nl}} = \frac{2\pi a}{(s_{nl} \text{ or } t_{nl})} = \frac{(12.7 \text{ cm})\pi}{(s_{nl} \text{ or } t_{nl})} \geq \lambda_{\text{air}} = 15 \text{ cm}$$

resulting in $(s_{nl} \text{ or } t_{nl}) \leq 2.660$. Therefore, using Tables C.2 and C.3, only TE_{11} and TM_{01} modes propagate at $\lambda_{\text{air}} = 15$ cm.

C.30 Barrow's experiments.

For a $\lambda_{\text{air}} = 50$ cm signal source, $f = c/\lambda_{\text{air}} \simeq 600$ MHz. Professor Barrow used a hollow cylindrical waveguide with radius $a = 2.25$ cm. The cutoff frequency of the lowest-order TE₁₁ mode for this waveguide is given by

$$f_{c_{\text{TE}_{11}}} \simeq \frac{1.8412c}{2\pi a} \simeq \frac{1.8412(3 \times 10^{10})}{2\pi(2.25)} \simeq 3.91 \times 10^9 \text{ Hz} = 3.91 \text{ GHz} > 600 \text{ MHz}$$

Therefore, the experiment was unsuccessful because no propagation mode exists on this waveguide at 600 MHz.

(b) $\lambda_{\text{air}} = 40$ cm $\rightarrow f \simeq 750$ MHz. Using $a = 22.85$ cm, the cutoff frequency of the lowest-order TE₁₁ mode in this guide is given by

$$f_{c_{\text{TE}_{11}}} \simeq \frac{1.8412(3 \times 10^{10})}{2\pi(22.85)} \simeq 3.85 \times 10^8 \text{ Hz} = 385 \text{ MHz} > 750 \text{ MHz}$$

Therefore, TE₁₁ mode propagates at 750 MHz and as a result, the experiment in this case was successful. Did Professor Barrow observe any other propagating modes in this experiment?

C.31 The Channel Tunnel.

(a) Equating the cutoff frequency of a mode to the highest AM frequency, we have

$$f_{c_{nl}} = \frac{(s_{nl} \text{ or } t_{nl})c}{2\pi a} = 1.605 \times 10^6 \text{ Hz} \rightarrow (s_{nl} \text{ or } t_{nl}) \simeq 0.128!$$

Therefore, AM radio waves do not propagate along the 7.6 m diameter tunnel.

(b) Using 108 MHz and following a similar approach as in part (a), we find $(s_{nl} \text{ or } t_{nl}) \simeq 8.595$. Therefore, using a source such as Beattie (see footnote 22 in Chapter 5), the maximum number of propagating modes at 108 MHz FM frequency is found to be 21.

(c) Following a similar approach as in part (a), again, we find out that AM does not propagate. Using 108 MHz, we find $(s_{nl} \text{ or } t_{nl}) \simeq 5.429$ and as a result, maximum of 9 different modes can propagate.

C.32 Unknown circular waveguide mode.

(a) Comparing the H_ϕ expression with (C.48) and (C.50), we conclude that this mode is a TM_{*nl*} mode and that $n = 0$. To find the value of l , we use

$$\frac{t_{nl}}{a} = \frac{t_{nl}}{0.04} \simeq 138 \rightarrow t - nl \simeq 5.520$$

Comparing with the roots provided in Table C.2, this mode is identified as the TM₀₂ mode. This is a propagating mode, as is evident from the $e^{j48\pi z}$ term.

(b) Using (C.46), we can write

$$\bar{\beta}_{\text{TM}_{02}} \simeq \frac{(2\pi f)^2}{c^2} - (138)^2 \simeq (48\pi)^2 \rightarrow f \simeq \frac{c}{2\pi} \sqrt{(48\pi)^2 + (138)^2} \simeq 9.760 \text{ GHz}$$

(c) From (C.48), we have

$$-\frac{j\omega\epsilon a}{t_{nl}} C_0 \simeq C_1 \quad \rightarrow \quad C_0 \simeq j254.3 C_1$$

Therefore, the other nonzero field components of this TM_{02} mode can be written as

$$E_z \simeq j254.3 C_1 J_0(138r) e^{j48\pi z}$$

$$E_r = 277.9 C_1 J'_0(138r) e^{j48\pi z}$$

(d) From the cutoff frequency expression we have

$$f_{c_{nl}} = \frac{(t_{nl} \text{ or } s_{nl})c}{2\pi a} \leq \sim 9.760 \text{ GHz} \quad \rightarrow \quad (t_{nl} \text{ or } s_{nl}) \leq \sim 8.176$$

Using Tables C.2 and C.3, the total number of propagating modes possible at ~ 9.760 GHz is found to be 18 (i.e., 7 TM_{nl} and 11 TE_{nl}) modes.

C.33 Unknown circular waveguide mode.

(a) To find the unknown TE_{nl} mode propagating in the circular air waveguide with $a = 3.5$ cm, we use (C.50) which yields $n = 3$ and $s_{nl}/(0.035 \text{ m}) = 120 \rightarrow s_{3l} \simeq 4.200$ and from Table C.3, we find that $l = 1$. Therefore, this is the TE_{31} mode. It is a propagating mode because of the $e^{-j116.9z}$ term in the H_z phasor expression.

(b) The operation frequency can be calculated from the phase constant expression given by

$$\bar{\beta}_{31}^2 \simeq \frac{(2\pi)^2 f^2}{(3 \times 10^8)^2} \left[1 - \frac{(5.73 \times 10^9)^2}{f^2} \right] \simeq (116.9)^2$$

where we used $f_{c_{31}} = 4.201c/(2\pi a) \simeq 5.73$ GHz. Solving the operating frequency f from the above equation, we find $f \simeq 8.00$ GHz.

(c) To find the highest-order propagating mode at ~ 8 GHz, we have

$$f_{c_{nl}} = \frac{(s_{nl} \text{ or } t_{nl})c}{2\pi a} \simeq 8 \times 10^9 \quad \rightarrow \quad (s_{nl} \text{ or } t_{nl}) \simeq 5.864$$

Therefore, the highest-order propagating mode at ~ 8 GHz is the TM_{02} mode.

(d) For the TM_{02} mode propagating in the z direction, $H_z = 0$. Using $t_{02} \simeq 5.5201$ from Table C.2, the E_z phasor expression can be written as

$$E_z \simeq C_2 J_0 \left(\frac{5.5201}{0.035} r \right) e^{-j\bar{\beta}_{02}z} \simeq C_2 J_0(158r) e^{-j18\pi z}$$

where

$$\bar{\beta}_{02} = \frac{2\pi f}{c} \sqrt{1 - (f_{c_{02}}/f)^2} \simeq \frac{2\pi(8 \times 10^9)}{3 \times 10^8} \sqrt{1 - (7.53/8)^2} \simeq 18\pi$$

and

$$f_{c_{02}} \simeq \frac{5.5201c}{\pi(0.07)} \simeq 7.53 \text{ GHz}$$

are used.

C.34 Smallest circular waveguide dimension.

(a) From Table C.2, the cutoff frequency of the TM₂₁ mode in a circular air-filled waveguide is given by

$$f_{c_{\text{TM}_{21}}} \simeq \frac{5.135c}{2\pi a} \simeq \frac{5.136 \times 3 \times 10^{10}}{\pi d} = 25 \text{ GHz}$$

from which the smallest diameter d_{min} can be obtained as

$$d_{\text{min}} = 2a_{\text{min}} \simeq 0.510 \text{ cm}$$

(b) The cutoff frequency of the TM₁₂ mode is given by

$$f_{c_{\text{TM}_{21}}} \simeq \frac{7.016c}{2\pi a} = 25 \text{ GHz}$$

from which $d_{\text{min}} = 2a_{\text{min}} \simeq 0.373 \text{ cm}$.

C.35 Circular waveguide modes.

(a) Since the WC-80 ($a = 1.012 \text{ cm}$) circular air waveguide (i.e., $v_p = c \simeq 3 \times 10^8 \text{ m-s}^{-1}$) is operated at 16 GHz, the cutoff frequencies of all the propagating modes must satisfy the inequality

$$f_{c_{\text{TE or TM}}} = \frac{(s_{nl} \text{ or } t_{nl})c}{2\pi a} < 16 \text{ GHz} \rightarrow (s_{nl} \text{ or } t_{nl}) < \sim 3.391$$

Therefore, using Tables C.2 and C.3 ($t_{01} \simeq 2.405$, $s_{11} \simeq 1.841$ and $s_{21} \simeq 3.054$), we find that the only modes that will propagate in this waveguide at 16 GHz are TE₁₁, TM₀₁ and TE₂₁ respectively.

(b) The cutoff frequencies of the propagating modes are given by

$$\begin{aligned} f_{c_{\text{TE}_{11}}} &\simeq \frac{1.8412c}{2\pi a} \simeq 8.69 \text{ GHz} \\ f_{c_{\text{TM}_{01}}} &\simeq \frac{2.4048c}{2\pi a} \simeq 11.35 \text{ GHz} \\ f_{c_{\text{TE}_{21}}} &\simeq \frac{3.054c}{2\pi a} \simeq 14.4 \text{ GHz} \end{aligned}$$

Using these values, the phase velocity, guide wavelength, and the wave impedance of these propagating modes at 16 GHz can be calculated as

$$\bar{v}_{p_{11}} = \frac{v_p}{\sqrt{1 - (f_{c_{11}}/f)^2}} \simeq \frac{c}{\sqrt{1 - (8.69/16)^2}} \simeq 1.19c$$

$$\bar{v}_{01} \simeq 1.42c, \bar{v}_{21} \simeq 2.30c,$$

$$\bar{\lambda}_{11} = \frac{v_p/f}{\sqrt{1 - (f_{c_{11}}/f)^2}} \simeq \frac{3 \times 10^8 / (16 \times 10^9)}{\sqrt{1 - (8.69/16)^2}} \simeq 0.0223 \text{ m} = 2.23 \text{ cm}$$

$$\bar{\lambda}_{01} \simeq 2.66 \text{ cm}, \bar{\lambda}_{21} \simeq 4.31 \text{ cm},$$

$$Z_{\text{TE}_{11}} = \frac{\eta_{\text{air}}}{\sqrt{1 - (f_{c_{11}}/f)^2}} \simeq \frac{377}{\sqrt{1 - (8.69/16)^2}} \simeq 1.19(377\Omega) \simeq 449\Omega$$

$Z_{\text{TE}_{21}} \simeq 867\Omega$, and

$$Z_{\text{TM}_{01}} = \eta_{\text{air}} \sqrt{1 - (f_{c_{11}}/f)^2}$$

respectively.

C.36 Low-loss TE_{01} mode in a circular waveguide.

(a) For an air-filled circular waveguide with radius $a = 5$ cm, the cutoff frequency of the low-loss TE_{01} mode is given by

$$f_{c_{\text{TE}_{01}}} = \frac{s_{01}c}{2\pi a} \simeq \frac{3.832(3 \times 10^{10})}{2\pi(5)} \simeq 3.66 \times 10^9 \text{ Hz} = 3.66 \text{ GHz}$$

(b) If the same circular waveguide is filled with water (assume $\epsilon_r \simeq 81$), then, the new cutoff frequency of the TE_{01} mode is

$$f_{c_{\text{TE}_{01}}} \simeq \frac{3.832(3 \times 10^{10})}{2\pi(5)\sqrt{81}} \simeq 4.07 \times 10^8 \text{ Hz} = 407 \text{ MHz}$$

C.37 Low-loss TE_{01} mode in a highly overmoded waveguide.

(a) Using the E_ϕ expression in (C.50) along with the root $s_{01} \simeq 3.8317$ from Table C.3, we can calculate the diameter d of the air-filled waveguide as

$$\frac{s_{01}}{a} \simeq \frac{3.8317}{a} \simeq 238 \rightarrow d = 2a \simeq 3.22 \text{ cm}$$

Using the phase constant expression given by

$$\begin{aligned} \beta_{01} &= \frac{2\pi f}{c} \sqrt{1 - (f_{c_{01}}/f)^2} \simeq 716\pi \\ \rightarrow (716\pi)^2 &\simeq \left(\frac{2\pi}{c}\right)^2 [f^2 - f_{c_{01}}^2] \end{aligned}$$

where $f_{c_{01}} = s_{01}c/(2\pi a) \simeq 11.36 \text{ GHz}$ and $c \simeq 3 \times 10^{10} \text{ cm-s}^{-1}$, we can calculate the operating frequency to be $f \simeq 108 \text{ GHz}$.

(b) Using the cutoff frequency expression

$$f_{c_{nl}} = \frac{(s_{nl} \text{ or } t_{nl})c}{2\pi a} \simeq 108 \times 10^9 \text{ Hz}$$

from which we find $(s_{nl} \text{ or } t_{nl})_{\text{max}} \simeq 36.42$. Therefore, using a reference such as Beattie (see footnote 21 in Addendum C), the total number of propagating modes in this waveguide operating at $\sim 108 \text{ GHz}$ is found to be 339!

C.38 A highly overmoded circular waveguide.

(a) The radii of the two circular waveguides are $a_1 = 3.175$ cm and $a_2 = 1.39$ cm. Assuming air-filled waveguide, the cutoff frequencies of the propagating modes in the 6.35 cm diameter guide must satisfy the inequality

$$f_{c_{nl}} = \frac{(s_{nl} \text{ or } t_{nl})c}{2\pi a_1} < 60 \text{ GHz} \rightarrow (s_{nl} \text{ or } t_{nl})_{\max} < \sim 39.90$$

Therefore, using a reference such as Beattie (see footnote 21 in Addendum C), the total number of modes propagating in the 6.35 cm diameter air waveguide at 60 GHz is found to be 409.

(b) Repeating part (a) for the 2.78 cm diameter waveguide, we have

$$f_{c_{nl}} = \frac{(s_{nl} \text{ or } t_{nl})c}{2\pi a_2} < 60 \text{ GHz} \rightarrow (s_{nl} \text{ or } t_{nl})_{\max} < \sim 17.46$$

Therefore, using Beattie, the total number of propagating modes in the 2.78 cm diameter air waveguide at 60 GHz is 80.

C.39 TE₁₁ to TM₁₁ mode converter.

(a) For the input air waveguide with radius $a_1 \simeq 1.19$ cm, the cutoff frequency of any propagating mode at 9.94 GHz must satisfy

$$f_{c_{nl}} = \frac{(s_{nl} \text{ or } t_{nl})c}{2\pi a_1} < 9.94 \times 10^9$$

yielding $(s_{nl} \text{ or } t_{nl}) < \sim 2.477$. Therefore, using the values of s_{nl} and t_{nl} provided in Tables C.2 and C.3, the only modes that can propagate on the inner waveguide at 9.94 GHz are TE₁₁ and TM₀₁ respectively.

(b) Repeating part (a) for the output air waveguide with radius $a_2 \simeq 2.06$ cm, we find

$$(s_{nl} \text{ or } t_{nl}) < \sim 4.289$$

from which we determine the propagating modes on the outer waveguide at 9.94 GHz as TE₁₁, TM₀₁, TE₂₁, TM₁₁, TE₀₁, and TE₃₁ respectively.

C.40 Circular waveguide modes.

(a) Using Tables C.2 and C.3, the cutoff frequencies of the dominant TE₁₁ mode and the next higher TM₀₁ mode on a 1 cm inner diameter circular air waveguide are given by

$$f_{c_{\text{TE}_{11}}} = \frac{s_{11}c}{2\pi a} \simeq \frac{(1.8412)(3 \times 10^{10})}{\pi(1)} \simeq 17.58 \text{ GHz}$$

$$f_{c_{\text{TM}_{01}}} = \frac{t_{01}c}{2\pi a} \simeq \frac{(2.4049)(3 \times 10^{10})}{\pi(1)} \simeq 22.97 \text{ GHz}$$

Therefore, the frequency range over which only the dominant TE₁₁ mode can propagate can be found as $f_{c_{\text{TM}_{01}}} - f_{c_{\text{TE}_{11}}} \simeq 5.383$ GHz.

(b) The cutoff frequency of the TE₀₁ and TE₃₁ mode are

$$f_{c_{TE_{01}}} = \frac{s_{01}c}{2\pi a} \simeq \frac{(3.832)(3 \times 10^{10})}{\pi(1)} \simeq 36.59 \text{ GHz}$$

$$f_{c_{TE_{31}}} = \frac{s_{31}c}{2\pi a} \simeq \frac{(4.201)(3 \times 10^{10})}{\pi(1)} \simeq 40.12 \text{ GHz}$$

Therefore, excluding the possibility of the TM₀₁ and TE₂₁ modes, the frequency range over which only the TE₁₁ and TE₀₁ (and TM₁₁) modes can propagate can be found as $f_{c_{TE_{31}}} - f_{c_{TE_{01}}} \simeq 3.52 \text{ GHz}$.

C.41 Circular waveguide design.

(a) Using the first design criteria, we have

$$f_{c_{TE_{11}}} \simeq \frac{1.8412c}{2\pi a} \leq 0.8(6.4 \text{ GHz}) \rightarrow a_{\min} \simeq 1.717 \text{ cm}$$

where $c \simeq 3 \times 10^{10} \text{ cm-s}^{-1}$ is used. Using the second design criteria, we have

$$f_{c_{TE_{01}}} \simeq \frac{3.832c}{2\pi a} \geq 1.1(6.4 \text{ GHz}) \rightarrow a_{\max} \simeq 2.599 \text{ cm}$$

Therefore, the waveguide radius must lie in the range $\sim 1.717 \leq a \leq \sim 2.599 \text{ cm}$. But, since the third design criteria is to maximize the power delivering capability of the waveguide, we choose $a = a_{\max} \simeq 2.599 \text{ cm}$.

(b) The three possible modes that can propagate at 6.4 GHz are TE₁₁, TM₀₁, and TE₂₁, since the cutoff frequencies of these three modes are

$$f_{c_{TE_{11}}} \simeq \frac{1.8412c}{2\pi(2.599)} \simeq 3.38 \text{ GHz}$$

$$f_{c_{TM_{01}}} \simeq \frac{2.4049c}{2\pi(2.599)} \simeq 4.42 \text{ GHz}$$

$$f_{c_{TE_{21}}} \simeq \frac{3.0542c}{2\pi(2.599)} \simeq 5.61 \text{ GHz}$$

The next higher modes are TE₀₁ and TM₁₁, both of which have the same cutoff frequencies given by

$$f_{c_{TE_{01}}} = f_{c_{TM_{11}}} \simeq \frac{3.832c}{2\pi(2.599)} \simeq 7.04 \text{ GHz} > 6.4 \text{ GHz}$$

and therefore, these two modes do not propagate at 6.4 GHz.

(c) Similar to part (b), the possible propagating modes at 9.6 GHz can be found as TE₁₁, TM₀₁, TE₂₁, TE₀₁, TM₁₁, TE₃₁ (with $f_{c_{TE_{31}}} \simeq 7.72 \text{ GHz}$), and TM₂₁ (with $f_{c_{TM_{21}}} \simeq 9.44 \text{ GHz}$).

C.42 Circular waveguide modes.

(a) For the WC-109 circular polystyrene-filled waveguide with diameter $2a = 2.779$ cm, the modes that can propagate at 10 GHz can be TE₁₁, TM₀₁, TE₂₁, TE₀₁, TM₁₁, and TE₃₁ which have cutoff frequencies given by

$$f_{c_{TE_{11}}} \simeq \frac{1.8412(3 \times 10^{10})}{\pi(2.779)\sqrt{2.56}} \simeq 3.954 \text{ GHz}$$

$$f_{c_{TM_{01}}} \simeq \frac{2.4049(3 \times 10^{10})}{\pi(2.779)\sqrt{2.56}} \simeq 5.165 \text{ GHz}$$

$$f_{c_{TE_{21}}} \simeq \frac{3.0542(3 \times 10^{10})}{\pi(2.779)\sqrt{2.56}} \simeq 6.559 \text{ GHz}$$

$$f_{c_{TE_{01}}} = f_{c_{TM_{11}}} \simeq \frac{3.832(3 \times 10^{10})}{\pi(2.779)\sqrt{2.56}} \simeq 8.23 \text{ GHz}$$

$$f_{c_{TE_{31}}} \simeq \frac{4.201(3 \times 10^{10})}{\pi(2.779)\sqrt{2.56}} \simeq 9.022 \text{ GHz}$$

Note that the next higher mode (in this case TM₂₁) does not propagate since its cutoff frequency is $\sim 11.03 \text{ GHz} > \sim 10 \text{ GHz}$.

(b) The phase velocity, the guide wavelength, and the wave impedance of the dominant TE₁₁ mode at 10 GHz can be calculated as

$$\bar{v}_{p_{11}} \simeq \frac{(3 \times 10^8 \text{ m-s}^{-1})/\sqrt{2.56}}{\sqrt{1 - (3.954/10)^2}} \simeq 2.04 \times 10^8 \text{ m-s}^{-1}$$

$$\bar{\lambda}_{11} \simeq \frac{(3 \text{ cm})/\sqrt{2.56}}{\sqrt{1 - (3.954/10)^2}} \simeq 2.04 \text{ cm}$$

$$Z_{TE_{11}} \simeq \frac{(377\Omega)/\sqrt{2.56}}{\sqrt{1 - (3.954/10)^2}} \simeq 256.5\Omega$$

C.43 A circular waveguide used for microwave telecommunications.

At 4 GHz, the cutoff frequencies of all propagating modes on the WC--281 circular air waveguide ($d = 2a \simeq 7.14$ cm) must satisfy

$$\frac{(t_{nl} \text{ or } s_{nl})}{\pi(7.14)} < 4 \text{ GHz} \rightarrow (t_{nl} \text{ or } s_{nl}) < \sim 2.991$$

Using Tables C.2 and C.3, we find that only TE₁₁ and TM₀₁ modes can propagate at 4 GHz.

At 6 GHz, we find $(t_{nl} \text{ or } s_{nl}) < \sim 4.486$, which means that only six modes (TE₁₁, TM₀₁, TE₂₁, TE₀₁, TM₁₁, and TE₃₁) can propagate.

At 8 GHz, we find $(t_{nl} \text{ or } s_{nl}) < \sim 5.982$, which means that only ten modes (TE₁₁, TM₀₁, TE₂₁, TE₀₁, TM₁₁, TE₃₁, TM₂₁, TE₄₁, TE₁₂ and TM₀₂) can propagate.

At 11 GHz, we find $(t_{nl} \text{ or } s_{nl}) < \sim 8.225$, which means that only 18 modes (up to the TE₃₂ mode) can propagate.

C.44 Orthogonally polarized TE₁₁ modes.

(a) We have

$$\frac{s_{11}}{a} = 80 \rightarrow a = \frac{s_{11}}{80} = \frac{1.841}{80} = 2.3 \text{ cm}$$

$$\bar{\beta}_{11} = 47 = [\omega^2 \mu \epsilon - (s_{11}/a)^2] \rightarrow f = \frac{c}{2\pi} [(47)^2 + (80)^2]^{1/2} \simeq 4.43 \text{ GHz}$$

(b) Next lowest cutoff for TM modes is TM₀₁, with $f_c \simeq 5$ GHz, while for TE modes is TE₂₁, with $f_c \simeq 6.3$ GHz. Thus, the TE₁₁ mode at 4.43 GHz is indeed dominant.

(c) From (C.8) we have

$$\mathbf{H}_{\text{tr}} = \mathbf{H}_r + \mathbf{H}_\phi = -\frac{\bar{\gamma}}{\bar{\gamma}^2 + \omega^2 \mu \epsilon} \nabla_{\text{tr}} H_z \quad (\text{C.6a})$$

$$\mathbf{E}_{\text{tr}} = \mathbf{E}_r + \mathbf{E}_\phi = \frac{j\omega\mu}{\bar{\gamma}} \mathbf{H}_{\text{tr}} \times \hat{\mathbf{z}} \quad (\text{C.6b})$$

where $\bar{\beta} = [\omega^2 \mu \epsilon - (s_{nl}/a)^2]^{1/2}$, and $\bar{\gamma} = j\bar{\beta}$. Since $\hat{\phi} \times \hat{\mathbf{z}} = \hat{\mathbf{r}}$, we have from the above

$$H_\phi = \frac{\bar{\beta}}{\omega\mu} E_r = \frac{\bar{\beta}}{\omega\mu} \frac{C_1}{r} J_1(80r) [\sin \phi + \cos \phi] e^{-j47z}$$

$$= (1.34 \times 10^{-3}) \frac{C_1}{r} J_1(80r) [\sin \phi + \cos \phi] e^{-j47z}$$

The H_z component can be found by noting that

$$\bar{\gamma}^2 + \omega^2 \mu \epsilon = \left(\frac{s_{nl}}{a}\right)^2$$

$$\nabla_{\text{tr}} = \hat{\mathbf{r}} \frac{\partial}{\partial r} + \hat{\phi} \frac{1}{r} \frac{\partial}{\partial \phi}$$

and integrating (C.8a):

$$H_z = \frac{(s_{nl}/a)^2}{-j\bar{\beta}} \int H_\phi r d\phi = j \frac{(s_{nl}/a)^2}{\omega\mu} C_1 J_1(80r) e^{-j47z} \int [\sin \phi + \cos \phi] d\phi$$

$$= j \frac{(s_{nl}/a)^2}{\omega\mu} C_1 J_1(80r) e^{-j47z} [\cos \phi - \sin \phi] = j(0.183) C_1 J_1(80r) e^{-j47z} [\cos \phi - \sin \phi]$$

and from (C.6a) we have

$$H_r = \frac{-j\bar{\beta}}{(s_{nl}/a)^2} \frac{\partial H_z}{\partial r} = \bar{\beta} \omega \mu C_1 J'_1(80r) e^{-j47z} (80) [\cos \phi - \sin \phi]$$

$$= 0.107 C_1 J'_1(80r) e^{-j47z} [\cos \phi - \sin \phi]$$

whereas from (C.6a) we have

$$E_\phi = \frac{j\omega\mu}{j\bar{\beta}} = 80 C_1 J'_1(80r) e^{-j47z} [\cos \phi - \sin \phi]$$

(d) The form a choice of sines and cosines in the rectangular case are due to the boundary conditions, while in the circular case they are due to an arbitrary selection of the origin of ϕ .

C.45 Circular waveguide-to-microstrip transition.

The cutoff frequency of all the propagating modes on the 2.1 cm diameter circular air waveguide must satisfy

$$\frac{(t_{nl} \text{ or } s_{nl})c}{2\pi a} < 10.66 \text{ GHz} \rightarrow (t_{nl} \text{ or } s_{nl}) < \frac{\pi(2.1)(10.66 \times 10^9)}{3 \times 10^{10}} \simeq 2.344$$

Using Tables C.2 and C.3, we find that only the TE_{11} mode can propagate in this waveguide, for the frequency range specified.

C.46 Circular versus rectangular waveguides.

We separately consider parallel-plate, rectangular, and circular waveguides. For parallel-plate, examination of Figure 10.11 indicates that possible low loss modes are TEM and TE_1 . For TEM, we have $f_c = 0$, and $\alpha_{c_{TEM}} = R_s/(\eta a)$. From the given sheet size we can choose $b = \frac{6.3}{2} = 3.15$ cm, and select a value of a small enough so that fringing fields can be negligible, e.g., $a \leq b/(10) = 0.315$ cm. The attenuation constant is then

$$\alpha_{c_{TEM}} = \frac{1}{0.315 \times 10^{-2}} 317.46 \frac{R_s}{\eta a} = 317.46 \frac{R_s}{\eta a}$$

For TE_1 , we have

$$f_{c1} = \frac{c}{(2a)} \leq 25 \text{ GHz} \rightarrow a \geq \frac{c}{2.25 \times 10^9} = 0.6 \text{ cm}$$

since we must have $a \leq 0.315$ cm to minimize fringing fields, it appears that any parallel-plate guide we can make from the given material would not be suitable for propagating the TE_1 mode.

For rectangular waveguide, we see from Figure C.8 that the best mode to consider is the TE_{10} mode. We have

$$f_{c10} = \frac{c}{2a} \leq 25 \text{ GHz} \rightarrow a \geq 0.6 \text{ cm}$$

$$\text{Also } a \geq b \text{ and } a + b = \frac{6.3}{2} = 3.15 \text{ cm} \rightarrow a \geq \frac{3.15}{2} = 1.5757 \text{ cm}$$

$$\text{and } a < 3.15 \text{ cm} \text{ whereas } b = 3.15 - a \text{ cm}$$

The attenuation constant is

$$\alpha_{c_{TE_{10}}} = \frac{R_s [1 + (2b/a)(f_{c10}/f)^2]}{\eta b \sqrt{1 - (f_{c10}/f)^2}} = \frac{R_s}{\eta} \frac{1 + [(6.3 - 2a)/a][c/(2\pi f)]^2}{(3.15 - a) \times 10^{-2} \sqrt{1 - [c/(2\pi f)]^2}} \simeq 372.91 \frac{R_s}{\eta}$$

for $f = 25$ GHz, and $a = b = 1.575$ cm.

For circular waveguide, we note from Figure C.13 that possible modes are TE₁₁ and TE₀₁. We consider these separately:

$$\text{TE}_{01} : f_{c_{\text{TE}_{01}}} = \frac{s_{01}}{2\pi a \sqrt{\mu\epsilon}} = \frac{3.832c}{2\pi a} \leq 25 \text{ GHz} \rightarrow a \geq \frac{3.8232c}{2\pi(25 \times 10^9)} = 0.73 \text{ cm}$$

$$\text{Also } 2\pi a \leq 6.3 \text{ cm} \rightarrow a \leq 1.00 \text{ cm}$$

$$\alpha_{c_{\text{TE}_{01}}} = \frac{R_s}{\eta} \frac{1}{a} \left[1 - \left(\frac{f_{c_{\text{TE}_{01}}}}{f} \right)^2 \right]^{1/2} \left[\left(\frac{f_{c_{\text{TE}_{01}}}}{f} \right)^2 + \frac{1}{(3.832)^2 - 1} \right] \simeq 89.34 \frac{R_s}{\eta}$$

for $f = 25 \text{ GHz}$ and $a = 1 \text{ cm}$.

$$\text{TE}_{11} : f_{c_{\text{TE}_{11}}} = \frac{s_{11}}{2\pi a \sqrt{\mu\epsilon}} = \frac{1.841c}{2\pi a} \leq 25 \text{ GHz} \rightarrow a \geq \frac{3.8232c}{2\pi(25 \times 10^9)} = 0.35 \text{ cm}$$

$$\text{Also } 2\pi a \leq 6.3 \text{ cm} \rightarrow a \leq 1.00 \text{ cm}$$

$$\alpha_{c_{\text{TE}_{11}}} = \frac{R_s}{\eta} \frac{1}{a} \left[1 - \left(\frac{f_{c_{\text{TE}_{11}}}}{f} \right)^2 \right]^{1/2} \left[\left(\frac{f_{c_{\text{TE}_{11}}}}{f} \right)^2 + \frac{1}{(1.841)^2 - 1} \right] \simeq 57.91 \frac{R_s}{\eta}$$

Comparison of the α_c values for the three different waveguides indicates that circular waveguide is the best from the point of view of minimizing attenuation due to conductive losses.

C.47 Attenuation in a coaxial line.

The expression for the attenuation constant for a coaxial line is

$$\alpha_c = \frac{R_s}{2\eta \ln(b/a)} \left[\frac{1}{a} + \frac{1}{b} \right] = 0.003 \text{ np-m}^{-1} \text{ at } 300 \text{ MHz}$$

where $R_s = \sqrt{\omega\mu_0/(2\sigma)}$ is the only frequency dependent term, for a nonmagnetic conductor such as copper, and assuming that $\eta = \sqrt{\mu/\epsilon}$ is not frequency dependent, which for an air-filled line is simply $\eta_{\text{air}} = \sqrt{\mu_0/\epsilon_0}$. We are told that the line is made of 'thick' walls, which at 300 MHz must definitely be much larger than the skin depth ($\delta \simeq 3.82 \mu\text{m}$ for copper at 300 MHz). Thus, the wall thickness does not explicitly appear in the expression for α_c , and doubling it does not significantly change the attenuation constant.

(a) At 600 MHz, the value of R_s is higher by a factor of $\sqrt{2}$, thus we have $\alpha_c \simeq 0.003\sqrt{2} \simeq 0.0042 \text{ np-m}^{-1}$.

(b) As mentioned above, doubling the thickness of the copper walls has no significant effect. When the conductor radii are $2a$ and $2b$, we have

$$\alpha_c = \frac{R_s}{2\eta \ln[2b/(2a)]} \left[\frac{1}{2a} + \frac{1}{2b} \right] = \frac{1}{2} \underbrace{\left\{ \frac{R_s}{2\eta \ln(b/a)} \left[\frac{1}{a} + \frac{1}{b} \right] \right\}}_{\alpha_c \text{ at } 300 \text{ MHz}} = 0.0015 \text{ np-m}^{-1}$$

(c) The attenuation rate due to dielectric losses for the TEM mode in a coaxial line filled with nonmagnetic material is given by (C.57), namely

$$\alpha_d \simeq \frac{\omega \epsilon'' \sqrt{\mu_0}}{2\sqrt{\epsilon'}} \quad \text{np-m}^{-1}$$

where $\epsilon'' = \epsilon' \tan \delta_c$. Using the values given for 300 MHz we find

$$\alpha_d \simeq \frac{(2\pi)(300 \times 10^6)(2\epsilon_0)[(15/\pi) \times 10^{-4}]}{2\sqrt{2\epsilon_0}} \simeq 6.36 \times 10^5 \sqrt{\epsilon_0} \simeq 1.89 \text{ np-m}^{-1}$$

so that the total attenuation rate is

$$\alpha_{\text{total}} = \alpha_c + \alpha_d = 0.003 + 1.89 \simeq 1.90 \text{ np-m}^{-1}$$

It thus appears that the dielectric losses are clearly dominant.

(d) At 600 MHz, α_d is twice as large, since it is proportional to frequency. Thus we have

$$\alpha_{\text{total}} = 0.0042 + (2)(1.89) = 3.78 \text{ np-m}^{-1}$$

C.48 Optimum coaxial lines.

There is a typo in the statement of this problem. As should be obvious from the wording, the condition for minimum α_c for a given outer conductor radius b is $b = 3.6a$, rather than $a = 3.6b$.

(a) The expression for α_c for TEM mode in a coaxial line is given by (C.56), namely

$$\alpha_c = \frac{R_s}{2\eta \ln(b/a)} \left[\frac{1}{a} + \frac{1}{b} \right]$$

For a given value of b , we can differentiate α_c with respect to a and equate to zero

$$\frac{\partial \alpha_c}{\partial a} = \frac{R_s}{2\eta} \left\{ \frac{\left[\frac{1}{a} + \frac{1}{b} \right]}{a[\ln(b/a)]^2} - \frac{1}{a^2 \ln(b/a)} \right\} = 0$$

which reduces to

$$a \left[\frac{1}{a} + \frac{1}{b} \right] = \ln(b/a) \quad \rightarrow \quad 1 + \frac{1}{b/a} = \ln(b/a) \quad \rightarrow \quad \zeta = e^{1+\zeta^{-1}} \quad \rightarrow \quad \zeta = \frac{b}{a} \simeq 3.591$$

(b) The characteristic impedance is given by (C.58)

$$Z_0 \simeq 60 \ln \frac{b}{a} \simeq 60 \ln \frac{3.6a}{a} \simeq 76.7 \Omega$$

(c) The answer is no. If we start with a fixed value of the inner conductor radius a , then the larger the value of b the better, since the average power transmitted (P_{av}) goes up proportional to the cross-sectional area while the wall losses (P_{loss}) are determined by the perimeter, thus α_c , which is determined by the ratio of P_{loss} to P_{av} can be made arbitrarily small by choosing an arbitrarily large value of b .

C.49 Power capacity of a coaxial line.

Our answer must be based on the expressions from Section C.2.2 for the electric and magnetic fields and the average power transmitted for a coaxial line. We have

$$\mathbf{H} = \hat{\phi} \frac{H_0}{r} e^{-j\beta z} \quad ; \quad \mathbf{E} = \hat{r} \frac{H_0 \eta}{r} e^{-j\beta z} \quad ; \quad P_{av} = \pi \eta H_0^2 \ln \left(\frac{b}{a} \right)$$

The surface current density $\mathbf{J}_s = \hat{\mathbf{n}} \times \mathbf{H}$, so that $|\mathbf{J}_s| = |\mathbf{H}|$. We note that both the electric field and the surface current density are maximum at the lowest radius, i.e., at $r = a$. Thus, we only need to pay attention to their values at $r = a$. For the given value of $a = 0.5$ mm, the maximum electric field and surface current conditions dictate the following:

$$\begin{aligned} |\mathbf{J}_s| \leq 10 \text{ A-mm}^{-1} &\rightarrow \frac{H_0}{0.5 \times 10^{-3}} \leq 10 \times 10^3 \rightarrow H_0 \leq 5 \\ |\mathbf{E}| \leq 10 \text{ kV-mm}^{-1} &\rightarrow \frac{H_0(377)}{0.5 \times 10^{-3}} \leq 10 \times 10^6 \rightarrow H_0 \leq 13.26 \end{aligned}$$

Thus, it appears that the surface current criteria is the one that limits the maximum power handling capacity. For $H_0 = 5$ we have

$$P_{av} = \pi \eta H_0^2 \ln \left(\frac{b}{a} \right) = \pi(377)(5) \ln \left(\frac{2.5}{0.5} \right) = 9.53 \text{ kW}$$

C.50 Higher-order modes on a coaxial line.

(a) For the air-filled coaxial line with $a \simeq 1.49$ cm and $b \simeq 3.429$ cm, the mode with the lowest nonzero cutoff frequency is the TE_{11} mode with cutoff frequency approximately given by (C.59) as

$$f_{c11} \simeq \frac{c}{\pi(a+b)} \simeq \frac{3 \times 10^{10}}{\pi(1.49 + 3.429)} \simeq 1.941 \text{ GHz}$$

Thus, TE_{11} mode can propagate on the coaxial line only at frequencies above 1.941 GHz.

(b) Repeating part (a) for the same coaxial line filled with Noryl EN265 material ($\epsilon'_r \simeq 2.65$), we find

$$f_{c11} \simeq \frac{3 \times 10^{10} / \sqrt{2.65}}{\pi(1.49 + 3.429)} \simeq 1.193 \text{ GHz}$$

(c) Based on the cutoff frequency calculated in part (b), it is clear that the TEM approximation is not valid for frequencies above ~ 1.2 GHz, since the higher-order modes such as the TE_{11} can also propagate on the line and can contribute to the results obtained in the measurements.

C.51 Group velocity for the TE₁₀ mode.

The field expressions for the TE₁₀ mode in a rectangular waveguide are:

$$\begin{aligned}
 H_z^o &= C \cos\left(\frac{\pi x}{a}\right) \\
 H_x^o &= \frac{j\bar{\beta}aC}{\pi} \sin\left(\frac{\pi x}{a}\right) \\
 E_y^o &= -\frac{j\omega\mu aC}{\pi} \sin\left(\frac{\pi x}{a}\right) \\
 E_x^o &= H_y^o = 0 \\
 \bar{\beta}_{10} &= \sqrt{\omega^2\mu\epsilon - \left(\frac{\pi}{a}\right)^2} = \left[\left(\frac{2\pi}{\lambda}\right)^2 - \left(\frac{\pi}{a}\right)^2\right]^{1/2}
 \end{aligned}$$

Following an analysis similar to that in Section 10.3.3, we can consider a unit length (1 m) of waveguide. The time average energy stored in a volume $V = (a)(b)(1)$, including both electric and magnetic parts, is

$$\begin{aligned}
 \bar{W}_{\text{str}} &= \frac{1}{4} \int_0^a \int_0^b \int_0^1 [\epsilon \mathbf{E} \cdot \mathbf{E}^* + \mu \mathbf{H} \cdot \mathbf{H}^*] dz dy dx \\
 &= \frac{\mu\omega^2\mu\epsilon ab}{4(\pi/a)^2}
 \end{aligned}$$

The time average power transmitted can be found as

$$P_{\text{av}} = \int_0^b \int_0^a \frac{1}{2} \text{Re}\{\mathbf{E} \times \mathbf{H}^*\} dx dy = \frac{\omega\mu\bar{\beta}_{10}ab}{a(\pi/a)^2}$$

so that the velocity of energy travel is given by

$$v_{\text{en}} = \frac{\mathbf{S}_{\text{av}}}{W} = \frac{\omega\bar{\beta}_{10}}{\omega^2\mu\epsilon} = \frac{v_p^2}{v_p} = \frac{1}{\sqrt{\mu\epsilon}} \sqrt{1 - \left(\frac{f_{c10}}{f}\right)^2} \rightarrow v_{\text{en}} = v_g$$

Thus we see that the group velocity is indeed the velocity of energy transport for the TE₁₀ mode.

2

Transient Response of Transmission Lines

2.1 Lumped or distributed circuit element?

(a) Using (2.9),

$$Z_0 = \sqrt{\frac{L}{C}} = \sqrt{\frac{4 \times 10^{-9} \text{ H-cm}^{-1}}{1.6 \times 10^{-12} \text{ F-cm}^{-1}}} = 50\Omega$$

Using (2.7),

$$\begin{aligned} v_p &= \frac{1}{\sqrt{LC}} = \frac{1}{\sqrt{(4 \times 10^{-9} \text{ H-cm}^{-1})(1.6 \times 10^{-12} \text{ F-cm}^{-1})}} \\ &= 1.25 \times 10^{10} \text{ cm-s}^{-1} \\ &= 12.5 \text{ cm-(ns)}^{-1} \end{aligned}$$

Hence the one-way time delay t_d is given by

$$t_d = \frac{l}{v_p} = \frac{5 \text{ cm}}{12.5 \text{ cm-(ns)}^{-1}} = 0.4 \text{ ns}$$

(b) The ratio between the step source rise-time and the one-way time delay is

$$\frac{t_r}{t_d} = \frac{0.1 \text{ ns}}{0.4 \text{ ns}} = 0.25 < 2.5$$

From (1.1), it is not appropriate to model the transmission line in this circuit as a lumped element.

2.2 Lumped- or distributed-circuit element?

(a) Using (2.7) and (2.9), we have

$$v_p = \frac{1}{\sqrt{LC}} = \frac{2c}{3} \simeq 2 \times 10^8 \text{ m-s}^{-1}$$

$$Z_0 = \sqrt{\frac{L}{C}} = 50\Omega$$

Multiplying the above two equations yields

$$v_p Z_0 = \frac{1}{C} \simeq (2 \times 10^8 \text{ m-s}^{-1})(50\Omega)$$

$$\rightarrow C \simeq 10^{-10} \text{ F-m}^{-1} = 1 \text{ pF-(cm)}^{-1}$$

Dividing the above two equations into one another results in

$$\frac{v_p}{Z_0} = \frac{1}{L} \simeq \frac{2 \times 10^8 \text{ m-s}^{-1}}{50\Omega}$$

$$\rightarrow L \simeq 2.5 \times 10^{-7} \text{ H-m}^{-1} = 2.5 \text{ nH-(cm)}^{-1}$$

(b)

$$t_d = \frac{l}{2c/3} \simeq \frac{1 \text{ m}}{2 \times 10^8 \text{ m-s}^{-1}} \simeq 5 \text{ ns}$$

(c)

$$\lambda = \frac{2c/3}{f} \simeq \frac{2 \times 10^8 \text{ m-s}^{-1}}{10^9 \text{ Hz}} = 0.2 \text{ m}$$

Using (1.6), we have

$$l = 1 \text{ m} > 0.01\lambda = 0.002 \text{ m}$$

Therefore, this transmission line should not be treated as a lumped element.

2.3 Open-circuited line.

Since we have an ideal unit step source, $R_s = 0$. As a result, the source-end reflection coefficient is

$$\Gamma_s = \frac{R_s - Z_0}{R_s + Z_0} = \frac{0 - Z_0}{0 + Z_0} = -1$$

At the load end (open circuit, i.e., $R_L = \infty$), the reflection coefficient is

$$\Gamma_L = \frac{R_L - Z_0}{R_L + Z_0} = \frac{\infty - Z_0}{\infty + Z_0} = +1$$

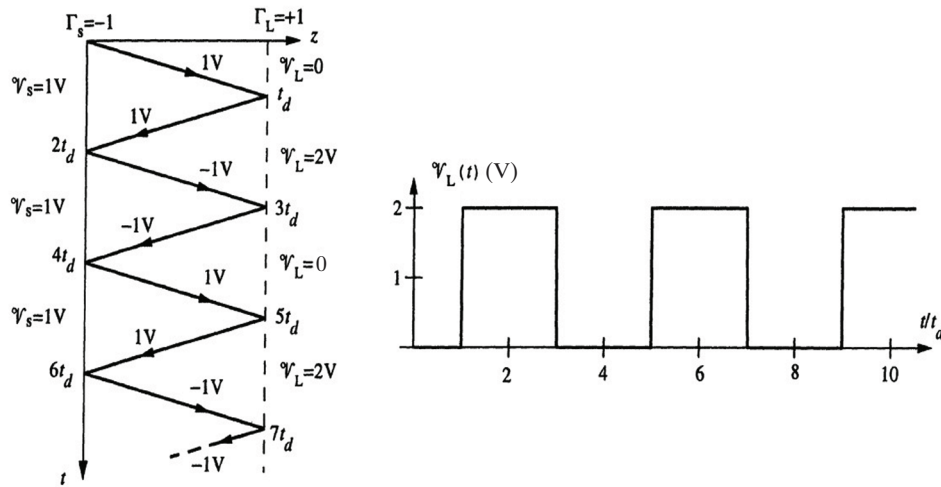


Figure 2.1 Figure for Problem 2.3

At $t = 0$, an incident voltage of amplitude

$$V_1^+ = \frac{Z_0}{R_s + Z_0} V_0 = \frac{50}{0 + 50} (1 \text{ V}) = 1 \text{ V}$$

is launched at the source end of the line. Using these values, we have the bounce diagram shown. The load end voltage $V_L(t)$ shown is sketched in Figure 2.1 using the bounce diagram.

2.4 Step and pulse excitation of a lossless line.

(a) We first calculate the reflection coefficients at the source and load, and the amplitude of the V_1^+ voltage wave that is launched at $t = 0^+$:

$$\begin{aligned}\Gamma_s &= \frac{R_s - Z_0}{R_s + Z_0} = \frac{10 - 90}{10 + 90} = -0.8 \\ \Gamma_L &= \frac{R_L - Z_0}{R_L + Z_0} = \frac{630 - 90}{630 + 90} = 0.75 \\ V_1^+ &= \frac{V_0 Z_0}{R_s + Z_0} = \frac{(10)(90)}{10 + 90} = 9 \text{ V}\end{aligned}$$

Using these values, we can sketch the bounce diagram in Figure 2.2a. The successive V^- and V^+ step amplitudes are calculated using the load and source reflection coefficients. For example, V_1^- and V_2^+ are found from V_1^+ as:

$$V_1^- = \Gamma_L V_1^+ = (0.75)(9) = 6.75 \text{ V}$$

$$V_2^+ = \Gamma_s V_1^- = (-0.8)(6.75) = -5.4 \text{ V}$$

The bounce diagram can be used to sketch the load- and source-end voltages, as shown in Figure 2.2b.

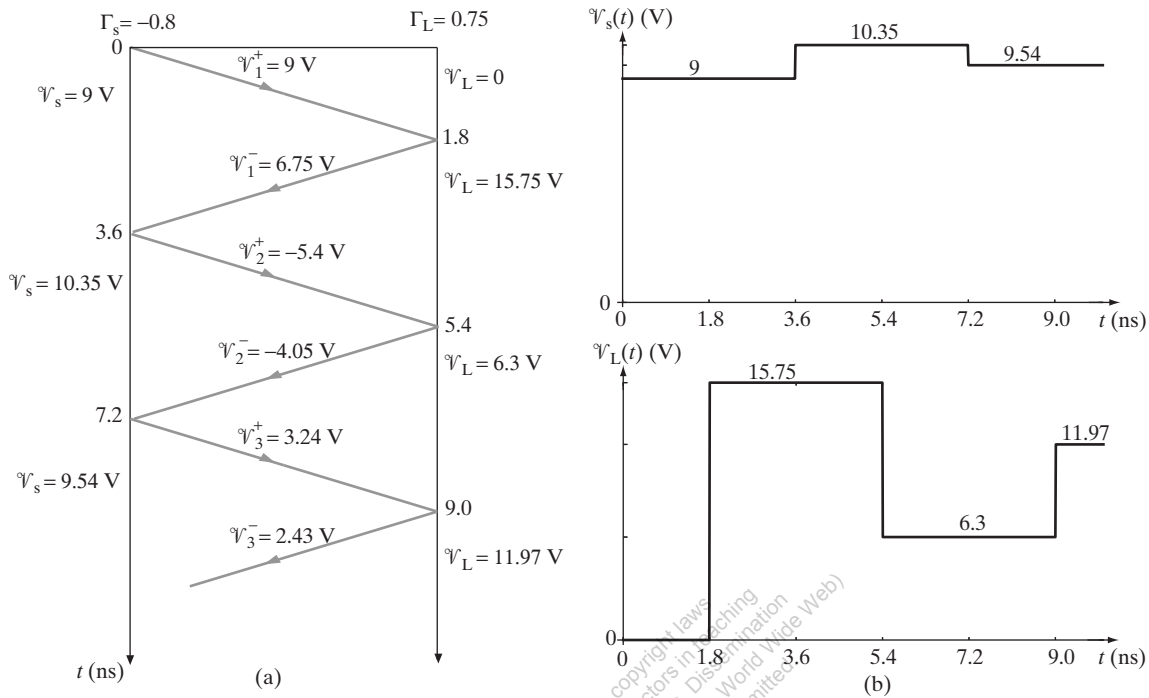


Figure 2.2 Figure for Problem 2.4(a). (a) Bounce diagram. (b) V_s and V_L versus time t .

(b) We can derive the sketches for V_s and V_L from the sketches in part (a) by delaying the plots by 0.3 ns and subtracting the result. The resulting sketches are shown in Figure 2.3.

2.5 Resistive loads.

Since $R_s = 0$, $\Gamma_s = -1$.

(a) For $R_L = 25\Omega$, we have

$$\Gamma_L = \frac{R_L - Z_0}{R_L + Z_0} = \frac{25 - 50}{25 + 50} = -\frac{1}{3}$$

At $t = 0$, an incident voltage of amplitude given by

$$V_1^+ = \frac{Z_0}{R_L + Z_0} V_0 = \frac{50}{0 + 50} (3 \text{ V}) = 3 \text{ V}$$

is launched at the source end of the line. Using these values, the bounce diagram and the load voltage $V_L(t)$ versus t are as shown in Figure 2.4.

(b) For $R_L = 50\Omega$, $\Gamma_L = 0$. The bounce diagram and the sketch of the load voltage for this case are as shown in Figure 2.5.

(c) For $R_L = 100\Omega$, the load reflection coefficient is

$$\Gamma_L = \frac{100 - 50}{100 + 50} = +\frac{1}{3}$$

Again, the bounce diagram and $V_L(t)$ versus t are as shown in Figure 2.6.

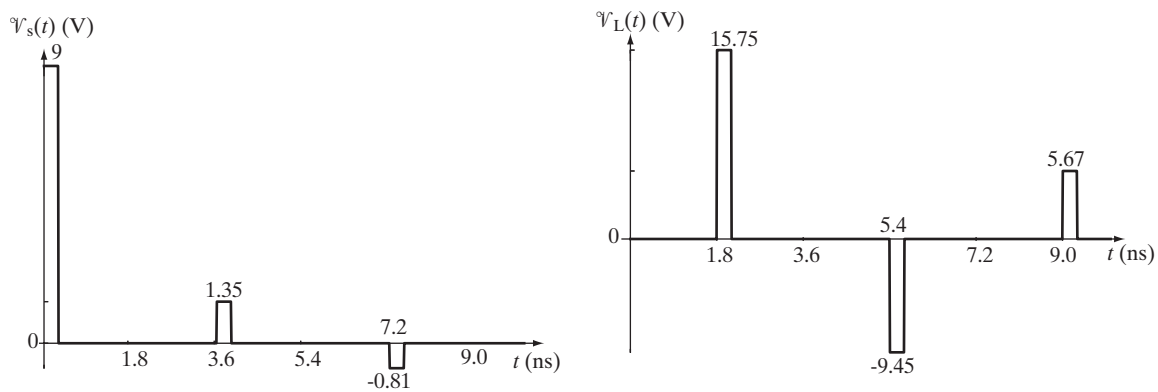


Figure 2.3 Figure for Problem 2.4(b). V_s and V_L versus time t .

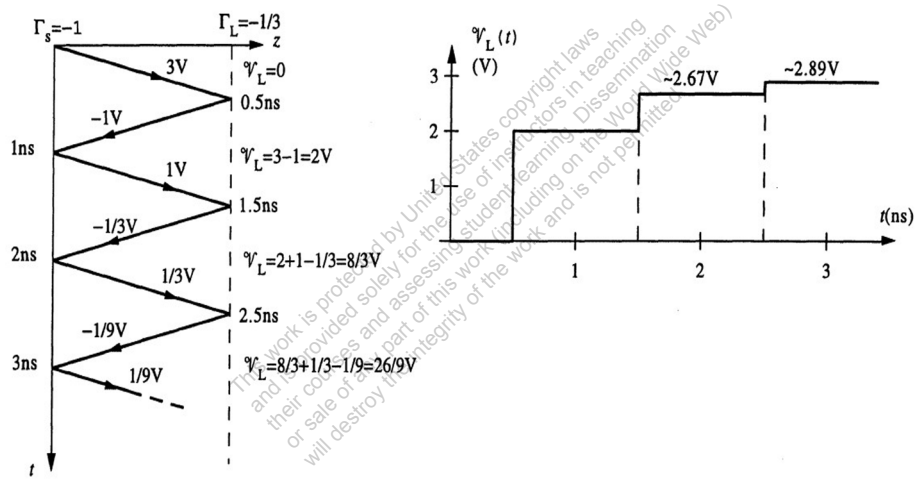


Figure 2.4 Figure for Problem 2.5a. $R_L = 25 \Omega$

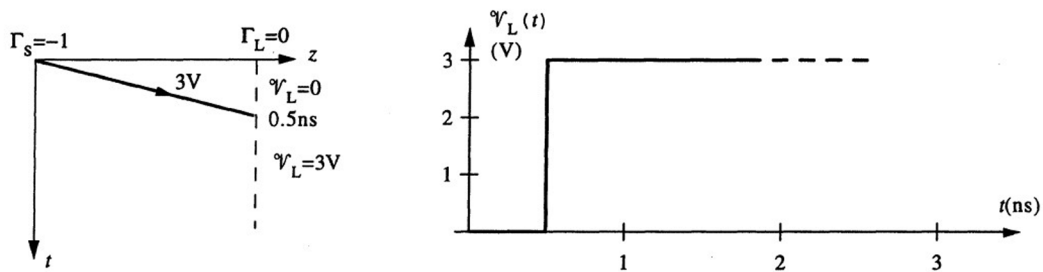


Figure 2.5 Figure for Problem 2.5b. $R_L = 50 \Omega$

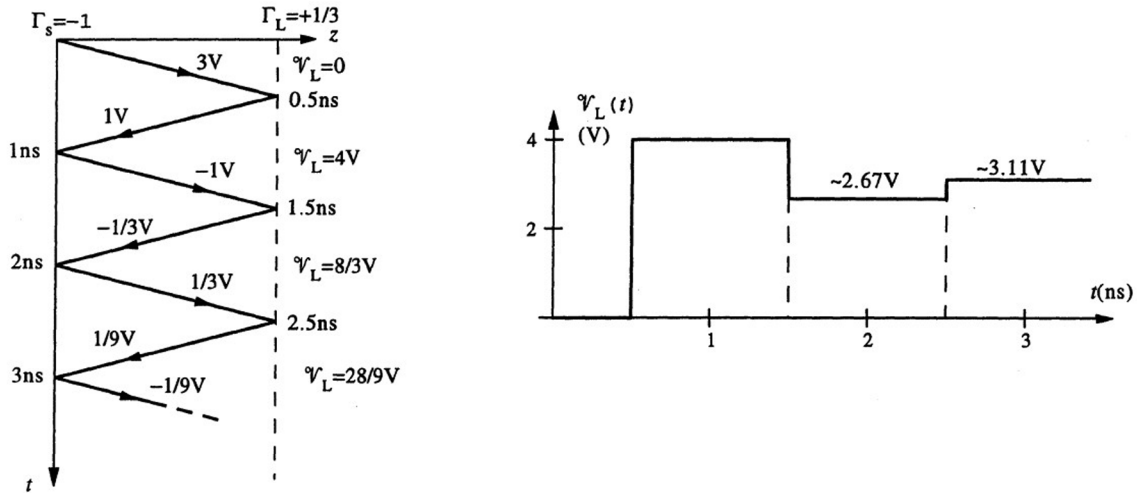


Figure 2.6 Figure for Problem 2.5c. $R_L = 100 \Omega$

2.6 Ringing.

Using (2.7) and (2.9), we have

$$v_p = \frac{1}{\sqrt{LC}} = \frac{1}{\sqrt{0.5 \times 10^{-6} \text{ H-m}^{-1} \times 0.2 \times 10^{-9} \text{ F-m}^{-1}}} = 10^8 \text{ m-s}^{-1}$$

$$Z_0 = \sqrt{\frac{L}{C}} = \sqrt{\frac{0.5 \times 10^{-6} \text{ H-m}^{-1}}{0.2 \times 10^{-9} \text{ F-m}^{-1}}} = 50 \Omega$$

The one-way time delay can be found as

$$t_d = \frac{l}{v_p} = \frac{15 \text{ cm}}{10^{10} \text{ cm-s}^{-1}} = 1.5 \text{ ns}$$

The incident voltage wave launched at the source-end at $t = 0$ can be found using the voltage divider principle as

$$V_1^+ = \frac{V_0 Z_0}{R_s + Z_0} = \frac{(50)(3.6)}{10 + 50} = 3 \text{ V}$$

The load-end and source-end reflection coefficients can be found using (2.12) and (2.14):

$$\Gamma_L = \frac{R_L - Z_0}{R_L + Z_0} \bigg|_{R_L \rightarrow \infty} = +1$$

$$\Gamma_s = \frac{R_s - Z_0}{R_s + Z_0} = \frac{10 - 50}{10 + 50} = -\frac{2}{3}$$

Next, we draw a bounce diagram up to $t = 10 \text{ ns}$, shown in Figure 2.7a. Using the load-end voltage values on the bounce diagram, we can sketch the load-end voltage $V_L(t)$ versus time, as shown in Figure 2.7b.

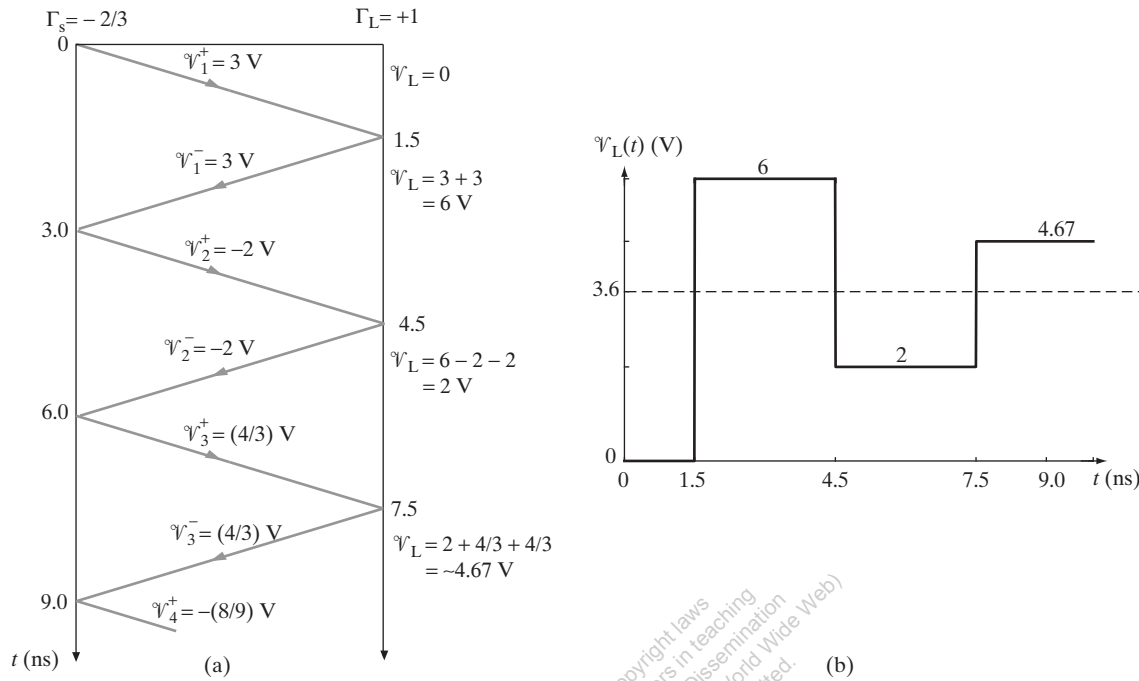


Figure 2.7 Figure for Problem 2.6. (a) Bounce diagram. (b) V_L versus time t .

2.7 Discharging of a charged line.

At $t = 0^-$ (i.e., immediately before the switch opens when steady-state conditions are in effect), the source end current \mathcal{I}_s is given by $\mathcal{I}_s(0^-) = V_0/R_L = 3/R_L$. At $t = 0^+$ (i.e., immediately after the switch opens), the source end current is suddenly forced to go to zero, i.e., $\mathcal{I}_s(0^+) = 0$. We can represent this change in \mathcal{I}_s as a new disturbance launched from the source end of the line starting at $t = 0$. The amplitude of this new current wave and its accompanying voltage wave are given respectively by $\mathcal{I}_1^+ = \mathcal{I}_s(0^+) - \mathcal{I}_s(0^-) = -3/R_L$ and $V_1^+ = Z_0 \mathcal{I}_1^+ = -3Z_0/R_L$. This disturbance will not affect the value of the load end voltage until $t = t_d = 0.5$ ns. So, for $t < t_d$, $V_L(t) = 3$ V, regardless of the value of R_L . Using the reflection coefficient values calculated in Problem 2.5, we draw the bounce diagram and sketch $V_L(t)$ as a function of t for each value of R_L , as shown in Figures 2.8, 2.9, and 2.10.

2.8 Two step voltage sources.

The reflection coefficients at source 1 and source 2 ends are, respectively,

$$\Gamma_1 = \frac{R_{s1} - Z_0}{R_{s1} + Z_0} = \frac{\frac{Z_0}{3} - Z_0}{\frac{Z_0}{3} + Z_0} = -0.5$$

$$\Gamma_2 = \frac{R_{s2} - Z_0}{R_{s2} + Z_0} = \frac{Z_0 - Z_0}{Z_0 + Z_0} = 0$$

At $t = 0^-$, the system is at a steady state, and so

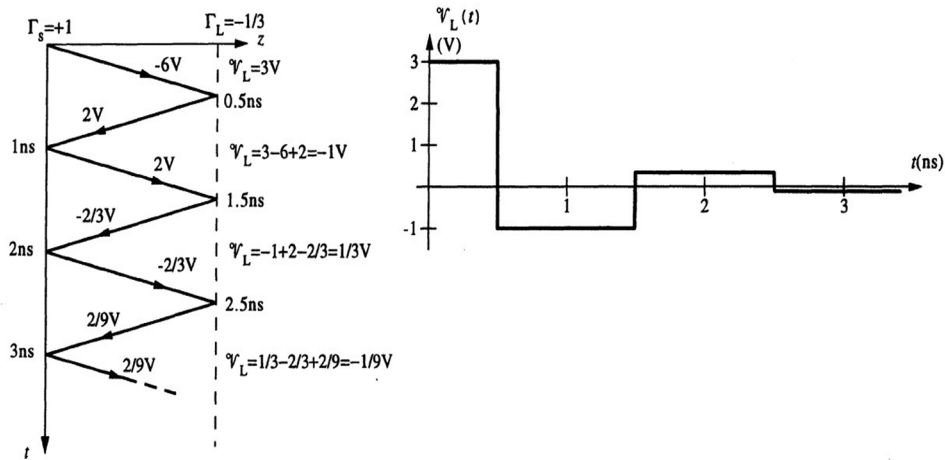


Figure 2.8 Figure for Problem 2.7a. Bounce diagram and $V_L(t)$ versus t for $R_L = 25 \Omega$.

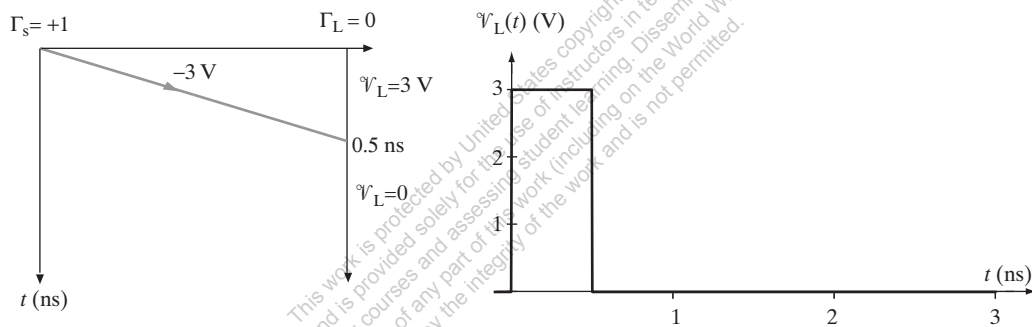


Figure 2.9 Figure for Problem 2.7b. Bounce diagram and $V_L(t)$ versus t for $R_L = 50 \Omega$.

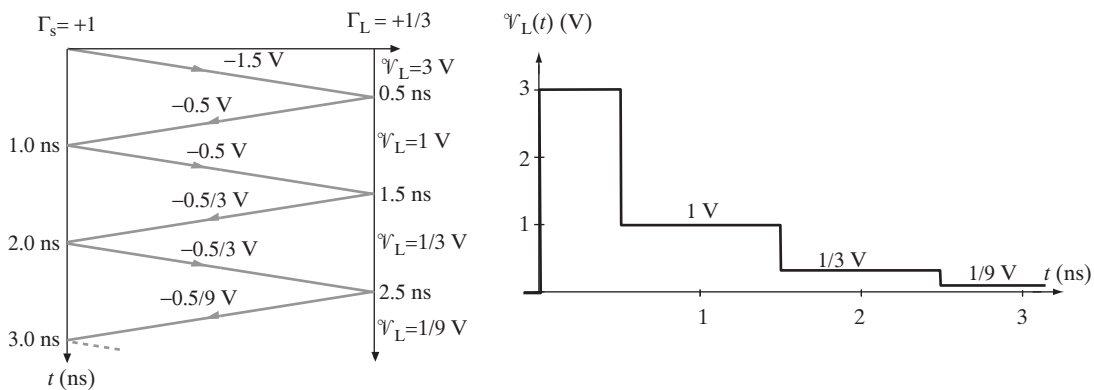


Figure 2.10 Figure for Problem 2.7c. Bounce diagram and $V_L(t)$ versus t for $R_L = 100 \Omega$.

$$\mathcal{V}_1(0^-) = \mathcal{V}_2(0^-) = \frac{R_{s2}}{R_{s1} + R_{s2}} V_0 = \frac{Z_0}{\frac{Z_0}{3} + Z_0} V_0 = 0.75V_0$$

At $t = 0$, $V_0 u(-t)$ turns off and $2V_0 u(t)$ turns on. As a result, we have the bounce diagram shown in Figure 2.11a. Note that \mathcal{V}_{1A}^+ is a voltage wave launched due to source $V_0 u(-t)$ turning off at $t = 0$. Similarly, \mathcal{V}_{1A}^- is a voltage wave launched due to $2V_0 u(t)$ turning on at $t = 0$.

Calculating the voltage wave amplitudes, we have

$$\begin{aligned}\mathcal{V}_{1A}^+ &= -\frac{Z_0}{R_{s1} + Z_0} V_0 = -0.75V_0 \\ \mathcal{V}_{1A}^- &= \frac{Z_0}{R_{s2} + Z_0} (2V_0) = V_0 \\ \mathcal{V}_{2A}^+ &= \Gamma_1 \mathcal{V}_{1A}^- = (-0.5)(V_0) = -0.5V_0\end{aligned}$$

Using these values, we have

$$\mathcal{V}_1(t) = \begin{cases} 0.75V_0, & t < 0 \\ 0, & 0 < t < t_d \\ 0.5V_0, & t > t_d \end{cases}$$

and

$$\mathcal{V}_2(t) = \begin{cases} 0.75V_0, & t < 0 \\ 1.75V_0, & 0 < t < t_d \\ V_0, & t_d < t < 2t_d \\ 0.5V_0, & t > 2t_d \end{cases}$$

The voltage sketches are shown in Figure 2.11b.

2.9 Pulse excitation.

The one-way time delay and the reflection coefficients at the ends of the line are $t_d = l/v_p = (10 \text{ cm})/(20 \text{ cm-ns}^{-1}) = 0.5 \text{ ns}$,

$$\Gamma_s = \frac{R_s - Z_0}{R_s + Z_0} = \frac{25 - 75}{25 + 75} = -0.5$$

$$\Gamma_L = \frac{R_L - Z_0}{R_L + Z_0} = \frac{0 - 75}{0 + 75} = -1$$

respectively. At $t = 0$, an incident voltage is launched at the source end of the line given by

$$\mathcal{V}_1^+ = \frac{75}{25 + 75} (1 \text{ V}) = 0.75 \text{ V}$$

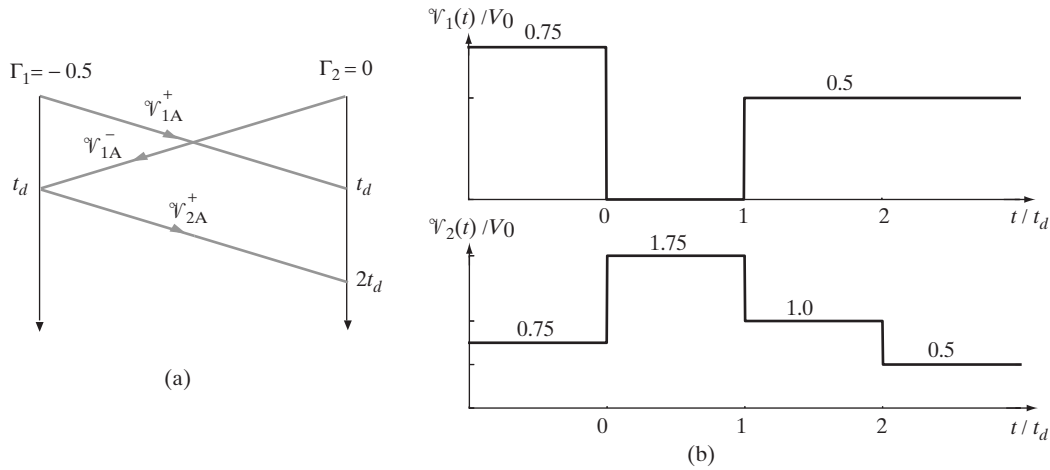


Figure 2.11 Figure for Problem 2.8. (a) Bounce diagram. (b) V_1 and V_2 versus time t .

(a) The input voltage has a pulse width of $t_w = 10$ ns, that is the input voltage turns off at $t = t_w = 10$ ns. We represent this change in the input voltage as a new incident voltage of amplitude $V_1^{+*} = -V_1^+ = -0.75$ V launched at the source end of the line at $t_w = 10$ ns. The bounce diagram and the variation of the source voltage $V_s(t)$ versus t are as shown in Figure 2.12a.

(b) For the case of $t_w = 1$ ns, the source end voltage $V_s(t)$ can easily be obtained by shifting the second-half of the $V_s(t)$ sketched in part (a) by 9 ns to the left and adding it with the first half. The final plot for $V_s(t)$ versus t is as shown in Figure 2.12b.

2.10 Pulse excitation.

The reflection coefficients at the two ends of the line are (using (2.12) and (2.14))

$$\Gamma_s = \frac{R_s - Z_0}{R_s + Z_0} = \frac{Z_0 - Z_0}{Z_0 + Z_0} = 0$$

$$\Gamma_L = \frac{R_L - Z_0}{R_L + Z_0} = \frac{100Z_0 - Z_0}{100Z_0 + Z_0} \simeq +1$$

At $t = 0$, an incident voltage of amplitude

$$V_1^+ = \frac{Z_0}{R_s + Z_0} A = \frac{Z_0}{Z_0 + Z_0} A = \frac{A}{2}$$

is launched at the source end of the line. When the input pulse turns off at $t = t_w$, this change can be represented as a new voltage disturbance

$$V_1^{+*} = -V_1^+ = -\frac{A}{2}$$

launched at the source end of the line at $t = t_w$. One by one, the new voltage cancels out the existing voltage disturbances $V_1^+, V_1^-, V_2^+, V_2^-$, etc. along the line. The bounce diagram and the load voltage $V_L(t)$ versus t are provided in Figures 2.13, 2.14, and 2.15. for each case corresponding to a different input pulse lengths.

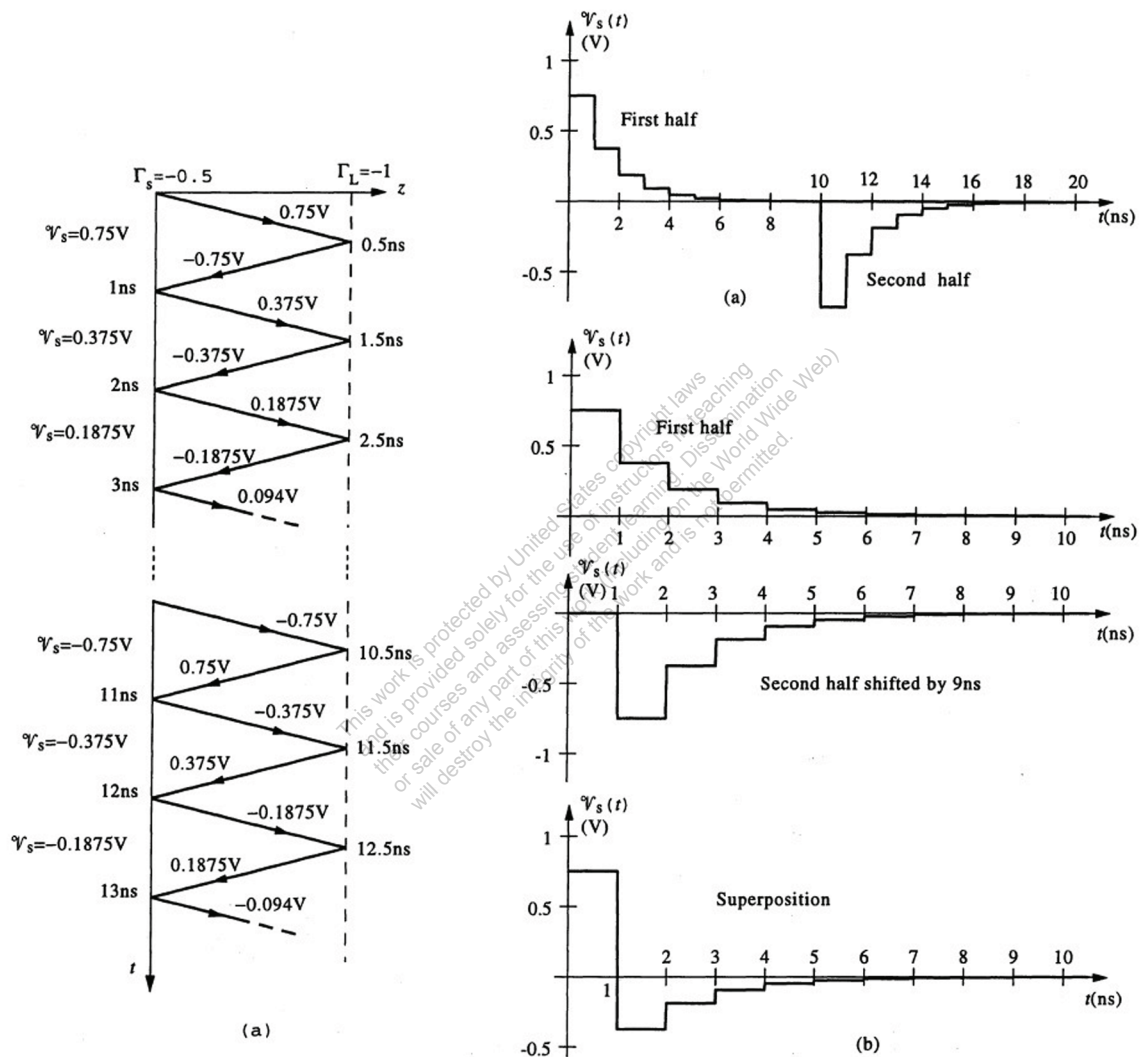


Figure 2.12 Figure for Problem 2.9. (a) Bounce diagram and $V_s(t)$ versus t . (b) $V_s(t)$ versus t , obtained via superposition.

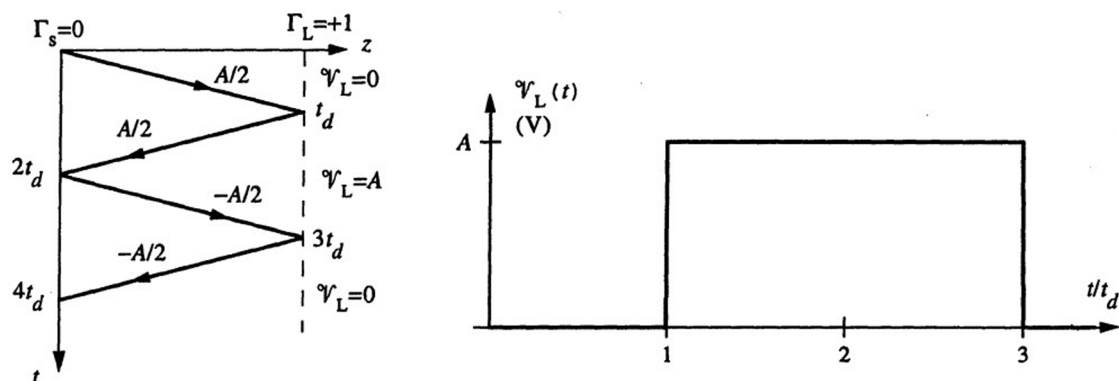


Figure 2.13 Figure for Problem 2.10a. (a) Bounce diagram and $V_L(t)$ versus t for $t_\omega = 2t_d$, where t_d is the one-way time delay along the line.

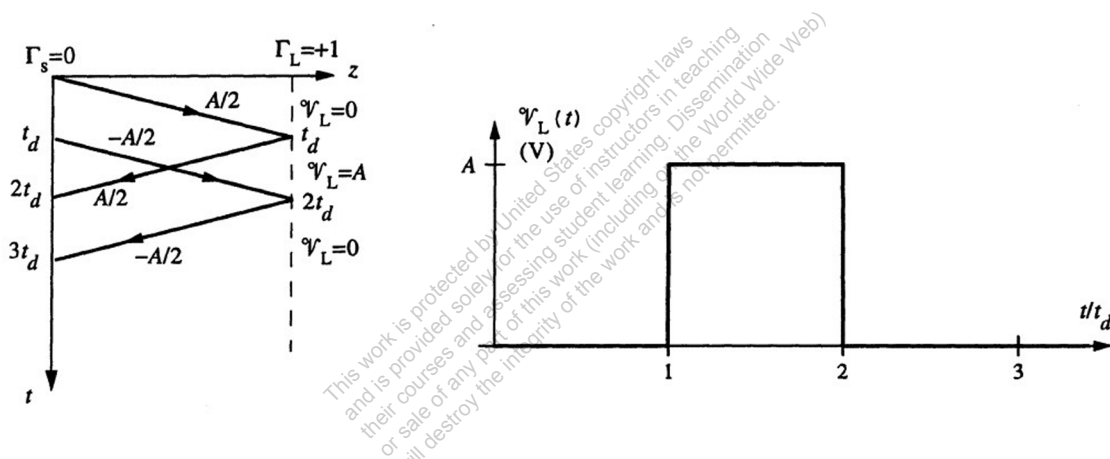


Figure 2.14 Figure for Problem 2.10b. (a) Bounce diagram and $V_L(t)$ versus t for $t_\omega = t_d$.

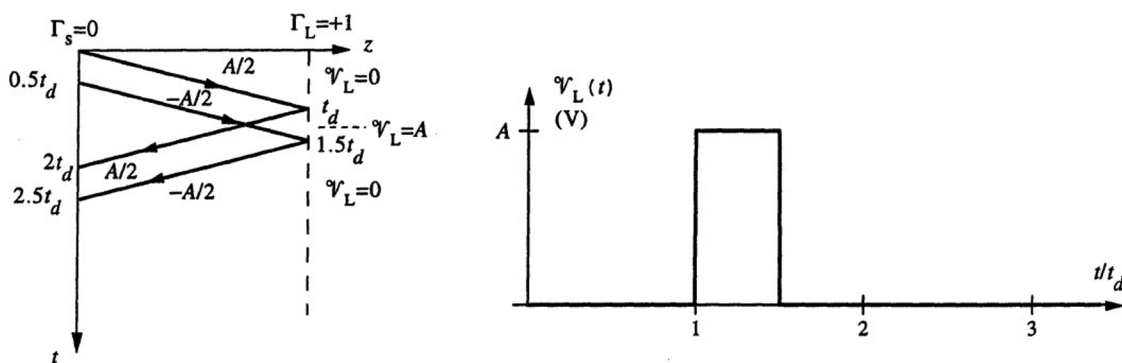


Figure 2.15 Figure for Problem 2.10c. (a) Bounce diagram and $V_L(t)$ versus t for $t_\omega = t_d/2$.

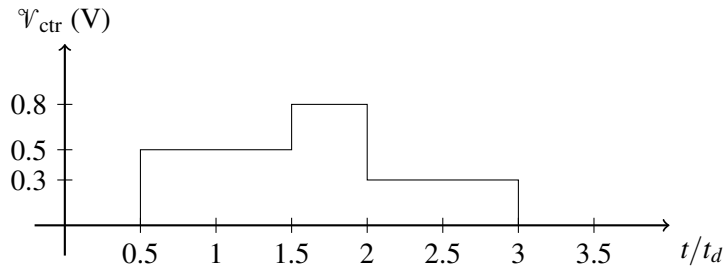


Figure 2.16 Figure for Problem 2.11.

2.11 Observer on the line.

(a) Using the sketch of \mathcal{V}_{ctr} versus t provided, the initial voltage launched on the line is given by

$$\mathcal{V}_1^+ = \frac{Z_0}{R_s + Z_0} V_0 = \frac{Z_0}{100 + Z_0} (1 \text{ V}) = 0.5 \text{ V} \rightarrow Z_0 = 100 \Omega$$

The reflected voltage is given by

$$\mathcal{V}_1^- = \Gamma_L \mathcal{V}_1^+ = \frac{R_L - Z_0}{R_L + Z_0} \mathcal{V}_1^+ = \frac{R_L - 100}{R_L + 100} (0.5 \text{ V}) = 0.3 \text{ V}$$

Solving for R_L , we have $R_L = 400 \Omega$.

(b) Superimposing the direct and reflected pulses, the voltage $\mathcal{V}_{\text{ctr}}(t)$ is as drawn in Figure 2.16.

2.12 Cascaded transmission lines.

The reflection coefficients are $\Gamma_s = 0$ (since $R_s = 50 \Omega$),

$$\Gamma_{12} = -\Gamma_{21} = \frac{Z_{02} - Z_{01}}{Z_{02} + Z_{01}} = \frac{75 - 50}{75 + 50} = +0.2$$

and $\Gamma_L = +1$ (since $R_L = \infty$) respectively. The bounce diagram and the sketches of voltages $\mathcal{V}_s(t)$ and $\mathcal{V}_L(t)$ are as shown in Figure 2.17.

2.13 Time-domain reflectometry (TDR).

The initial voltage \mathcal{V}_1^+ launched from the source end of the line is given by

$$\mathcal{V}_1^+ = \frac{Z_{01}}{R_s + Z_{01}} V_0 = \frac{Z_{01}}{50 + Z_{01}} (1 \text{ V}) = 0.5 \text{ V} \rightarrow Z_{01} = R_s = 50 \Omega$$

The source end voltage $\mathcal{V}_s(t)$ changes from 0.5 V to 0.375 V when the voltage wave reflected from the junction point between the two lines reaches the source end of the line, i.e., at time $2t_{d1} = 1 \text{ ns}$ or $t_{d1} = 0.5 \text{ ns}$. The length of the first line l_1 can then be found as $l_1 = v_p t_{d1} = (20 \text{ cm} \cdot (\text{ns})^{-1})(0.5 \text{ ns}) = 10 \text{ cm}$. The voltage \mathcal{V}_1^- reflected from the junction point can be expressed in terms of \mathcal{V}_1^+ as

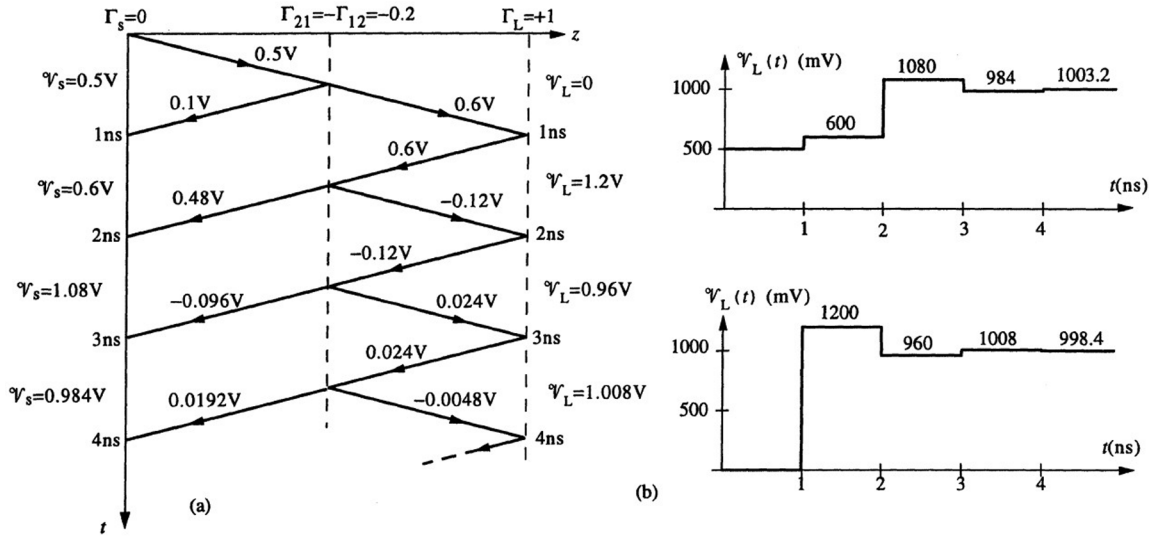


Figure 2.17 Figure for Problem 2.12. (a) Bounce diagram for the cascaded lines. (b) V_s and V_L versus t .



Figure 2.18 Figure for Problem 2.13. V_{R1} versus t .

$$V_1^- = \frac{(R_1 \parallel Z_{02}) - Z_{01}}{(R_1 \parallel Z_{02}) + Z_{01}} V_1^+ \quad \text{where} \quad R_1 \parallel Z_{02} = \frac{R_1 Z_{02}}{R_1 + Z_{02}}$$

When the reflected voltage V_1^- reaches the source end of the line, no reflection takes place since $\Gamma_s = 0$. Thus, we have $V_1^+ + V_1^- = 0.375 \text{ V} \rightarrow V_1^- = -0.125 \text{ V}$. Using this value in the above expression with $V_1^+ = 0.5 \text{ V}$ and $Z_{01} = 50 \Omega$, we find $R_1 \parallel Z_{02} = 30 \Omega$. Since $Z_{02} = 75 \Omega$, we have $R_1 = 50 \Omega$. The voltage $V_{R1}(t)$ versus t is plotted as shown in Figure 2.18.

2.14 Time-domain reflectometry (TDR).

(a) The initial voltage launched at the source end of the transmission line system is given by

$$V_1^+ = \frac{Z_{01}}{R_s + Z_{01}} V_0 = \frac{Z_{01}}{100 + Z_{01}} (3 \text{ V}) = 1.5 \text{ V} \rightarrow Z_{01} = R_s = 100 \Omega$$

The one-way time delay of the two transmission lines can be found as $t_{d1} = 3 \text{ ns}/2 = 1.5 \text{ ns}$ and $t_{d2} = (7.5 \text{ ns} - 3 \text{ ns})/2 = 2.25 \text{ ns}$. Since $\Gamma_s = 0$, the source end voltage V_s at $t = 2t_{d1}^+$ can be written as

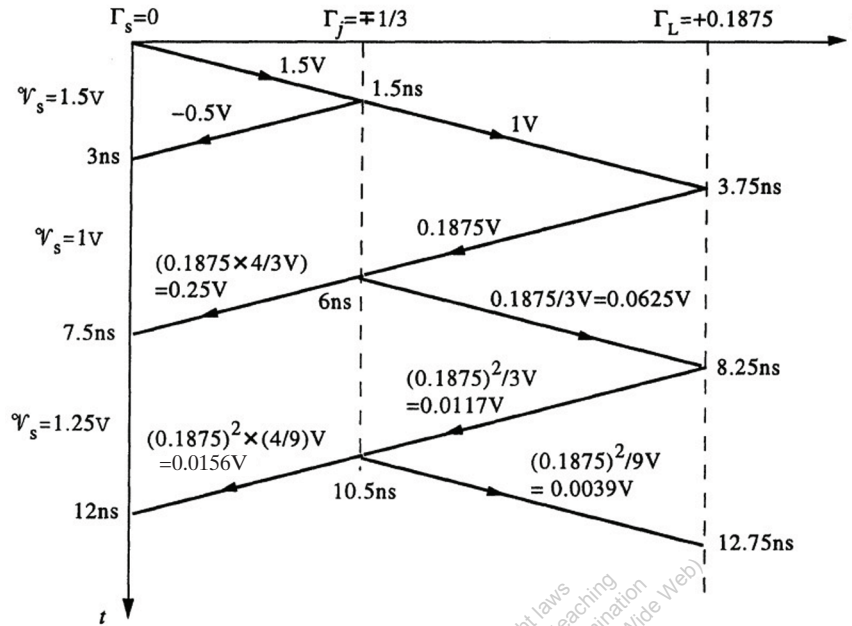


Figure 2.19 Figure for Problem 2.14. Bounce diagram.

$$V_s(2t_{d1}^+) = V_1^+(1 + \Gamma_{12}) = (1.5\text{V})(1 + \Gamma_{12}) = 1\text{V} \rightarrow \Gamma_{12} = -\frac{1}{3}$$

where

$$\Gamma_{12} = \frac{Z_{02} - Z_{01}}{Z_{02} + Z_{01}} = \frac{Z_{02} - 100}{Z_{02} + 100} \rightarrow Z_{02} = 50\Omega$$

At $t = 7.5^+$ ns, the source end voltage V_s is given by

$$V_s(t = 7.5^+) = V_1^+(1 + \Gamma_{12})[1 + \Gamma_L(1 + \Gamma_{21})] = 1.25\text{V}$$

where

$$\Gamma_{21} = -\Gamma_{12} = \frac{Z_{01} - Z_{02}}{Z_{01} + Z_{02}} = +\frac{1}{3} \text{ and } \Gamma_L = \frac{R_L - Z_{02}}{R_L + Z_{02}}$$

Substituting $V_1^+ = 1.5\text{V}$, $Z_{01} = 100\Omega$ and $Z_{02} = 50\Omega$, we find

$$\Gamma_L = \frac{R_L - 50}{R_L + 50} = 0.1875 \rightarrow R_L \simeq 73.1\Omega$$

(b) From the bounce diagram shown we note that the source end voltage V_s changes again at $t = 12$ ns, increasing by an amount of about $\sim 15.6\text{mV}$.

2.15 Time-domain reflectometry (TDR).

The initial voltage launched on the line is given by

$$\mathcal{V}_1^+ = \frac{Z_{01}}{R_s + Z_{01}} V_0 = \frac{Z_{01}}{50 + Z_{01}} (5 \text{ V}) = 3 \text{ V} \rightarrow Z_{01} = 75 \Omega$$

Since $v_p = 15 \text{ cm} \cdot (\text{ns})^{-1}$ and the one-way time delay of each line is $t_d = 5 \text{ ns}/2 = 2.5 \text{ ns}$, the length of each line is $l = v_p t_d = (15 \text{ cm} \cdot (\text{ns})^{-1})(2.5 \text{ ns}) = 37.5 \text{ cm}$.

At $t = 2t_d^+$, the source end voltage can be expressed as

$$\mathcal{V}_s(t = 2t_d^+) = \mathcal{V}_1^+ + \Gamma_{12}\mathcal{V}_1^+ + \Gamma_{12}\Gamma_s\mathcal{V}_1^+ = \mathcal{V}_1^+[1 + \Gamma_{12}(1 + \Gamma_s)] = 3.6 \text{ V}$$

where

$$\Gamma_{12} = \frac{Z_{02} - Z_{01}}{Z_{02} + Z_{01}} = \frac{Z_{02} - 75}{Z_{02} + 75}$$

$$\Gamma_s = \frac{R_s - Z_{01}}{R_s + Z_{01}} = \frac{50 - 75}{50 + 75} = -0.2$$

Substituting, we have

$$(3 \text{ V})[1 + \Gamma_{12}(1 - 0.2)] = 3.6 \text{ V} \rightarrow \Gamma_{12} = 0.25 \rightarrow Z_{02} = 125 \Omega$$

At $t = 4t_d^+$, the source end voltage is given by

$$\mathcal{V}_s(4t_d^+) = 3.6 \text{ V} + \Gamma_{12}^2\Gamma_s(1 + \Gamma_s)\mathcal{V}_1^+ + (1 + \Gamma_{12})\Gamma_L(1 + \Gamma_{21})(1 + \Gamma_s)\mathcal{V}_1^+ = 5.82 \text{ V}$$

$$\rightarrow \mathcal{V}_1^+[\Gamma_{12}^2\Gamma_s + (1 + \Gamma_{12})\Gamma_L(1 + \Gamma_{21})](1 + \Gamma_s) = 2.22 \text{ V}$$

where $\Gamma_{21} = -\Gamma_{12} = -0.25$. Substituting numerical values, we have

$$(3 \text{ V})[(0.25)^2(-0.2) + (1.25)\Gamma_L(0.75)](0.8) = 2.22 \text{ V}$$

from which we solve for $\Gamma_L = +1$, and $R_L = \infty$ (i.e., open circuit).

The bounce diagram for this problem is shown in Figure 2.20.

2.16 Multiple lines.

We start by calculating the reflection coefficients at the source, resistor loads, and at the junction.

$$\Gamma_s = \frac{R_s - Z_{01}}{R_s + Z_{01}} = \frac{50 - 100}{50 + 100} = -\frac{1}{3}$$

$$\Gamma_{L1} = \frac{R_{L1} - Z_{02}}{R_{L1} + Z_{02}} = \frac{150 - 50}{150 + 50} = \frac{1}{2} = 0.5$$

$$\Gamma_{L2} = \frac{R_{L2} - Z_{03}}{R_{L2} + Z_{03}} = \frac{100 - 100}{100 + 100} = 0$$

$$\Gamma_{j1 \rightarrow 2,3} = \frac{(Z_{02} \parallel Z_{03}) - Z_{01}}{(Z_{02} \parallel Z_{03}) + Z_{01}} = \frac{100/3 - 100}{100/3 + 100} = -0.5$$

$$\Gamma_{j2 \rightarrow 1,3} = \frac{(Z_{01} \parallel Z_{03}) - Z_{02}}{(Z_{01} \parallel Z_{03}) + Z_{02}} = \frac{50 - 50}{50 + 50} = 0$$

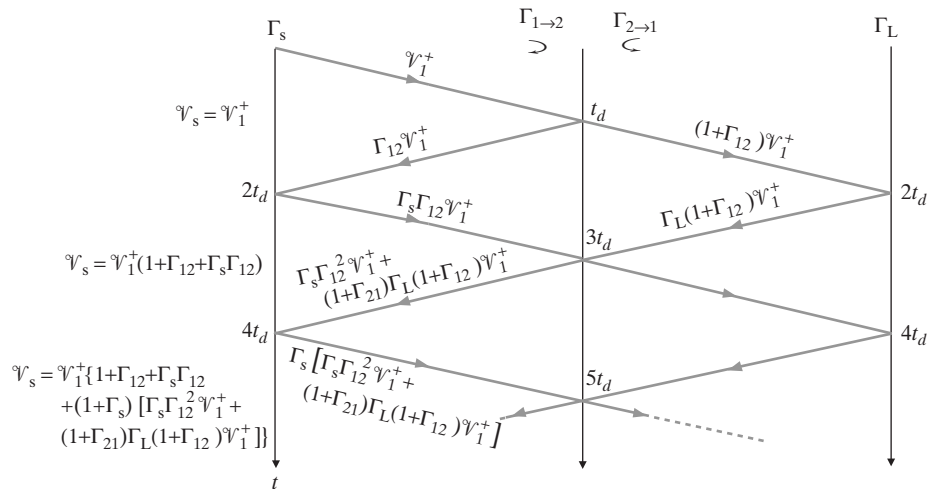


Figure 2.20 Figure for Problem 2.15. Bounce diagram.

Since the R_{L2} resistor is matched to line 3, there is no reflection on that transmission line and thus no need to calculate the reflection coefficient at the junction from line 3.

The amplitude of the voltage wave launched at $t = 0^+$ is

$$V_{1A}^+ = \frac{Z_{01} V_0}{R_s + Z_{01}} = \frac{(100)(4.5)}{50 + 100} = 3 \text{ V}$$

The resulting bounce diagrams for lines 1, 2, and 3, together with sketches for $V_s(t)$, $V_{L1}(t)$, and $V_{L2}(t)$ are shown in Figure 2.21.

2.17 Digital IC chips.

(a) The one-way time delay of each interconnect can be calculated as $t_d = l/v_p = (15 \text{ cm})/(10 \text{ cm} \cdot (\text{ns})^{-1}) = 1.5 \text{ ns}$. The reflection coefficients at the source and load ends of the interconnects are $\Gamma_s = 0$ and $\Gamma_{L1} = \Gamma_{L2} = 0$ respectively. When the incident voltage wave of amplitude

$$V_1^+ = \frac{50}{50 + 50}(1 \text{ V}) = 0.5 \text{ V}$$

(launched at the driver end of the 50Ω interconnect) reaches the junction between the three interconnects at $t = 1.5 \text{ ns}$, where no reflection occurs since $(100 \parallel 100) = 50\Omega$. As a result, a voltage wave of amplitude 0.5 V is launched on each of the 100Ω interconnects. At $t = 3 \text{ ns}$, these voltage waves reach the load ends where they are completely absorbed. The bounce diagram and the voltages V_{L1} and V_{L2} are sketched as shown.

(b) Since the load end of one of the 100Ω interconnects (point A) is now an open circuit (i.e., $\Gamma_{L2} = +1$), reflection occurs. The reflected voltage wave $V_1^- = 0.5 \text{ V}$ arrives the junction at $t = 4.5 \text{ ns}$ where another reflection occurs sending back a voltage wave $V_2^+ = \Gamma_j V_1^- = -0.25 \text{ V}$ toward point A where

$$\Gamma_j = \frac{(50 \parallel 100) - 100}{(50 \parallel 100) + 100} = -0.5$$

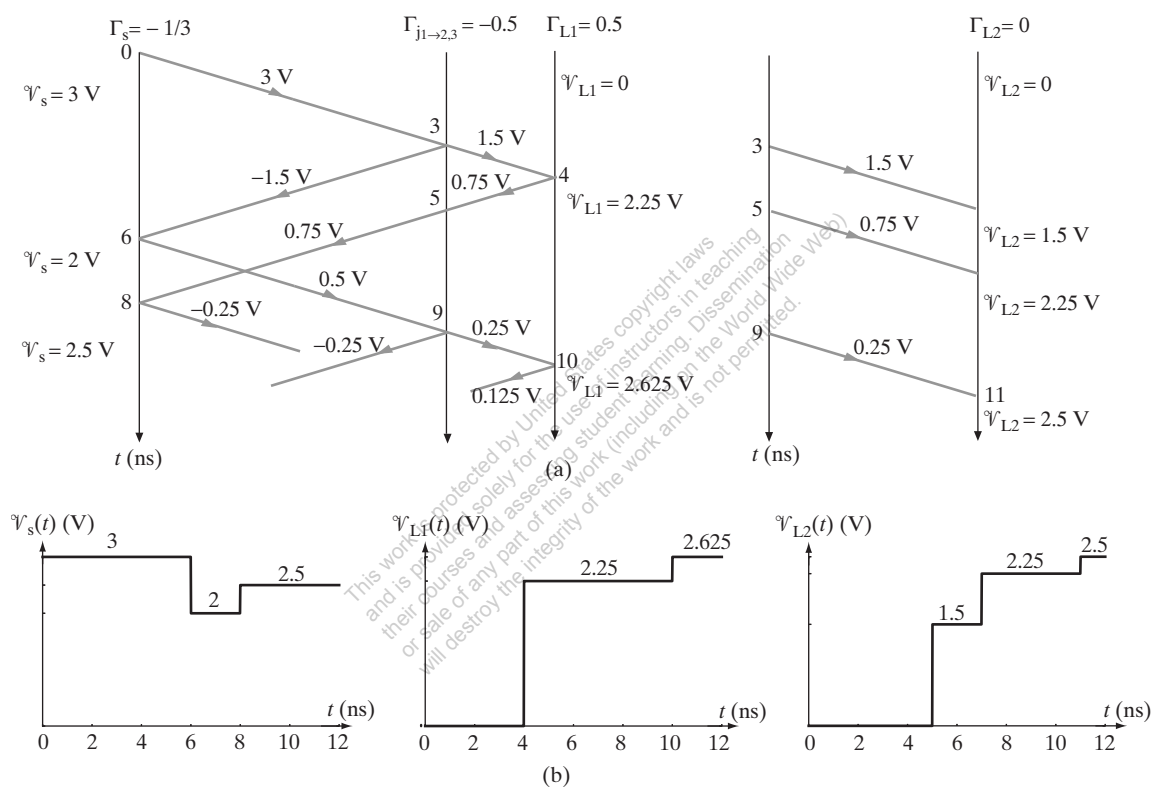


Figure 2.21 Figure for Problem 2.16. (a) Bounce diagram. (b) V_s , V_{L1} , and V_{L2} versus time t .

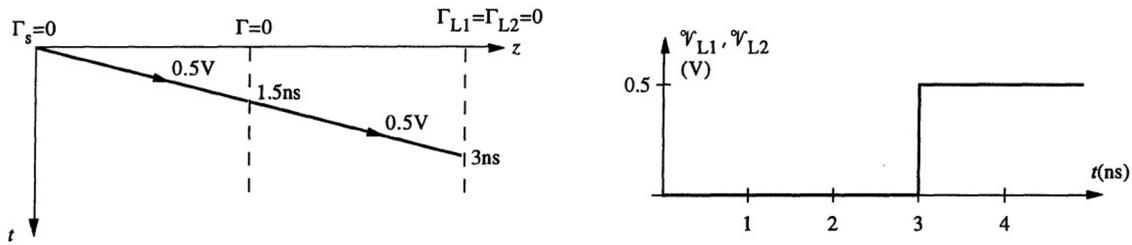


Figure 2.22 Figure for Problem 2.17a. Bounce diagram and V_{L1} , and V_{L2} versus t .

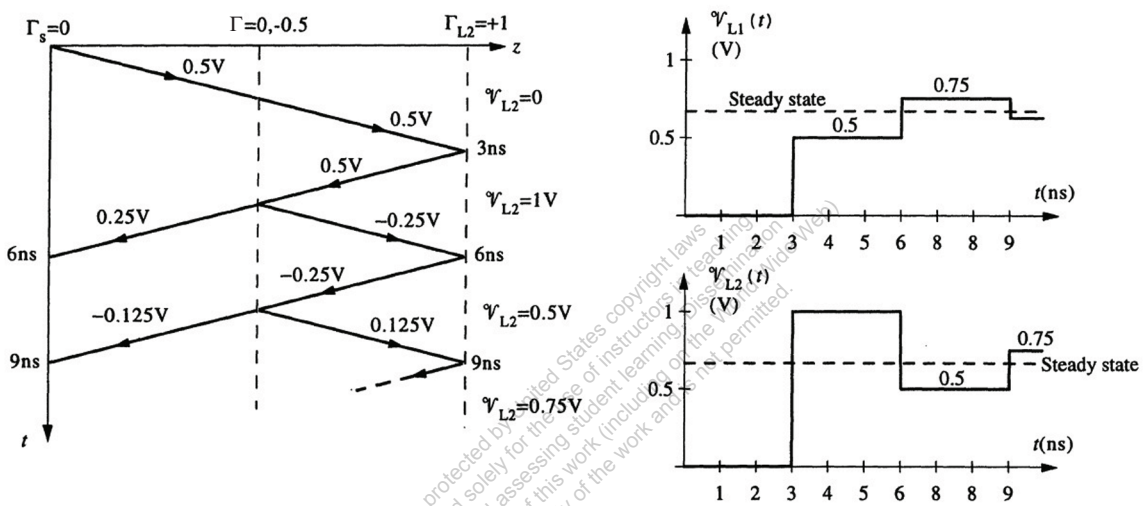


Figure 2.23 Figure for Problem 2.17b. Bounce diagram and V_{L1} , and V_{L2} versus t .

and launching a voltage of $V_1^- + V_2^+ = 0.5 - 0.25 = 0.25$ V on each of the other two lines. This process continues on. The bounce diagram and the variation of the voltages V_{L1} and V_{L2} are as shown. Note that at steady-state,

$$V_{L1} = V_{L2} = V_{ss} = \frac{100}{50 + 100}(1 \text{ V}) \simeq 0.667 \text{ V}$$

2.18 Multiple lines.

(a) A voltage disturbance of

$$V_1^+ = \frac{50}{50 + 50}(5 \text{ V}) = 2.5 \text{ V}$$

is launched on the line A-B at point A. This voltage wave reaches point B at $t = 1$ ns when $V_1^- = \Gamma_B V_1^+ = -2.5/3$ V reflects back to line A-B since

$$\Gamma_B = \frac{(50 \parallel 50) - 50}{(50 \parallel 50) + 50} = \frac{25 - 50}{25 + 50} = -\frac{1}{3}$$

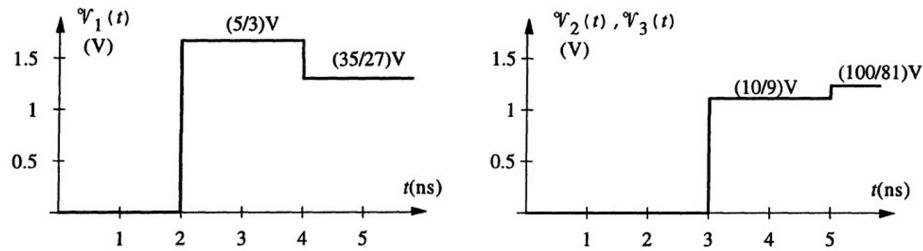


Figure 2.24 Figure for Problem 2.18a. V_1 , V_2 , and V_3 versus t .

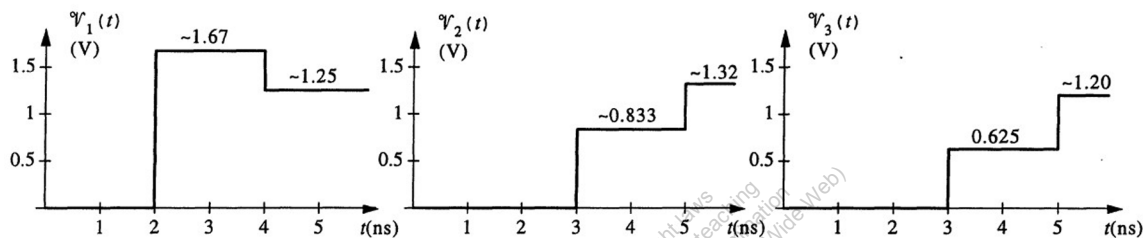


Figure 2.25 Figure for Problem 2.18b. V_1 , V_2 , and V_3 versus t .

and $V_2^+ = (1 + \Gamma_B)V_1^+ = +5/3$ V is transmitted to lines B-C and B-E respectively. At $t = 2$ ns, V_1^- reaches the source and is completely absorbed since $\Gamma_A = 0$. Also at $t = 2$ ns, V_2^+ reaches points C and E. At point E, V_2^+ is completely absorbed since $\Gamma_E = 0$. At point C, $V_2^- = \Gamma_C V_2^+ = -5/9$ V reflects back to line B-C and $V_3^+ = 5/3 - 5/9 = +10/9$ V is launched on lines C-D and C-F. At $t = 3$ ns, V_2^- reaches point B where $\Gamma_B V_2^- = +5/27$ V reflects back to line B-C and $(1 + \Gamma_B)V_2^- = -10/27$ V is launched to lines B-A and B-E. This process continues on until the reflections die out. The variation of the voltages V_1 , V_2 and V_3 are shown in Figure 2.24 up to 5 ns. Note that at steady-state, all of these voltages reach a final value of $V_{ss} = 1.25$ V.

(b) Now, since $Z_{01} = 25\Omega$, the value of the reflection coefficient at point B varies depending on from which line the voltage disturbance reaches point A. For example, when the signal reaches B from line A-B,

$$\Gamma_B = \frac{(50 \parallel Z_{01}) - 50}{(50 \parallel Z_{01}) + 50} = -0.5$$

whereas if the signal reaches B from line E-B, then

$$\Gamma_B = \frac{(50 \parallel 50) - 25}{(50 \parallel 50) + 25} = 0$$

Similar case applies at point C where we have $Z_{02} = 25\Omega$. The voltages V_1 , V_2 and V_3 are sketched up to 5 ns as shown in Figure 2.25. Again, at steady-state, all the voltages reach 1.25 V.

2.19 Reflections due to parasitic effects.

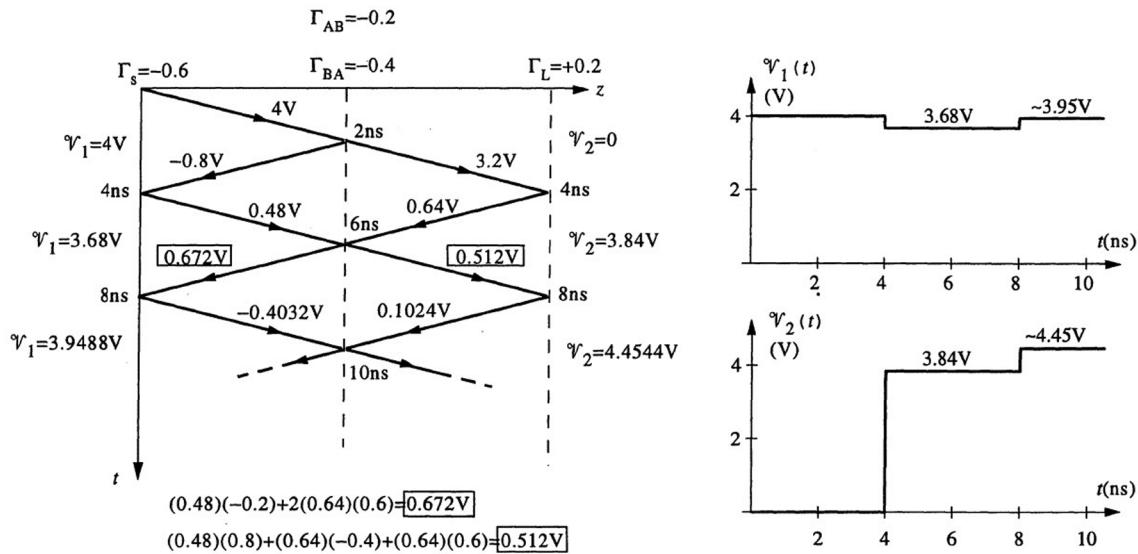


Figure 2.26 Figure for Problem 2.19. Bounce diagram and V_1 , and V_2 versus t .

The source and the load reflection coefficients are respectively given as

$$\Gamma_s = \frac{15 - 60}{15 + 60} = -0.6 \text{ and } \Gamma_L = \frac{120 - 80}{120 + 80} = +0.2$$

The value of the reflection coefficient at the junction point between the three interconnects varies depending on the line from which the voltage disturbance arrives at the junction. If a voltage signal reaches the junction from interconnect A, then

$$\Gamma_{A \rightarrow BC} = \frac{(Z_0 \parallel Z_0) - 60}{(Z_0 \parallel Z_0) + 60} = \frac{40 - 60}{40 + 60} = -0.2$$

whereas for a signal which reaches the junction from line B or C, we have

$$\Gamma_{B \rightarrow AC} = \Gamma_{C \rightarrow AB} = \frac{(Z_0 \parallel 60) - Z_0}{(Z_0 \parallel 60) + Z_0} = \frac{(80 \parallel 60) - 80}{(80 \parallel 60) + 80} = -0.4$$

Using these values, the bounce diagram and the voltages V_1 and V_2 are sketched as shown in Figure 2.26. Note that if $Z_0 = 120\Omega$ (i.e., no parasitic effects present), then no reflection occurs since $\Gamma_{A \rightarrow BC} = 0$ and both load reflection coefficients $\Gamma_L = 0$. Thus, the parasitic effects cause extra time delay before the voltages reach their steady-state values.

2.20 Parallel multiple lines.

(a) The reflection coefficients at the source end, load end and the junction between the three lines are respectively $\Gamma_s = 0$, $\Gamma_L = +1$, and

$$\Gamma_j = \frac{(50 \parallel 50) - 50}{(50 \parallel 50) + 50} = -\frac{1}{3}$$

The amplitude of the initial voltage wave launched from the source end is

$$\mathcal{V}_1^+ = \frac{50}{50 + 50}(3 \text{ V}) = 1.5 \text{ V}$$

The bounce diagram and the voltages $\mathcal{V}_s(t)$ and $\mathcal{V}_L(t)$ corresponding to these values are shown in Figure 2.27.

(b) When the load ends are terminated by $R_L = 50\Omega$ each, then $\Gamma_L = 0$. The bounce diagram and the voltages \mathcal{V}_s and \mathcal{V}_L for this case are shown in Figure 2.28.

2.21 Optimized multiple lines.

Using the line parameters $L = 364.5 \text{ nH}\cdot\text{m}^{-1}$ and $C = 125 \text{ pF}\cdot\text{m}^{-1}$, and using (2.7) and (2.9), the characteristic impedance and the phase velocity of each line can be found as

$$Z_0 = \sqrt{\frac{L}{C}} = \sqrt{\frac{364.5 \times 10^{-9}}{125 \times 10^{-12}}} = 54 \Omega$$

$$v_p = \frac{1}{\sqrt{LC}} = \frac{1}{\sqrt{(364.5 \times 10^{-9})(125 \times 10^{-12})}} \simeq 14.8 \text{ cm}\cdot(\text{ns})^{-1}$$

The one-way time delay of each line can be found as $t_d = l/v_p \simeq (40 \text{ cm})/(14.8 \text{ cm}\cdot(\text{ns})^{-1}) \simeq 2.7 \text{ ns}$. The reflection coefficients at the source- and the load-ends of the lines and at the junction point where the lines meet are

$$\Gamma_s = \frac{R_s - Z_0}{R_s + Z_0} = \frac{6 - 54}{6 + 54} = -0.8$$

$$\Gamma_L = \frac{R_L - Z_0}{R_L + Z_0} = \frac{66 - 54}{66 + 54} = +0.1$$

$$\Gamma_j = \frac{(Z_0 \parallel Z_0) - Z_0}{(Z_0 \parallel Z_0) + Z_0} = \frac{27 - 54}{27 + 54} = -\frac{1}{3}$$

respectively. The initial voltage launched at the source end of the line is

$$\mathcal{V}_1^+ = \frac{Z_0}{R_s + Z_0} V_0 = \frac{54}{6 + 54}(5 \text{ V}) = 4.5 \text{ V}$$

using these values, the bounce diagram and the voltages \mathcal{V}_s and \mathcal{V}_L are sketched as shown in Figure 2.29. As seen from the bounce diagram, at $t = 3t_d^+ \simeq 8.1^+ \text{ ns}$, the voltage $\mathcal{V}_{A2}^- = \Gamma_j \mathcal{V}_{A2}^+ = (-1/3)(1.2 \text{ V}) = -0.4 \text{ V}$ reflected from the junction back onto line A propagating toward the source cancel completely with the two voltage disturbances transmitted to line A from lines B and C, each having an amplitude given by $\mathcal{V}_{A2}^{+*} = (1 + \Gamma_j)\mathcal{V}_{B1}^- = (2/3)(0.3 \text{ V}) = 0.2 \text{ V}$ (where \mathcal{V}_{B1}^- is a voltage disturbance reflected back to line B from the load R_L). As a result, no reflections from the source end occurs for the time interval $5.4 \text{ ns} \leq t \leq 16.2 \text{ ns}$. This cancellation plays a significant role in minimizing the effects of reflections due to impedance mismatches in the circuit, and is the basis in which the configuration in hand is considered to be 'optimized'.

2.22 Transient response of a cascaded transmission-line circuit.

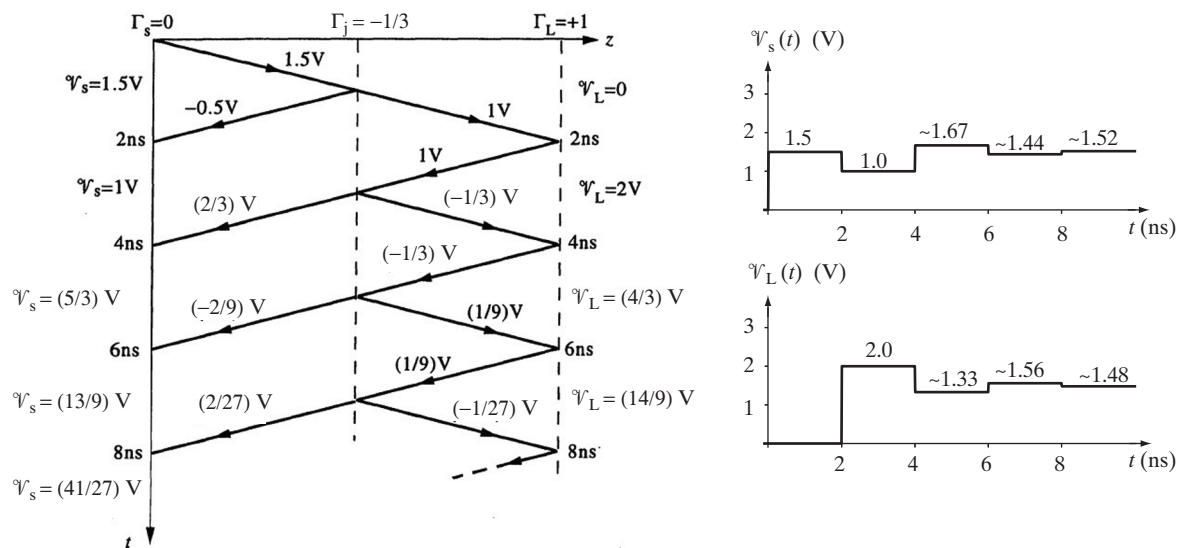


Figure 2.27 Figure for Problem 2.20a. Bounce diagram and V_s , and V_L versus t .

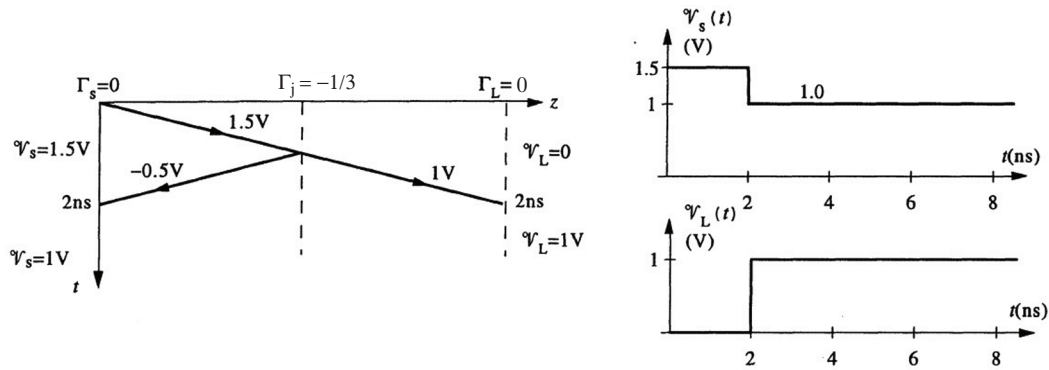


Figure 2.28 Figure for Problem 2.20b. Bounce diagram and V_s , and V_L versus t .

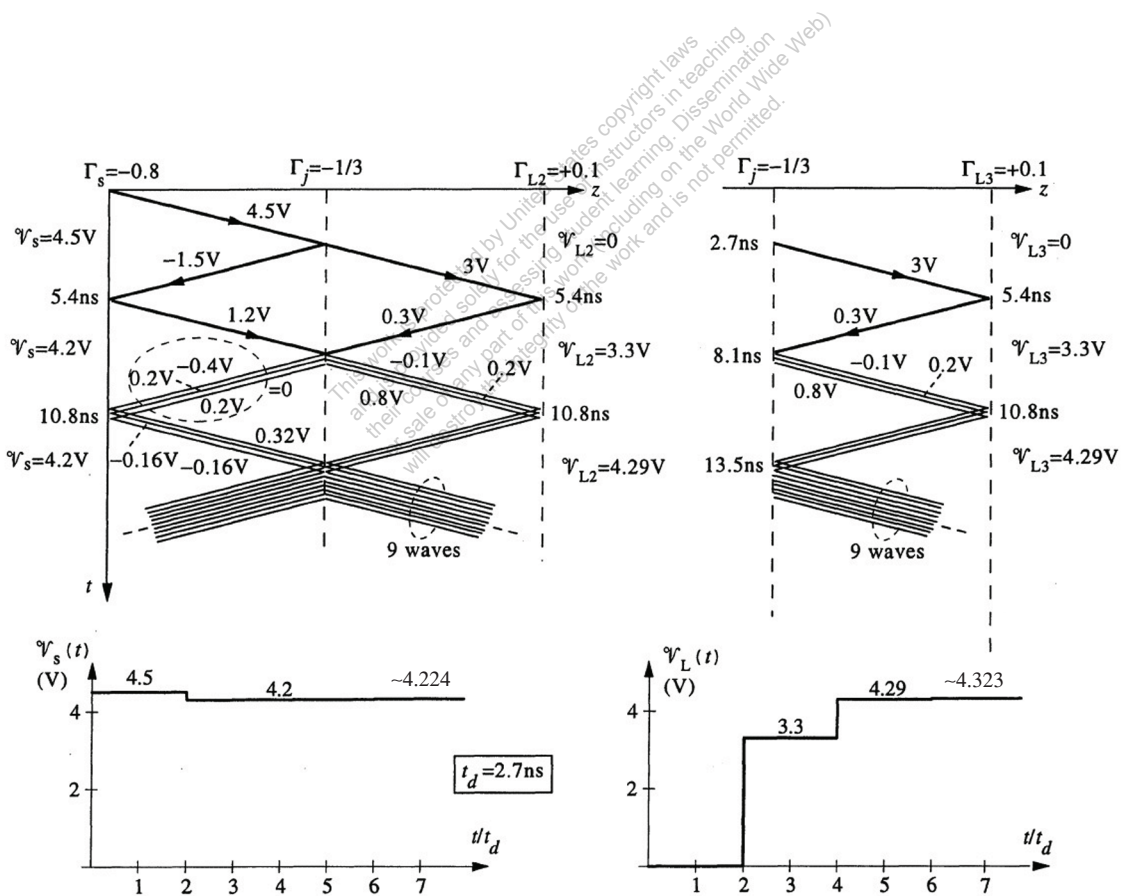


Figure 2.29 Figure for Problem 2.21. Bounce diagram and V_s , and V_L versus t .

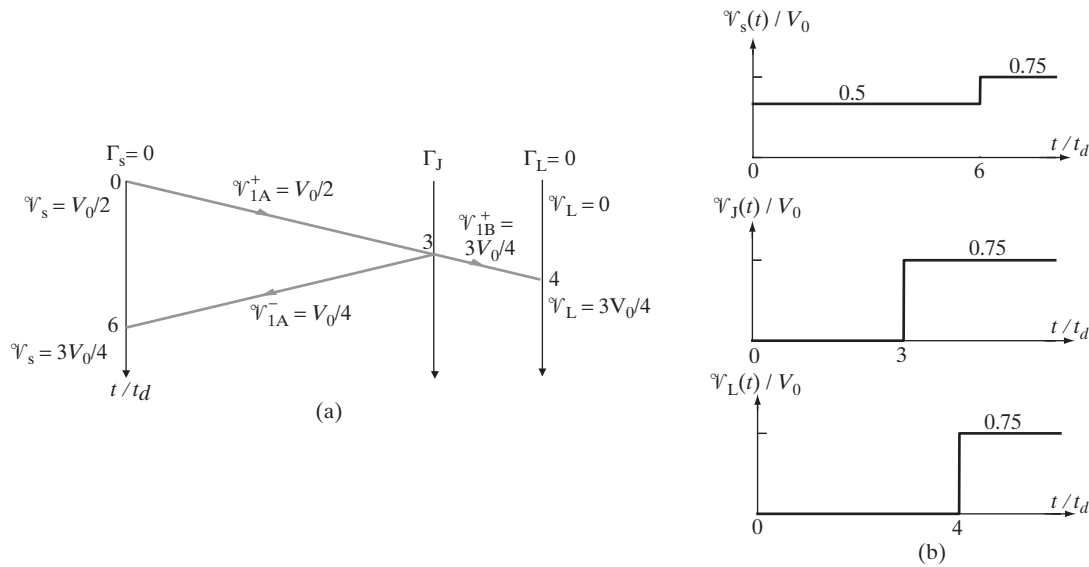


Figure 2.30 Figure for Problem 2.22a. (a) Bounce diagram (b) V_s , V_J , and V_L versus t .

(a) We begin by calculating the source, load, and junction reflection coefficients:

$$\begin{aligned}\Gamma_s &= \frac{R_s - Z_{01}}{R_s + Z_{01}} = \frac{Z_0 - Z_0}{Z_0 + Z_0} = 0 \\ \Gamma_L &= \frac{R_L - Z_{02}}{R_L + Z_{02}} = \frac{3Z_0 - 3Z_0}{3Z_0 + 3Z_0} = 0 \\ \Gamma_{J_{A \rightarrow B}} &= \frac{Z_{02} - Z_{01}}{Z_{02} + Z_{01}} = \frac{3Z_0 - Z_0}{3Z_0 + Z_0} = \frac{1}{2} \\ \Gamma_{J_{B \rightarrow A}} &= \frac{Z_{01} - Z_{02}}{Z_{01} + Z_{02}} = -\frac{1}{2}\end{aligned}$$

The amplitudes of the voltage waves in the bounce diagram shown in Figure 2.30 can be calculated as

$$\begin{aligned}V_{1A}^+ &= \frac{Z_{01} V_0}{R_s + Z_{01}} = \frac{Z_0 V_0}{Z_0 + Z_0} = \frac{V_0}{2} \\ V_{1A}^- &= \Gamma_{J_{A \rightarrow B}} V_{1A}^+ = \frac{V_0}{4} \\ V_{1B}^+ &= V_{1A}^+ + V_{1A}^- = \frac{3V_0}{4}\end{aligned}$$

The voltage plots are also shown in Figure 2.30.

(b) In this case,

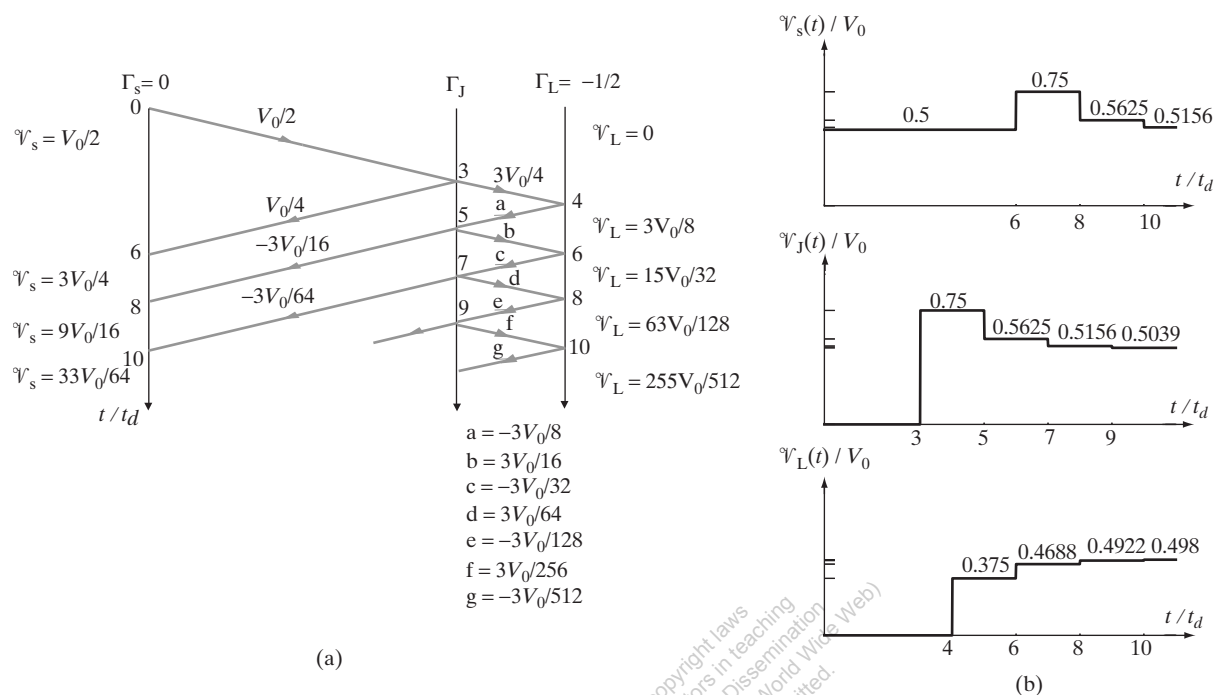


Figure 2.31 Figure for Problem 2.22b. (a) Bounce diagram (b) V_s , V_J , and V_L versus t .

$$\Gamma_s = 0$$

$$\Gamma_L = \frac{Z_0 - 3Z_0}{Z_0 + 3Z_0} = -\frac{1}{2}$$

from which we can generate the bounce diagram and voltage plots in Figure 2.31.

(c) In this case,

$$\Gamma_s = \frac{Z_0/3 - Z_0}{Z_0/3 + Z_0} = -\frac{1}{2}$$

$$\Gamma_L = 0$$

Note also that

$$V_{1A}^+ = \frac{Z_0 V_0}{Z_0/3 + Z_0} = \frac{3V_0}{4}$$

Using a similar approach, we can generate the bounce diagram and the voltage plots shown in Figure 2.32.

2.23 Charging and discharging of a line.

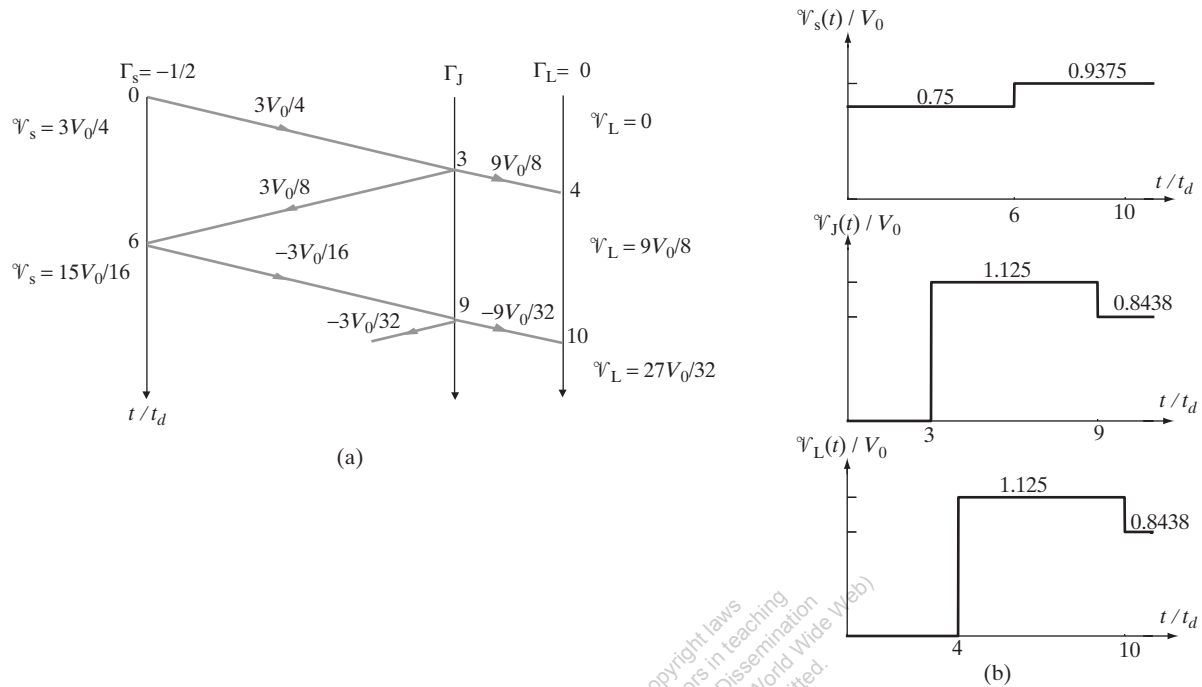


Figure 2.32 Figure for Problem 2.22c. (a) Bounce diagram (b) V_s , V_J , and V_L versus t .

At $t = 0^+$ (i.e., immediately after switch S_1 closes), an incident voltage wave of amplitude

$$V_1^+ = \frac{60}{15 + 60} (1 \text{ V}) = 0.8 \text{ V}$$

is launched at the source end of the line. This voltage wave reaches the load end at $t = 2t_d$ when it is completely absorbed since $\Gamma_L = 0$. However, at $t = 2t_d$, the switch S_2 closes and causes a discontinuity at the junction between the two lines. As a result, a voltage wave of amplitude

$$V_1^- = \Gamma_J V_1^+ = \frac{(60 \parallel 60) - 60}{(60 \parallel 60) + 60} (0.8 \text{ V}) = \left(-\frac{1}{3}\right) (0.8 \text{ V}) = -\frac{0.8}{3} \text{ V}$$

reflects back toward the source and a voltage wave of amplitude

$$V_1^{+*} = (1 + \Gamma_J) V_1^+ = \left(\frac{2}{3}\right) (0.8 \text{ V}) = +\frac{1.6}{3} \text{ V}$$

is transmitted to the line connected to the load. Note that on the bounce diagram, this wave appears to be $-0.8/3 \text{ V}$ since the existing transmitted wave of 0.8 V right before switch S_2 is closed and $-0.8/3 \text{ V}$ add up to $V_1^{+*} = 1.6/3 \text{ V}$. When the reflected voltage wave reaches the source end at $t = 3t_d$, a voltage wave of amplitude

$$V_2^+ = \Gamma_s V_1^- = \frac{15 - 60}{15 + 60} \left(-\frac{0.8}{3} \text{ V}\right) = (-0.6) \left(-\frac{0.8}{3} \text{ V}\right) = +0.16 \text{ V}$$

reflects back to the line. This voltage wave reaches the junction at $t = 4t_d$, when a voltage wave of amplitude

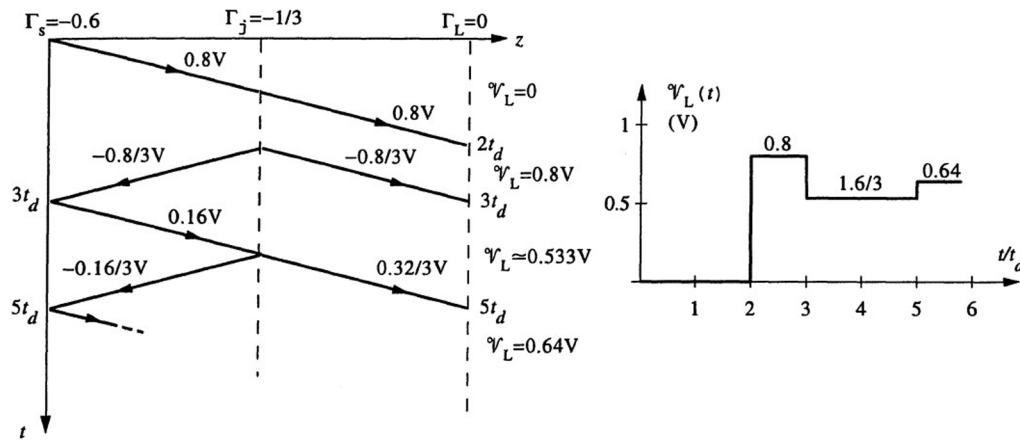


Figure 2.33 Figure for Problem 2.23. Bounce diagram and V_L versus t .

$$V_2^- = \Gamma_j V_2^+ = \left(-\frac{1}{3}\right)(+0.16 \text{ V}) = -\frac{0.16}{3} \text{ V}$$

reflects back toward the source and a voltage wave of amplitude

$$V_2^{+*} = (1 + \Gamma_j)V_2^+ = \left(\frac{2}{3}\right)(+0.16 \text{ V}) = +\frac{0.32}{3} \text{ V}$$

is transmitted to the line connected to the load. This process continues on. The bounce diagram and the variation of the load voltage $V_L(t)$ are as shown in Figure 2.33.

2.24 A digital IC interconnect.

(a) At $t = 0$, the driver gate changes from LOW to HIGH state launching a voltage disturbance of amplitude

$$V_1^+ = \frac{50}{14 + 50}(5 \text{ V}) \simeq 3.91 \text{ V}$$

at the driver end of the interconnect traveling toward the load. When this voltage arrives the load end of the interconnect at $t = t_d = 1.5 \text{ ns}$, a reflected voltage wave of amplitude $V_1^- = \Gamma_L V_1^+ \simeq (+1)(3.91 \text{ V}) = 3.91 \text{ V}$ is launched back on the interconnect traveling toward the driver gate. So, at $t = 1.5 \text{ ns}$, the load-end voltage of the interconnect changes from $V_L = 0$ to $V_L \simeq 7.81 \text{ V} > 3.75 \text{ V}$ and as a result of this change, the load gate turns ON.

(b) When the reflected voltage wave arrives the driver-gate end of the interconnect at $t = 2t_d = 3 \text{ ns}$, a new voltage wave of amplitude

$$V_2^+ = \Gamma_s V_1^- \simeq \frac{14 - 50}{14 + 50}(3.91 \text{ V}) \simeq (-0.563)(3.91 \text{ V}) \simeq -2.20 \text{ V}$$

is launched on the interconnect traveling toward the load gate. This voltage arrives at the load gate at $t = 4.5 \text{ ns}$ when a new voltage wave of amplitude $V_2^- = V_2^+ \simeq -2.20 \text{ V}$ is launched

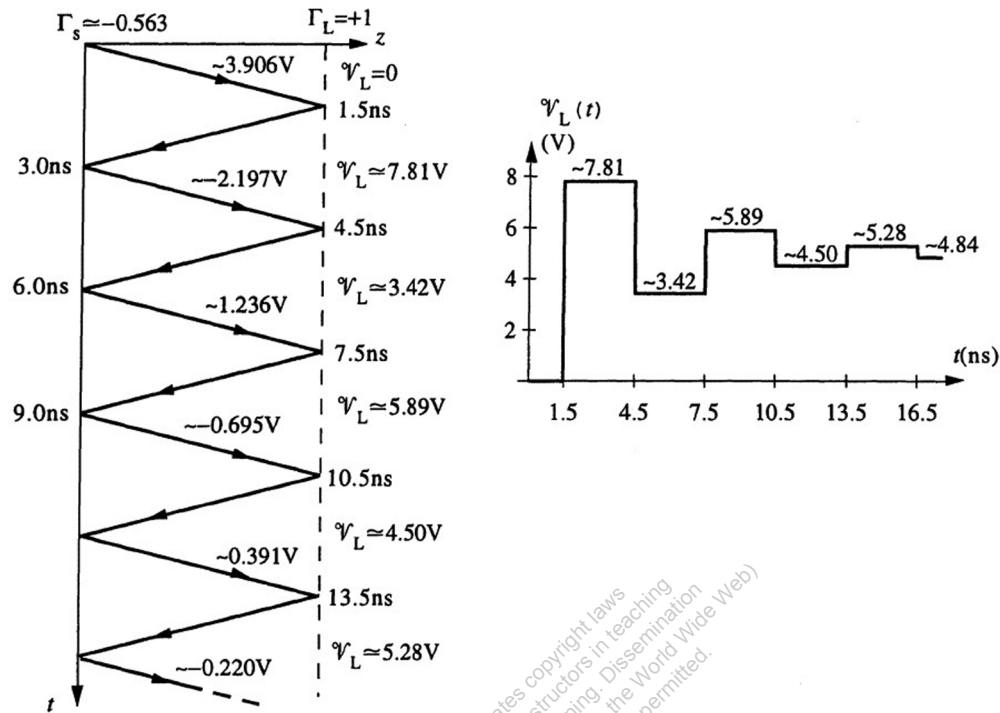


Figure 2.34 Figure for Problem 2.24. Bounce diagram and V_L versus t .

on the interconnect traveling toward the driver gate. As a result, the load-end voltage drops at $t = 3t_d = 4.5$ ns from $V_L \approx 7.81$ V to $V_L \approx 3.42$ V < 3.75 V and so the load gate turns OFF. This process continues on. As seen from the bounce diagram and the sketch of the load-end voltage V_L versus t , the load gate turns on permanently (i.e., $V_L > 3.75$ V afterwards) at $t = 5t_d = 7.5$ ns.

2.25 Terminated IC interconnects.

(a) In the series termination network, $R_T = Z_0 - R_s = 50 - 14 = 36\Omega$ so that $\Gamma_s = 0$. In the parallel termination network, $R_T = Z_0 = 50\Omega$ so that $\Gamma_L = 0$. In both circuits, the load gate at the end of the interconnect reaches steady state at $t = t_d = 1.5$ ns.

However, the steady-state voltages are different from one another. In the series termination network, the steady-state load-end voltage at HIGH state is $V_{ss} = V_{HIGH} = 5$ V whereas in the parallel termination network, it is

$$V_{ss} = \frac{R_T}{R_s + R_T} V_{HIGH} = \frac{50}{14 + 50} (5 \text{ V}) \approx 3.91 \text{ V}$$

This difference makes the parallel termination network more vulnerable to noise at HIGH state. Series termination network is the natural choice for low-power dissipation at steady-state since the steady-state current $I_{ss} = 0$ and as a result, no power is dissipated at steady state. In the parallel termination network however, a steady-state current flows through the circuit at HIGH state given by

$$I_{ss} = \frac{V_{HIGH}}{R_s + R_T} = \frac{5 \text{ V}}{14\Omega + 50\Omega} \simeq 78.1 \text{ mA}$$

resulting in a steady-state power dissipation of $P = I_{ss}^2(R_s + R_T) \simeq 0.39 \text{ W}$.

2.26 Digital IC gate interconnects.

Using $v_p \simeq 14.3 \text{ cm-(ns)}^{-1}$, the one-way time delay over 1 ft of the interconnect is

$$t_d \simeq (1 \text{ ft})(12 \text{ in-(ft)}^{-1})(2.54 \text{ cm-in}^{-1})/(14.3 \text{ cm-(ns)}^{-1}) \simeq 2.13 \text{ ns}$$

Thus, using this time delay and noting that no reflections occur at points A and B (since the load gates connected at these points present a very high impedance to the interconnect), in the series termination network, gate C switches to HIGH state at $t = 3t_d \simeq 6.39 \text{ ns}$ when the voltage \mathcal{V}_C changes from 0 to 5 V, gate B switches at $t = 4t_d \simeq 8.53 \text{ ns}$ after the voltage wave reflected from point C arrives at point B changing \mathcal{V}_B from 2.5 V to 5 V, and gate A switches at $t = 5t_d \simeq 10.7 \text{ ns}$ after the reflected voltage wave arrives at point A changing \mathcal{V}_A from 2.5 V to 5 V. In the parallel termination network, no reflections occur. Gate A switches to HIGH state at $t = 3t_d \simeq 2.13 \text{ ns}$ when \mathcal{V}_A changes from 0 to $\sim 3.91 \text{ V}$, gate B switches at $t = 2t_d \simeq 4.26 \text{ ns}$ when \mathcal{V}_B changes from 0 to $\sim 3.91 \text{ V}$, and gate C switches at $t = 3t_d \simeq 6.39 \text{ ns}$ when \mathcal{V}_C changes from 0 to $\sim 3.91 \text{ V}$. Therefore, the parallel termination network provides a faster overall speed because all of the three load gates reach steady state earlier.

2.27 Digital IC circuit.

At $t = 0$, an incident voltage wave of amplitude

$$\mathcal{V}_I = \frac{50}{50 + 50}(5 \text{ V}) = 2.5 \text{ V}$$

is launched at the driver-gate end of the line. This voltage wave arrives the junction of the three lines at $t = (2 \text{ ft})(2 \text{ ns-ft}^{-1}) = 4 \text{ ns}$ when it is completely absorbed since the junction reflection coefficient in this case is given by

$$\Gamma_{1 \rightarrow 23} = \frac{(100 \parallel 100) - 50}{(100 \parallel 100) + 50} = 0$$

The two voltage waves transmitted on lines 2 and 3 each with 2.5 V peak value arrive at the load gates at different times (one at $t = 6 \text{ ns}$ and the other at $t = 7 \text{ ns}$) where reflections occur. The load reflection coefficient at each load is given by $\Gamma_L = +1$ since $Z_{in} \gg Z_0$. When the reflected voltages arrive back at the junction joining the three lines, both reflections and transmissions occur since

$$\Gamma_{2 \rightarrow 13} = \Gamma_{3 \rightarrow 12} = \frac{(100 \parallel 50) - 100}{(100 \parallel 50) + 100} = -0.5$$

This process continues on. Using the above values, the bounce diagram and the variation of the voltage \mathcal{V}_1 and \mathcal{V}_2 versus t are as shown in Figure 2.35. According to these figures, gate 1 turns ON permanently at $t = 22 \text{ ns}$ and gate 2 turns ON permanently at $t = 19 \text{ ns}$.

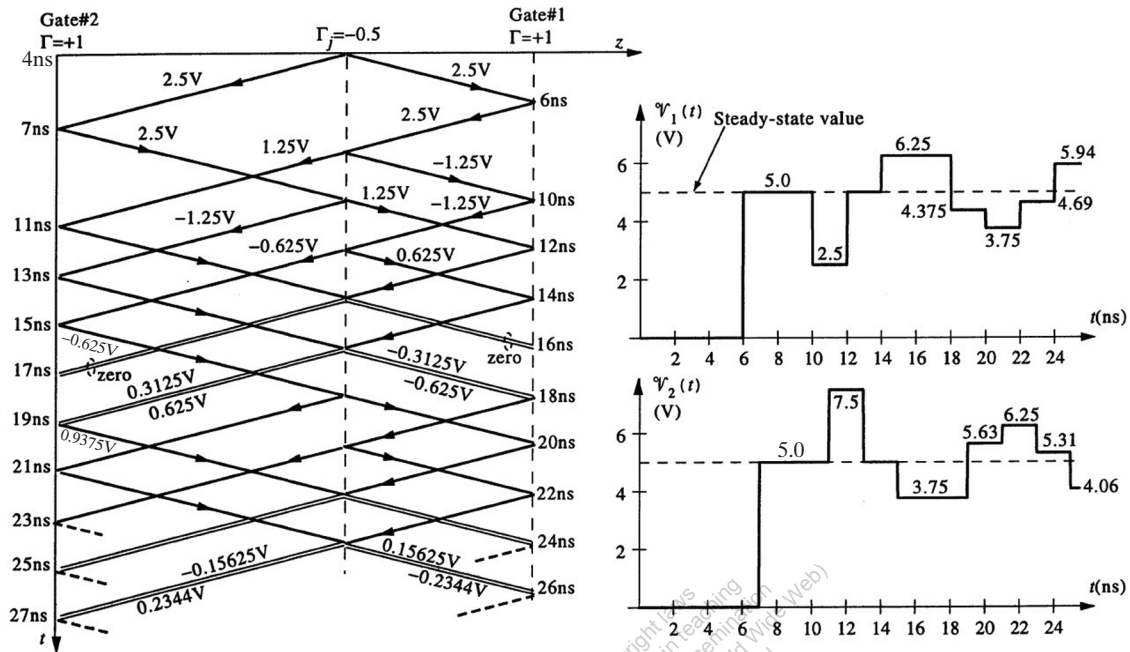


Figure 2.35 Figure for Problem 2.27. Bounce diagram, V_1 versus t and V_2 versus t .

2.28 Two driver gates.

(a) Let the two interconnects connected to each driver gate be driver interconnects D1 and D2 and the third one connected to the load gate be the load interconnect. At $t = 0$, an incident voltage wave of amplitude

$$V_1^+ = \frac{Z_0}{R_s + Z_0} V_0 = \frac{Z_0}{Z_0 + Z_0} V_0 = \frac{V_0}{2}$$

is launched at the driver end of each driver interconnect. When these voltage waves arrive the junction between the three interconnects at $t = t_d$, reflections and transmissions occur. The voltage wave reflected back to each of the driver interconnects is given by

$$V_{1r}^- = \Gamma_j V_1^+ = \frac{(Z_0 \parallel Z_0) - Z_0}{(Z_0 \parallel Z_0) + Z_0} \left(\frac{V_0}{2} \right) = \left(-\frac{1}{3} \right) \left(\frac{V_0}{2} \right) = -\frac{V_0}{6}$$

and the voltage wave transmitted to each driver interconnect follows as

$$V_{1t}^+ = (1 + \Gamma_j) V_1^+ = \left(\frac{2}{3} \right) \left(\frac{V_0}{2} \right) = \frac{V_0}{3}$$

Thus, the total voltage wave launched from the junction onto each driver interconnect at $t = t_d$ is

$$V_1^- = V_{1r}^- + V_{1t}^+ = \Gamma_j V_1^+ + (1 + \Gamma_j) V_1^+ = -\frac{V_0}{6} + \frac{V_0}{3} = \frac{V_0}{6}$$

In addition, the total voltage wave launched onto the load interconnect at $t = t_d$ is given by

$$\mathcal{V}_{lt}^{+*} = 2(\mathcal{V}_1^+ + \mathcal{V}_{lr}^-) = 2\mathcal{V}_{lt}^+ = \frac{2V_0}{3}$$

When the voltage wave \mathcal{V}_1^- arrives at the driver end of one of the driver interconnects at $t = 2t_d$, it is completely absorbed since $\Gamma_s = 0$. However, when the voltage wave \mathcal{V}_{lt}^{+*} arrives the load gate at $t = 2t_d$, it completely reflects back since $\Gamma_L \simeq +1$ (since $Z_{in} \gg Z_0$). The voltage wave reflected from the load gate reaches the junction at $t = 3t_d$ where again, reflection and transmission occurs. This process continues on. The bounce diagram and the sketch of the load-end voltage \mathcal{V}_L versus t are as shown in Figure 2.36. At steady state, the value of the load-end voltage is $\mathcal{V}_L(t = \infty) = V_0$.

(b) Before $t = 0$ (when driver gate 1 is at HIGH state and driver gate 2 is at LOW state), steady state applies and the load-end voltage is $\mathcal{V}_L(t = 0) = V_0/2$. When driver gate 1 changes to LOW state at $t = 0$, a voltage wave of amplitude

$$\mathcal{V}_{D1,1}^+ = -\frac{V_0}{2}$$

is launched at the driver end of the driver interconnect D1. At the same time, when driver gate 2 switches to HIGH state, a voltage wave of amplitude

$$\mathcal{V}_{D2,1}^+ = \frac{V_0}{2}$$

is launched at the driver end of the driver interconnect D2. These two voltages arrive the junction at $t = t_d$ when the total voltage which is transmitted onto the load interconnect can be found as

$$\mathcal{V}_{lt}^{+*} = (1 + \Gamma_j) \underbrace{(\mathcal{V}_{D1,1}^+ + \mathcal{V}_{D2,1}^+)}_{=0} = 0$$

Therefore, in this case, as shown in Figure 2.36b, the load voltage \mathcal{V}_L is not affected by the changes in the states of the two driver gates and stays equal to $\mathcal{V}_L = V_0/2$ for $t > 0$.

2.29 Capacitive load.

At $t = 0$, an incident voltage wave of amplitude

$$\mathcal{V}_1^+ = \frac{100}{100 + 100}(5 \text{ V}) = 2.5 \text{ V}$$

is launched at the source end of the 100Ω line. This voltage wave reaches the resistance $R_1 = 100\Omega$ at $t = t_d = 2 \text{ ns}$. The reflection coefficient at this junction for a voltage wave arriving from the 100Ω onto the 50Ω line is

$$\Gamma_{1 \rightarrow 2} = \frac{(R_1 \parallel 50) - 100}{(R_1 \parallel 50) + 100} = -0.5$$

Therefore, a voltage wave of $\mathcal{V}_1^- = \Gamma_{1 \rightarrow 2}\mathcal{V}_1^+ = (-0.5)(2.5 \text{ V}) = -1.25 \text{ V}$ reflects back to the 100Ω line and $\mathcal{V}_1^{+*} = \mathcal{V}_1^+ + \mathcal{V}_1^- = 1.25 \text{ V}$ is transmitted onto the 50Ω line. Hence, $\mathcal{V}_1(t) = \mathcal{V}_1^{+*}$, or using step function notation, $\mathcal{V}_1(t) = 1.25u(t - 2 \text{ ns}) \text{ V}$ until a new voltage wave disturbance arrives this position. The reflected voltage wave \mathcal{V}_1^- reaches the source end at $t = 2t_d = 4 \text{ ns}$ and is completely absorbed since $\Gamma_s = 0$. The transmitted voltage wave reaches the 5 pF capacitor at

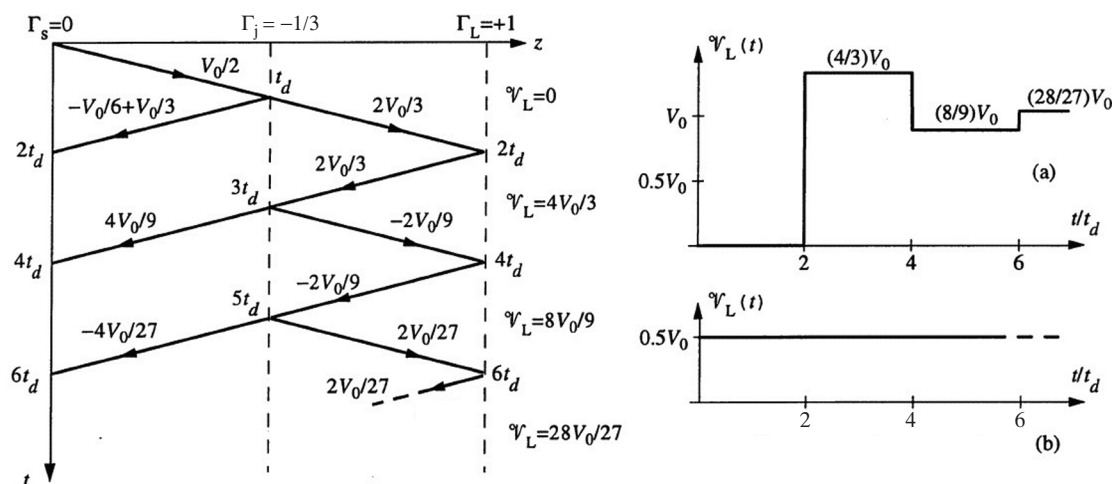


Figure 2.36 Figure for Problem 2.28. (a) Bounce diagram and V_L versus t . (b) V_L versus t .

$t = 2t_d = 4$ ns. Since this is a first-order circuit, the voltage wave reflected from the capacitor is of the form

$$V_1^{-*}(t) = u(t - 4 \text{ ns})[K_1 + K_2 e^{-(t-4 \text{ ns})/\tau}]$$

where τ is the time constant of the circuit given by $\tau = (50\Omega)(5 \text{ pF}) = 0.25$ ns and $2t_d = 4$ ns is the total transmission line delay for the step voltage wave to travel from the source to the 5 pF capacitor. Initially the capacitor is uncharged and appears like a short circuit, i.e., the capacitor voltage at $t = 4$ ns is $V_c(t = 4 \text{ ns}) = V_1^{+*} + V_1^{-*}(t = 4 \text{ ns}) = 0$ from which $V_1^{-*}(t = 4 \text{ ns}) = -V_1^{+*} = -1.25$ V, therefore $K_1 + K_2 = -1.25$ V. At $t = \infty$, $V_1^{-*}(\infty) = K_1 = V_1^{+*} = +1.25$ V since the capacitor is fully charged and appears as an open circuit. Thus, $K_1 = 1.25$ V. Hence $K_2 = -2.5$ V and so the reflected voltage wave at the capacitor load position is given by

$$V_1^{-*}(t) = 1.25u(t - 4 \text{ ns})[1 - 2e^{-(t-4 \text{ ns})/(0.25 \text{ ns})}] \text{ V}$$

This voltage wave reaches R_1 at $t = 6$ ns where no reflection back to the 50Ω line occurs since the reflection coefficient for a voltage arriving from the 50Ω line onto the 100Ω line is

$$\Gamma_{2 \rightarrow 1} = \frac{(100 \parallel 100) - 50}{(100 \parallel 100) + 50} = 0$$

Therefore, the voltage $V_1^{-*}(t)$ continues to travel on the 100Ω line towards the source. Hence, the voltage $V_1(t)$ across the R_1 resistor is now given by $V_1(t) = V_1^{+*}u(t - 2 \text{ ns}) + V_1^{-*}(t - 2 \text{ ns})$ which can also be written as

$$V_1(t) = 1.25u(t - 2 \text{ ns}) + 1.25u(t - 6 \text{ ns})[1 - 2e^{-(t-6 \text{ ns})/(0.25 \text{ ns})}] \text{ V}$$

When $V_1^{-*}(t)$ arrives the source end, it is completely absorbed since $\Gamma_s = 0$. The sketch of $V_1(t)$ versus t is as shown in Figure 2.37.

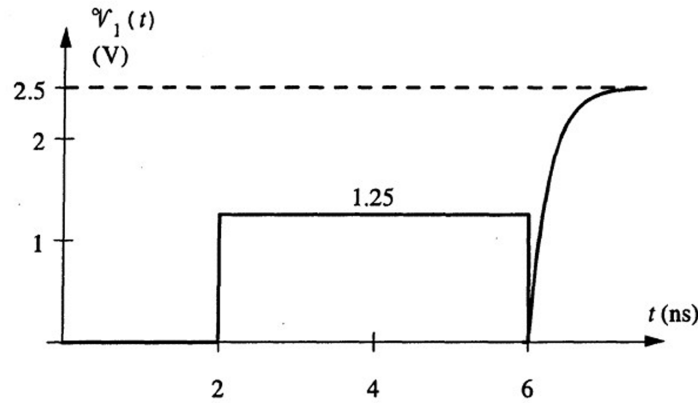


Figure 2.37 Figure for Problem 2.29. V_1 versus t .

2.30 Unknown lumped element.

Reading from the TDR waveform, the amplitude of the initial voltage wave launched on the Z_{01} transmission line is

$$\begin{aligned} V_{1A}^+ &= \frac{Z_{01}V_0}{R_s + Z_{01}} \\ &= \frac{Z_{01}(3)}{50 + Z_{01}} \\ &= 1.5 \text{ V} \end{aligned}$$

from which we can solve for Z_{01} as

$$Z_{01} = 50\Omega$$

We can also infer from the TDR waveform that $2t_{d1} = 6$ ns, so $t_{d1} = 3$ ns.

Since the source-end voltage drops to 0 at $t = 6$ ns, the initial value of the reflected voltage wave is given by

$$V_{1A}^-(t = t_{d1}) = \Gamma_{jA \rightarrow B}(t = t_{d1})V_{1A}^+ = -V_{1A}^+$$

which means that we must have

$$\Gamma_{jA \rightarrow B}(t = t_{d1}) = -1$$

where we define $\Gamma_{jA \rightarrow B}$ to be the reflection coefficient at the junction with respect to a voltage wave approaching the junction from the direction of the Z_{01} transmission line. Hence the unknown lumped element must be a capacitor, which acts like a short circuit at $t = t_{d1}$ (to maintain its zero voltage initially) and results in $V_{1A}^-(t = t_{d1}) = -V_{1A}^+$.

To find the time constant given by $\tau = R_T C$, we need to determine the Thevenin resistor R_T seen between the terminals of the capacitor:

$$R_T = Z_{01} \parallel Z_{02} = \frac{Z_{01}Z_{02}}{Z_{01} + Z_{02}}$$

Noting from the TDR waveform that $\tau = 2 \text{ ns}$, the time constant is given by

$$2 \text{ ns} = \tau = \frac{Z_{01}Z_{02}}{Z_{01} + Z_{02}} C = \frac{(50)Z_{02}}{50 + Z_{02}} C$$

Also, based on the TDR waveform, as $t \rightarrow \infty$ (when the circuit reaches steady state), the capacitor acts like an open circuit. As a result, we have

$$\begin{aligned} \mathcal{V}_{1A}^-(t \rightarrow \infty) &= \underbrace{\frac{Z_{02} - Z_{01}}{Z_{02} + Z_{01}}}_{\Gamma_{JA \rightarrow B}(t \rightarrow \infty)} \mathcal{V}_{1A}^+ \\ &= \frac{Z_{02} - 50}{Z_{02} + 50} (1.5) \\ &= 2.4 - 1.5 \end{aligned}$$

where we used the $\mathcal{V}_s(t = 0^+)$ and $\mathcal{V}_s(t \rightarrow \infty)$ values from the TDR waveform. Solving for Z_{02} , we get

$$Z_{02} = 200 \Omega$$

Substituting Z_{02} into the time constant equation above, we have

$$\frac{(50)(200)}{50 + 200} C = 2 \text{ ns} \rightarrow C = 0.05 \text{ nF} = 50 \text{ pF}$$

2.31 Unknown lumped element.

The unknown lumped element is a capacitor, because at first it presents itself to the incident voltage wave as a short circuit (since it is initially uncharged) and as a result, the initial value of the reflected voltage is $\mathcal{V}_1^-(t = d_1) = -\mathcal{V}_1^+ = -V_0/2$ and so when the front of the reflected voltage arrives the source end of the line at $t = 2t_{d1}$, the value of the source-end voltage reduces to $\mathcal{V}_s(t = 2t_{d1}) = V_0/2 - V_0/2 = 0$. At steady state (when the capacitor behaves like an open circuit), no reflection occurs since both lines have the same characteristic impedance and the second line is terminated with Z_0 , and so $\mathcal{V}_s(\infty) = \mathcal{V}_1^+ = V_0/2$ as seen in Figure 2.61 of the text. To relate the value of the capacitor to the shaded area, we shift the $\mathcal{V}_s(t)$ curve down by $V_0/2$ and integrate it. This yields

$$A = - \int_{2t_{d1}}^{\infty} \left(\mathcal{V}_s(t) - \frac{V_0}{2} \right) dt = \int_{2t_{d1}}^{\infty} \frac{V_0}{2} e^{-(t-2t_{d1})/\tau} dt$$

where $\tau = (Z_0 \parallel Z_0)C = Z_0C/2$. Substituting $t' = t - 2t_{d1}$, the above integral can be evaluated as

$$A = \frac{V_0}{2} \int_{t'=0}^{\infty} e^{-t'/\tau} dt' = \frac{V_0\tau}{2} = \frac{V_0Z_0C}{4}$$

from which the capacitor value can be found as

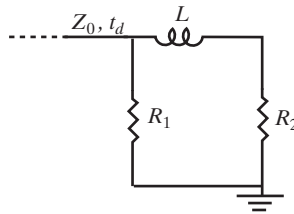


Figure 2.38 Figure for Problem 2.32. Identified unknown elements.

$$C = \frac{4A}{V_0 Z_0}$$

2.32 Source-end TDR waveform.

(a) Form the TDR waveform, we have

$$V_1^+ = \frac{Z_0 V_0}{R_s + Z_0} = \frac{Z_0(4)}{50 + Z_0} = 2 \text{ V}$$

Solving for Z_0 , we have

$$Z_0 = 50 \Omega$$

Hence the source-end reflection coefficient is 0. Also, based on the TDR waveform, since the reflected voltage wave arrives at the source at $t = 1 \text{ ns}$, we have

$$2t_d = 1 \text{ ns} \rightarrow t_d = 0.5 \text{ ns}$$

(b) Based on the TDR waveform, we can identify the unknown elements, as shown in Figure 2.38. When the unit step wavefront reaches the lumped element network at $t = t_{d1}$, the inductor at first behaves as an open circuit (to maintain its zero initial current), so the front value of the reflected voltage wave is given by

$$V_1^-(t = 0.5 \text{ ns}^+) = \frac{R_1 - Z_0}{R_1 + Z_0} V_1^+$$

Using the TDR waveform, we find the front value of the reflected voltage wave as

$$\begin{aligned} \frac{10}{3} - 2 &= V_1^-(t = 0.5 \text{ ns}^+) = \frac{R_1 - 50}{R_1 + 50} (2) \\ \rightarrow 2R_1 + 100 &= 3R_1 - 150 \rightarrow R_1 = 250 \Omega \end{aligned}$$

At steady state, the inductor is equivalent to a short circuit, so at the load network we have

$$V_1^-(t \rightarrow \infty) = \frac{(R_1 \parallel R_2) - Z_0}{(R_1 \parallel R_2) + Z_0} V_1^+$$

Using the TDR waveform, we determine the steady-state value of V_1^-

$$(1.25 - 2) = \frac{(R_1 \parallel R_2) - 50}{(R_1 \parallel R_2) + 50} (2)$$

$$\rightarrow R_1 \parallel R_2 = \frac{250}{11} \Omega \rightarrow R_2 = 25 \Omega$$

The inductor value can be determined from the time constant of the exponential decay of the source-end voltage after $t = 1$ ns:

$$\tau = \frac{L}{R_T} = \frac{L}{R_1 \parallel Z_0 + R_2} = \frac{L}{\frac{200}{3} \Omega} = 0.15 \text{ ns}$$

$$\rightarrow L = 10 \text{ nH}$$

2.33 Unknown Load.

We assume the source end to be at $z = 0$ and the load end to be at $z = L$. From Figure 2.63b in the text, we can write

$$\mathcal{V}_s(0^+) = \mathcal{V}_1^+(0, 0) = \frac{Z_0 V_0}{R_s + Z_0} = \frac{5Z_0}{75\Omega + Z_0} = 2.5 \text{ V}$$

Solving, we have $Z_0 = 75\Omega$. Therefore, there are no reflections from the source end.

Based on Figure 2.63b, one of the two unknown elements must be an inductor, since $\mathcal{V}_s \rightarrow 0$ as $t \rightarrow \infty$, and the other must be a resistor, since the $\mathcal{V}_s(t)$ waveform jumps at $t = 6$ ns. Note that to maintain its zero current, the inductor acts like an open circuit at $t = t_d$.

Let these two elements be represented as L and R . From Figure 2.63b in the text, we have

$$\mathcal{V}_s(2t_d^+) = \mathcal{V}_1^+(0, 2t_d^+) + \mathcal{V}_1^-(0, 2t_d^+) = 1.25 \text{ V}$$

and

$$\mathcal{V}_1^+(0, 2t_d^+) = \mathcal{V}_1^+(0, 0) = 2.5 \text{ V}$$

Hence

$$\mathcal{V}_1^-(0, 2t_d^+) = 1.25 - 2.5 = -1.25 \text{ V}$$

Hence we have

$$\Gamma_L(t_d^+) = \frac{\mathcal{V}_1^-(L, t_d^+)}{\mathcal{V}_1^+(L, t_d^+)} = \frac{-1.25}{2.5} = -\frac{1}{2}$$

Since

$$\Gamma_L(t_d^+) = \frac{R - Z_0}{R + Z_0} = \frac{R - 75}{R + 75} = -\frac{1}{2}$$

we can solve to find

$$R = 25\Omega$$

Using $\tau = 0.8$ ns, we have

$$\tau = \frac{L}{R \parallel Z_0} = \frac{(R + Z_0)L}{RZ_0} = \frac{(25 + 75)L}{(25)(75)} = 8 \times 10^{-10} \text{ s}$$

solving for L , we have

$$L = 1.5 \times 10^{-8} \text{ H} = 15 \text{ nH}$$

2.34 Capacitive load.

(a) At $t = 0$, an incident voltage wave of amplitude

$$\mathcal{V}_1^+ = \frac{Z_{01}}{R_s + Z_{01}} V_0 = \frac{75}{75 + 75} (3.6 \text{ V}) = 1.8 \text{ V}$$

is launched on line 1 from the source end. This voltage wave reaches the junction between the two lines at $t = t_{d1} = 6$ ns where a new voltage wave of amplitude

$$\mathcal{V}_1^- = \Gamma_{1 \rightarrow 2} \mathcal{V}_1^+ = \frac{(Z_{02} \parallel R_{sh}) - Z_{01}}{(Z_{02} \parallel R_{sh}) + Z_{01}} \mathcal{V}_1^+ = \frac{37.5 - 75}{37.5 + 75} (1.8 \text{ V}) = -0.6 \text{ V}$$

(where we have replaced $Z_{02} \parallel R_{sh} = 50 \parallel 150 = 37.5 \Omega$) reflects back to line 1 traveling toward the source and another new voltage wave of amplitude

$$\mathcal{V}_1^{+*} = \mathcal{V}_1^+ + \mathcal{V}_1^- = 1.8 - 0.6 = 1.2 \text{ V}$$

is transmitted to line 2 heading toward the capacitive load. The reflected voltage wave arrives at the source end at $t = 2t_{d1} = 12$ ns where it is completely absorbed since $R_s = Z_{01}$ and thus $\Gamma_s = 0$. The transmitted voltage wave arrives at the capacitive load at $t = t_{d1} + t_{d2} = 6 + 2 = 8$ ns where reflection occurs. Since this is a first-order circuit, the amplitude of the voltage wave reflected from the capacitive load varies with time and has the form given by

$$\mathcal{V}_1^{-*}(t) = \Gamma_L(t) \mathcal{V}_1^{+*} = u(t - 8 \text{ ns})(K_1 + K_2 e^{-(t-8 \text{ ns})/\tau})$$

where the time constant τ of the circuit is $\tau = [(50 \Omega \parallel 100 \Omega) + 100 \Omega](30 \text{ pF}) = 4$ ns. Note that this expression represents the reflected voltage wave at the load position. The constants K_1 and K_2 are determined by the initial and final conditions as follows: At $t = 8$ ns, the capacitor is uncharged and behaves like a short circuit. As a result, the load reflection coefficient at $t = 8$ ns is given by

$$\Gamma_L(t = 8 \text{ ns}) = \frac{(100 \parallel 100) - 50}{(100 \parallel 100) + 50} = 0$$

and so the reflected voltage wave at the load end at $t = 8$ ns is

$$\mathcal{V}_1^{-*}(8 \text{ ns}) = \Gamma_L(t = 8 \text{ ns}) \mathcal{V}_1^{+*} = 0 \rightarrow K_1 + K_2 = 0$$

At $t = \infty$ (or $t \geq \sim 5\tau$), the capacitor is fully charged and behaves like an open circuit. In this case, we have

$$\mathcal{V}_1^{-*}(t = \infty) = \Gamma_L(t = \infty) \mathcal{V}_1^{+*} = \frac{100 - 50}{100 + 50} (1.2 \text{ V}) = 0.4 \text{ V} = K_1$$

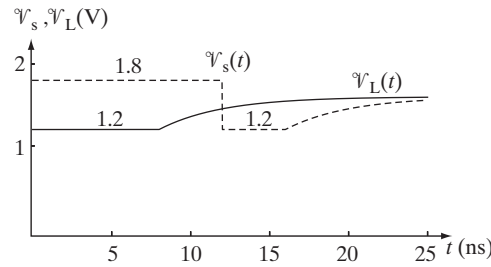


Figure 2.39 Figure for Problem 2.34. $V_L(t)$ and V_s versus t .

from which we can find K_2 as $K_2 = -K_1 = -0.4$ V. Therefore, the voltage reflected from the capacitive load at the load end can be written as

$$V_1^{-*}(t) = 0.4[1 - e^{-(t-8 \text{ ns})/(4 \text{ ns})}]u(t - 8 \text{ ns}) \text{ V}$$

Using this expression, the load end voltage $V_L(t)$ is given by

$$V_L(t) = V_1^{+*} + V_1^{-*}(t) = [1.6 - 0.4e^{-(t-8 \text{ ns})/(4 \text{ ns})}]u(t - 8 \text{ ns}) \text{ V}$$

The plot of V_L versus t is shown in Figure 2.39.

(b) Note that the voltage wave with an amplitude of $V_1^{-} = -0.6$ V reflected back toward the source from the junction point between lines 1 and 2 at $t = 6$ ns arrives at the source end of the line 1 at $t = 12$ ns, causing a change in the source end voltage from $V_s = 1.8$ V to $V_s = 1.2$ V. The voltage wave reflected from the capacitive load reaches back to the junction point between lines 1 and 2 at $t = t_{d1} + 2t_{d2} = 6 + 4 = 10$ ns where it is completely transmitted onto line 1 since

$$\Gamma_{2 \rightarrow 1} = \frac{(75 \parallel 150) - 50}{(75 \parallel 150) + 50} = 0$$

This voltage arrives at the source end of the line at $t = 2(t_{d1} + t_{d2}) = 16$ ns and is completely absorbed since $\Gamma_s = 0$. Therefore, the source-end voltage can be expressed mathematically as

$$V_s(t) = 1.8u(t) - 0.6u(t - 12 \text{ ns}) + 0.4[1 - e^{-(t-16 \text{ ns})/(4 \text{ ns})}]u(t - 16 \text{ ns}) \text{ V}$$

The plot V_s versus t is also shown in Figure 2.39.

2.35 Reactive element at the junction.

Using Z_{0A} to denote the characteristic impedance of the 50Ω transmission line, the voltage wave step at the input to the A transmission line at time $t = 0^+$ is given by

$$V_{1A}^+ = \frac{Z_{0A}V_0}{R_s + Z_{0A}} = \frac{(50)(6)}{50 + 50} = 3 \text{ V}$$

Since R_s is equal to Z_{0A} , the source reflection coefficient is 0:

$$\Gamma_s = \frac{R_s - Z_{0A}}{R_s + Z_{0A}} = \frac{50 - 50}{50 + 50} = 0$$

When the incident voltage wave reaches the junction at $t = t_{dA} = 2$ ns, the inductor initially acts as an open circuit (to maintain its zero initial current) and the junction reflection coefficient at 2 ns is thus given by

$$\Gamma_{AB}(t_{dA}^+) = \frac{150 - 50}{150 + 50} = \frac{1}{2}$$

Hence the voltage amplitude of the first reflected left-going wave on transmission line A is

$$V_{1A}^-(t_{dA}^+) = \Gamma_{AB}(t_{dA}^+)V_{1A}^+ = \left(\frac{1}{2}\right)(3) = \frac{3}{2} \text{ V}$$

and the initial input voltage wave traveling towards to the right-hand transmission line (which we denote as line B) is

$$V_{1B}^+(t_{dA}^+) = V_{1A}^+ + V_{1A}^-(t_{dA}^+) = 3 + \frac{3}{2} = \frac{9}{2} \text{ V}$$

As $t \rightarrow \infty$, the inductor turns into a short circuit at steady state and as a result we have

$$\Gamma_{AB}(t \rightarrow \infty) = \frac{(150||300) - 50}{(150||300) + 50} = \frac{100 - 50}{100 + 50} = \frac{1}{3}$$

and so

$$V_{1A}^-(t \rightarrow \infty) = \Gamma_{AB}(t \rightarrow \infty)V_{1A}^+ = \frac{1}{3}(3) = 1 \text{ V}$$

and

$$V_{1B}^+(t \rightarrow \infty) = V_{1A}^+ + V_{1A}^-(t \rightarrow \infty) = 3 + 1 = 4 \text{ V}$$

The load reflection coefficient is

$$\Gamma_L = \frac{R_L - Z_{0B}}{R_L + Z_{0B}} = \frac{300 - 300}{300 + 300} = 0$$

so there are no load reflections to consider.

Finally, the time constant is

$$\tau = \frac{0.27 \times 10^{-6}}{(50||150) + 300} = 8 \times 10^{-10} \text{ s} = 0.8 \text{ ns}$$

Considering the above results, we can make the sketches seen in Figure 2.40a and b. In functional form, we can write

$$\mathcal{V}_s(t) = 3u(t) + u(t - 4 \text{ ns}) + \frac{1}{2}e^{-(t-4 \text{ ns})/0.8 \text{ ns}}u(t - 4 \text{ ns}) \text{ V}$$

and

$$\mathcal{V}_L(t) = 4u(t - 4 \text{ ns}) + \frac{1}{2}e^{-(t-4 \text{ ns})/0.8 \text{ ns}}u(t - 4 \text{ ns}) \text{ V}$$

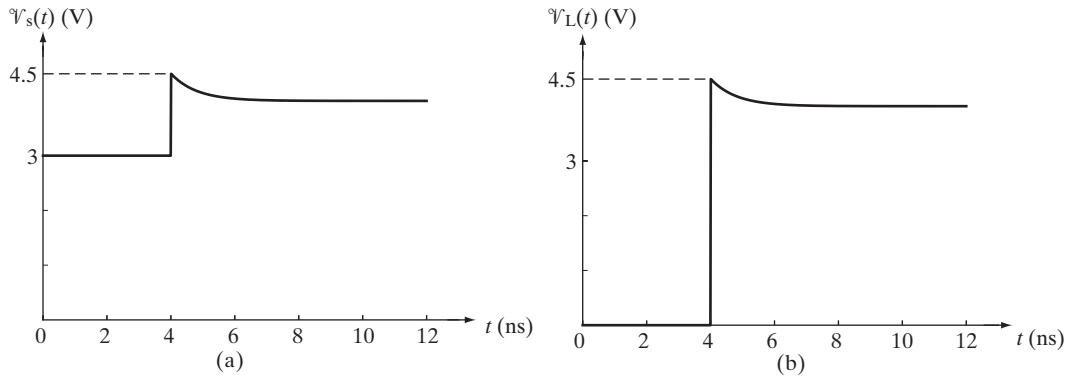


Figure 2.40 Figure for Problem 2.35. (a) $\mathcal{V}_s(t)$ versus t . (b) $\mathcal{V}_L(t)$ versus t .

2.36 Transmission line terminated with a capacitive load.

At $t = 0^-$ (just before the switch closes), steady state applies and we have

$$\mathcal{V}_s(0^-) = \mathcal{V}_L(0^-) = 5 \text{ V}$$

Following steps similar to Example 2.9, one can write the differential equation governing the reflected voltage wave $\mathcal{V}_1^-(l, t)$ at the load end as

$$\frac{d\mathcal{V}_1^-(l, t)}{dt} + \left(\frac{R_L + Z_0}{R_L Z_0 C_L} \right) \mathcal{V}_1^-(l, t) = \left(\frac{R_L - Z_0}{R_L Z_0 C_L} \right) \mathcal{V}_1^+(l, t)$$

where

$$\mathcal{V}_1^+(l, t) = \frac{Z_0 V_0}{R_s + Z_0} = \frac{V_0}{2} = 2.5 \text{ V}$$

The general solution for the above differential equation is given by

$$\begin{aligned} \mathcal{V}_1^-(l, t) &= K_1 + K_2 e^{-[(R_L + Z_0)/(R_L Z_0 C_L)]t} \\ &= K_1 + K_2 e^{-[(50+50)/((50)(50)(40 \times 10^{-12}))]t} \\ &= K_1 + K_2 e^{-10^9 t} \end{aligned}$$

where the K_1 and K_2 constants are to be determined using the initial and final conditions. Note that the reflected voltage wave at the load end must vary exponentially from 2.5 V at $t = 0$ (since $\mathcal{V}_L(0^+) = \mathcal{V}_L(0^-) = 5 \text{ V}$ and $\mathcal{V}_1^+(l, 0^+) + \mathcal{V}_1^-(l, 0^+) = 5 \text{ V}$) to

$$\Gamma_L(t \rightarrow \infty) \mathcal{V}_1^+(l, t \rightarrow \infty) = \left(\frac{R_L - Z_0}{R_L + Z_0} \right) \mathcal{V}_1^+(l, t \rightarrow \infty) = 0$$

for $t \rightarrow \infty$. So, $K_1 + K_2 = 2.5$ and since $K_1 = 0$, $K_2 = 2.5$. We thus have

$$\mathcal{V}_1^-(l, t) = 2.5 e^{-10^9 t} \text{ V}, \quad t \geq 0$$

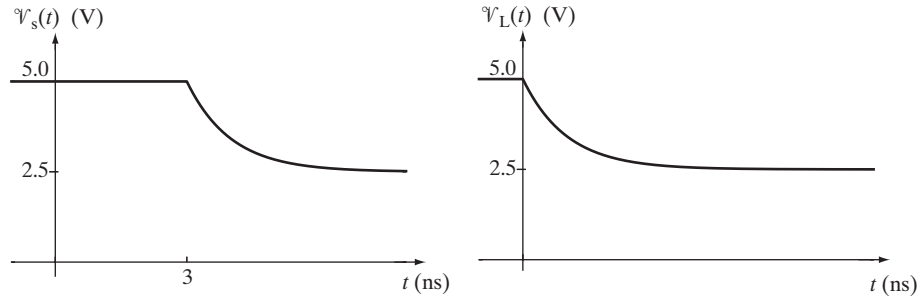


Figure 2.41 Figure for Problem 2.36. $V_s(t)$ and $V_L(t)$ versus t .

The load-end voltage $V_L(t)$ is given by

$$\begin{aligned} V_L(t) &= V_1^+(l, t) + V_1^-(l, t) \\ &= 2.5(1 + e^{-10^9 t}) \text{ V}, \quad t \geq 0 \end{aligned}$$

Since the variation in the reflected voltage wave affects the source-end voltage $t_d = 3$ ns later, the reflected voltage wave at the source-end can be written as

$$\begin{aligned} V_s(t) &= V_1^+(0, t) + V_1^-(0, t) \\ &= 2.5 + 2.5e^{-10^9(t-3 \text{ ns})} \\ &= 2.5 \left[1 + e^{-10^9(t-3 \text{ ns})} \right] \text{ V}, \quad t \geq 3 \text{ ns} \end{aligned}$$

The source- and load-end voltage waveforms are shown in Figure 2.41.

2.37 Transients on a transmission line.

At $t = 0^-$ (just before the switch opens), steady-state condition applies and the inductor acts like a short circuit. The incident and the reflected voltage waves at any position z on the line at $t = 0^-$ are given by

$$\begin{aligned} V_1^+(z, 0^-) &= \frac{Z_0}{R_s + Z_0} V_0 = \frac{50}{50 + 50} (6) = 3 \text{ V} \\ V_1^-(z, 0^-) &= \Gamma_L(0^-) V_1^+(z, 0^-) = (-1)(3) = -3 \text{ V} \end{aligned}$$

The source-end and load-end voltages and the inductor current at $t = 0^-$ are as follows:

$$\begin{aligned} V_s(0^-) &= V_1^+(0, 0^-) + V_1^-(0, 0^-) = 3 - 3 = 0 \\ V_L(0^-) &= V_1^+(l, 0^-) + V_1^-(l, 0^-) = 3 - 3 = 0 \\ i_{\text{ind}}(0^-) &= \frac{V_0}{R_s} = \frac{6 \text{ V}}{50 \Omega} = 0.12 \text{ A} \end{aligned}$$

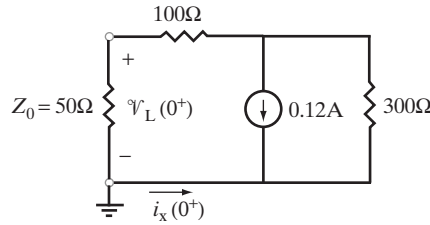


Figure 2.42 Figure for Problem 2.37. Lumped equivalent circuit at the load end of the transmission line at $t = 0^+$. The current source represents the inductor at $t = 0^+$.

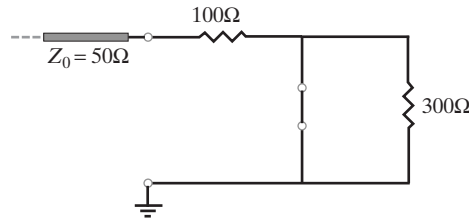


Figure 2.43 Figure for Problem 2.37. Equivalent circuit at the load end of the transmission line at steady state.

At $t = 0^+$ (right after the switch opens), the inductor current is $i_{\text{ind}}(0^+) = i_{\text{ind}}(0^-) = 0.12 \text{ A}$. The lumped equivalent circuit at the load end of the transmission line at $t = 0^+$ can be drawn as shown in Figure 2.42. Using Kirchhoff's circuit laws and Ohm's law, the load-end voltage at $t = 0^+$ can be found as

$$v_L(0^+) = Z_0 i_x(0^+) = (50)(-0.08) = -4 \text{ V}$$

Since

$$\begin{aligned} v_L(0^+) &= v_1^+(l, 0^+) + v_1^-(l, 0^+) \\ -4 \text{ V} &= 3 \text{ V} + v_1^-(l, 0^+) \rightarrow v_1^-(l, 0^+) = -7 \text{ V} \end{aligned}$$

Note however that this change in the value of the reflected voltage wave will not reach the source end until $t = t_d = 3 \text{ ns}$. Also, no reflection will occur at the source end since $\Gamma_s = 0$.

As $t \rightarrow \infty$, the inductor behaves like a short circuit and the lumped equivalent circuit at the load end at steady state can be drawn as shown in Figure 2.43. The load reflection coefficient as $t \rightarrow \infty$ can be found as

$$\Gamma_L(t \rightarrow \infty) = \frac{100 - 50}{100 + 50} = \frac{1}{3}$$

The reflected voltage wave as $t \rightarrow \infty$ is given by

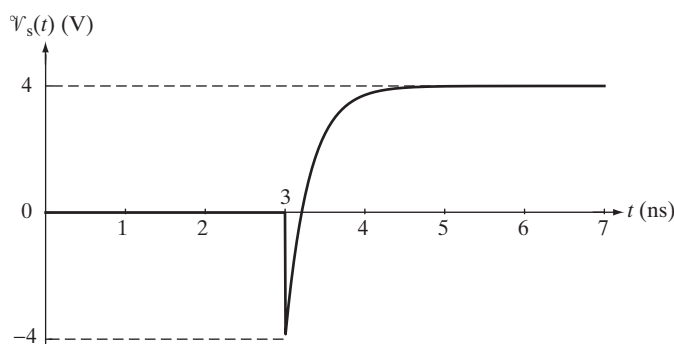


Figure 2.44 Figure for Problem 2.37. \mathcal{V}_s versus t .

$$\begin{aligned}\mathcal{V}_1^-(z, t \rightarrow \infty) &= \Gamma_L(t \rightarrow \infty) \mathcal{V}_1^+(z, t \rightarrow \infty) \\ &= \left(\frac{1}{3}\right)(3) = 1 \text{ V}\end{aligned}$$

So, the final steady-state value of the load-end and source-end voltages will be

$$\mathcal{V}_s(t \rightarrow \infty) = \mathcal{V}_L(t \rightarrow \infty) = \mathcal{V}_1^+ + \mathcal{V}_1^-(t \rightarrow \infty) = 3 + 1 = 4 \text{ V}$$

The time constant of the circuit can be found as

$$\tau = \frac{\mathcal{L}}{R_T} = \frac{30 \text{ nH}}{(50 + 100)\Omega \parallel 300\Omega} = 0.3 \text{ ns}$$

Using these values, the source-end voltage can be written as

$$\begin{aligned}\mathcal{V}_s(t) &= \begin{cases} 0, & t < 3 \text{ ns} \\ 4 - 8e^{-(t-3 \text{ ns})/0.3 \text{ ns}}, & t > 3 \text{ ns} \end{cases} \\ &= \left[4 - 8e^{-(t-3 \text{ ns})/0.3 \text{ ns}}\right] u(t - 3 \text{ ns}) \text{ V}\end{aligned}$$

$\mathcal{V}_s(t)$ is drawn in Figure 2.44.

2.38 Transient response.

We begin by calculating the reflection coefficient Γ_J at the junction. The two 100Ω parallel lines combine to contribute an impedance of $100 \parallel 100 = 50\Omega$. The effective impedance seen by the 50Ω line at the junction is $50 \parallel 25 \simeq 16.67\Omega$. The total reflection coefficient at the junction for a voltage wave approaching from the 50Ω line is therefore

$$\Gamma_J = \frac{16.67 - 50}{16.67 + 50} = -\frac{1}{2}$$

At $t = 0^+$, the step-source incident voltage wave with amplitude

$$\mathcal{V}_1^+ = \frac{50}{50 + 50} 12 = 6 \text{ V}$$

is launched down the 50Ω transmission line. When the voltage wave meets the junction at $t_{d1} = 1 \text{ ns}$, a reverse voltage wave of amplitude $\mathcal{V}_1^- = -0.5 \cdot 6 = -3 \text{ V}$ is reflected back to the source, and a $6 - 3 = 3 \text{ V}$ voltage waves are launched down the three parallel transmission lines at the junction. At $t = 2 \text{ ns}$, the transmitted voltage wave arrives at the capacitive load at $t_{d1} + t_{d2} = 2 \text{ ns}$. Initially, the capacitor is discharged and represents a short circuit. Noting the series 25Ω load resistor, the capacitive load is initially matched and the initial reflection coefficient is 0. With a time constant of

$$\tau = R_{\text{eq}}C = (25 + 25)(20 \times 10^{-12}) = 1 \text{ ns}$$

the capacitor eventually charges and becomes an effective open circuit. At this time, the reflection coefficient at the capacitive load is 1. Noting that the two 100Ω lines have matched terminations, and the parallel network seen by the 25Ω line is also matched, the bounce diagram in Figure 2.45a can be drawn. The right pointing arrow indicates the return voltage wave from the capacitive load builds from 0 to 3 V with a time constant of 1 ns.

When the switch is closed at $t = 7 \text{ ns}$, $\mathcal{V}_s \rightarrow 0$, which launches a -6 V step-type voltage wave down the 50Ω line. We can simply negate the voltages calculated in the bounce diagram for the $+6 \text{ V}$ incident voltage wave. The resulting voltages at the source and load are drawn in Figure 2.45b and c, respectively.

The functional form of the load and source voltages are

$$\mathcal{V}_L(t) = \begin{cases} 0 & 0 < t < 2 \text{ ns} \\ (6 - 3e^{-(t-2 \text{ ns})/1 \text{ ns}}) \text{ V} & 2 \text{ ns} < t < 9 \text{ ns} \\ 3e^{-(t-9 \text{ ns})/1 \text{ ns}} \text{ V} & t > 9 \text{ ns} \end{cases}$$

$$\mathcal{V}_s(t) = \begin{cases} 6 \text{ V} & 0 < t < 2 \text{ ns} \\ 3 \text{ V} & 2 \text{ ns} < t \leq 4 \text{ ns} \\ (6 - 3e^{-(t-4 \text{ ns})/1 \text{ ns}}) \text{ V} & 4 \text{ ns} \leq t < 7 \text{ ns} \\ 0 & 7 \text{ ns} < t < 9 \text{ ns} \\ 3 \text{ V} & 9 \text{ ns} < t \leq 11 \text{ ns} \\ 3e^{-(t-11 \text{ ns})/1 \text{ ns}} \text{ V} & t \geq 11 \text{ ns} \end{cases}$$

The problem statement asks for the voltage across the capacitor, not the voltage across the series combination of the resistor and capacitor at the load. Noting that the voltage across the capacitor cannot have a step discontinuity, we have

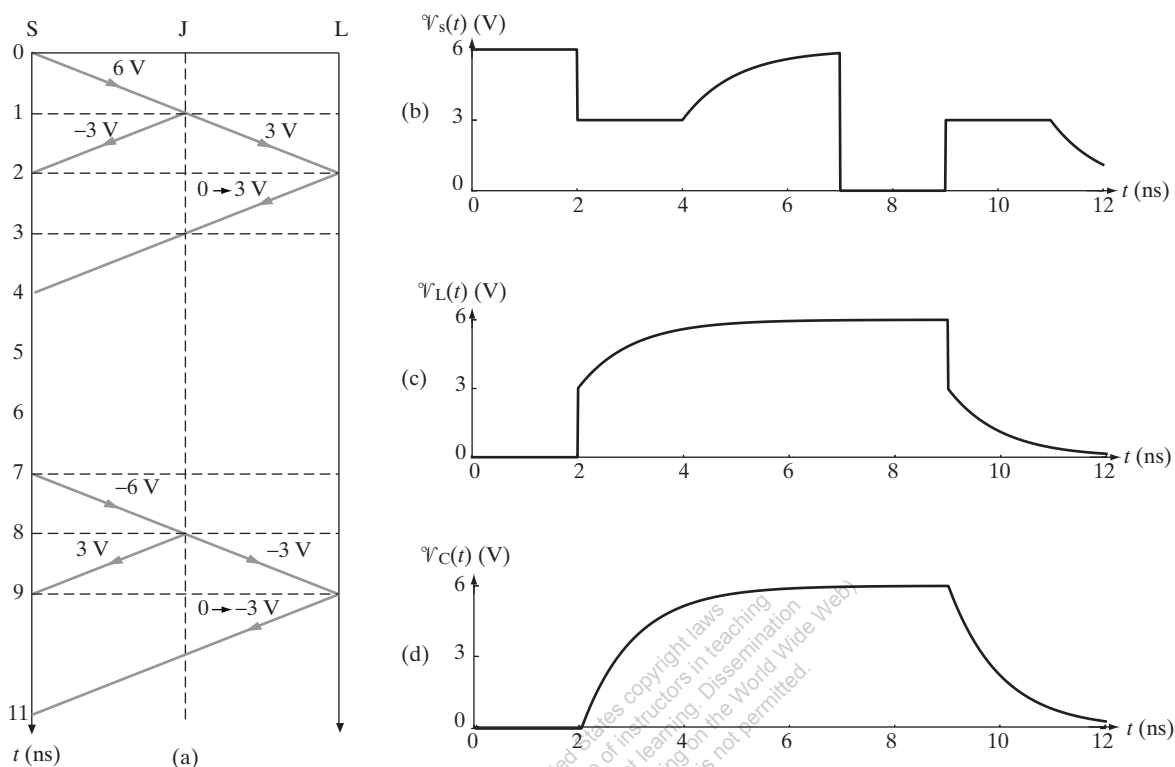


Figure 2.45 Figure for Problem 2.38. (a) Bounce diagram. The junction point is labeled J. (b) V_s versus t . (c) V_L versus t . (d) V_C versus t .

$$V_C(t) = \begin{cases} 0 & 0 < t \leq 2 \text{ ns} \\ 6(1 - e^{-(t-2 \text{ ns})/1 \text{ ns}}) \text{ V} & 2 \text{ ns} \leq t \leq 9 \text{ ns} \\ 6e^{-(t-9 \text{ ns})/1 \text{ ns}} \text{ V} & t > 9 \text{ ns} \end{cases}$$

The voltage across the capacitor is drawn in Figure 2.45d.

2.39 Inductive load.

At $t = 0$, an incident voltage wave of amplitude $V_1^+ = 2.5 \text{ V}$ is launched from the source end of the 50Ω line traveling toward the inductive load. This voltage wave reaches the 25Ω resistor at $t = 5 \text{ ns}$ where a voltage wave of amplitude

$$V_1^- = \frac{(25 + 75) - 50}{(25 + 75) + 50} V_1^+ = \left(\frac{1}{3}\right) (2.5 \text{ V}) = \frac{2.5}{3} \text{ V}$$

reflects back toward the source and another voltage wave of amplitude

$$V_1^{+*} = \frac{75}{25 + 75} \left(1 + \frac{1}{3}\right) V_1^+ = V_1^+ = 2.5 \text{ V}$$

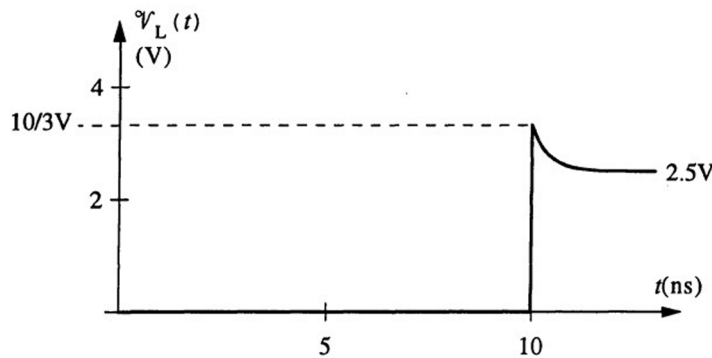


Figure 2.46 Figure for Problem 2.39. V_L versus t .

is launched on the 75Ω line traveling toward the load. When this voltage wave arrives at the inductive load at $t = 10$ ns, reflection occurs. Since this is a first-order circuit, the reflected voltage wave can be expressed as

$$V_1^{-*}(t) = \Gamma_L(t)V_1^{+*} = u(t - 10 \text{ ns})(K_1 + K_2 e^{-(t-10 \text{ ns})/\tau})$$

where K_1 and K_2 are to be found from the initial and final conditions and τ is the time constant given by

$$\tau = \frac{20 \text{ nH}}{(75\Omega + 75\Omega) \parallel 75\Omega} = \frac{20 \text{ nH}}{50\Omega} = 0.4 \text{ ns}$$

At $t = 10$ ns, the inductor acts like an open circuit and as a result, we have

$$V_1^{-*}(t = 10 \text{ ns}) = K_1 + K_2 = \Gamma_L(t = 10 \text{ ns})V_1^{+*} = \frac{(75 + 75) - 75}{(75 + 75) + 75}(2.5 \text{ V}) = \frac{2.5}{3} \text{ V}$$

As $t \rightarrow \infty$, the inductor becomes a short circuit and so we have

$$V_1^{-*}(t = \infty) = K_1 = \Gamma_L(\infty)V_1^{+*} = \frac{75 - 75}{75 + 75}(2.5 \text{ V}) = 0 \rightarrow K_1 = 0$$

from which we find $K_2 = 2.5/3$ V. Therefore, the reflected voltage wave follows as

$$V_1^{-*}(t) = u(t - 10 \text{ ns})\frac{2.5}{3}e^{-(t-10 \text{ ns})/0.4 \text{ ns}} \text{ V}$$

Thus, the load-end voltage can be found as

$$V_L(t) = V_1^{+*} + V_1^{-*}(t) = 2.5u(t - 10 \text{ ns}) \left[1 + \frac{1}{3}e^{-(t-10 \text{ ns})/(0.4 \text{ ns})} \right] \text{ V}$$

The sketch of $V_L(t)$ versus t is shown in Figure 2.46. Note that no other voltage reflects back toward the load since $V_1^{-*}(t)$ is completely absorbed both at the location of the 25Ω and at the source.

2.40 Capacitive load.

Using the results of Example 2.9, the general solution for the reflected voltage wave can be written as

$$\begin{aligned} \mathcal{V}_1^-(0, t) &= K_1 + K_2 e^{-[(R_L + Z_0)/(R_L Z_0 C_L)]t} \\ &= K_1 + K_2 e^{-[(300 + 100)/(300 \cdot 100 \cdot 20 \times 10^{-12})]t} \\ &= K_1 + K_2 e^{-t/(1.5 \text{ ns})} \end{aligned}$$

which is valid for $t > 0$. Since the capacitor will initially act like a short circuit at $t = 0$ to maintain its zero voltage,

$$\mathcal{V}_1^-(0, 0) = \underbrace{\Gamma_L(t=0)}_{-1} \underbrace{\mathcal{V}_1^+(0, 0)}_{1 \text{ V}} = -1 \text{ V}$$

On the other hand, since the capacitor will act like an open circuit as $t \rightarrow \infty$,

$$\begin{aligned} \mathcal{V}_1^-(0, t \rightarrow \infty) &= \Gamma_L(t \rightarrow \infty) \underbrace{\mathcal{V}_1^+(0, t \rightarrow \infty)}_{1 \text{ V}} \\ &= \frac{R_L - Z_0}{R_L + Z_0} = \frac{300 - 100}{300 + 100} = 0.5 \text{ V} \end{aligned}$$

Using the above initial and final conditions, the reflected voltage wave can be found as

$$\mathcal{V}_1^-(0, t) = 0.5 - 1.5e^{-t/(1.5 \text{ ns})}, \quad t > 0$$

To determine the approximate time at which the reflected voltage wave at $z = 0$ will equal to zero, we set $\mathcal{V}_1^-(0, t) = 0$ to find

$$0.5 - 1.5e^{-t/(1.5 \text{ ns})} = 0 \quad \rightarrow \quad t = -(1.5 \text{ ns}) \ln \left(\frac{0.5}{1.5} \right) \simeq 1.6479 \text{ ns}$$

2.41 Step excitation.

(a) At $t = 0^+$, an incident voltage wave of amplitude

$$\mathcal{V}_1^+ = \frac{2Z_0}{2Z_0 + 2Z_0} (5 \text{ V}) = 2.5 \text{ V}$$

is launched at the source end of the line. When this voltage wave reaches the stub junction at $t = t_d$, a new voltage wave of amplitude

$$\mathcal{V}_1^- = \Gamma_{j1} \mathcal{V}_1^+ = \frac{(Z_0 \parallel 2Z_0) - 2Z_0}{(Z_0 \parallel 2Z_0) + 2Z_0} (2.5 \text{ V}) = (-0.5)(2.5 \text{ V}) = -1.25 \text{ V}$$

reflects back toward the source and a transmitted voltage wave of amplitude

$$\mathcal{V}_1^{+*} = (1 + \Gamma_{j1}) \mathcal{V}_1^+ = +1.25 \text{ V}$$

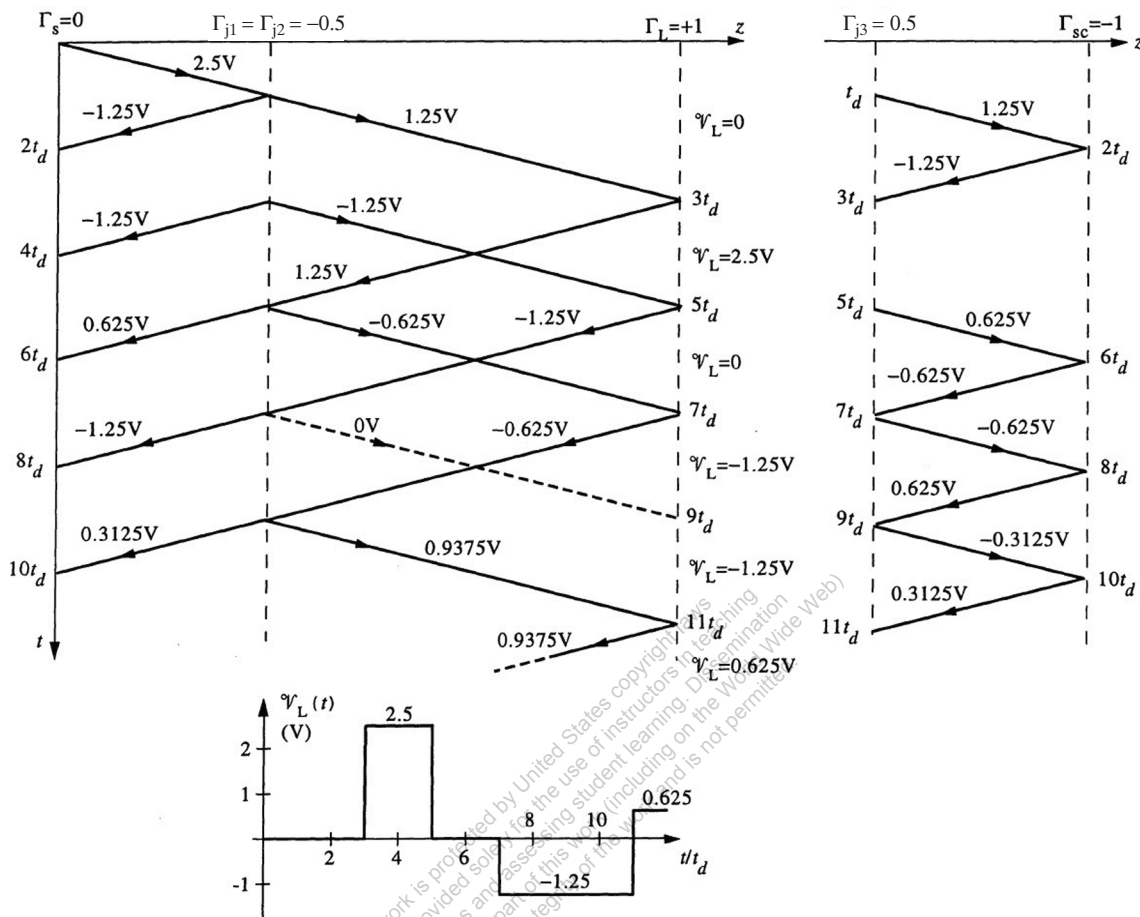


Figure 2.47 Figure for Problem 2.41. Bounce diagram and the load voltage V_L versus t .

is launched not only on the stub (V_{1s}^+) but also on the main line (V_{1m}^+) traveling toward the load. The V_{1s}^+ launched on the stub arrives at the short circuit at $t = 2t_d$ where $V_{1s}^- = \Gamma_{sc} V_{1s}^+ = -V_{1s}^+ = -1.25$ V reflects back toward the junction since $\Gamma_{sc} = -1$. When it reaches the junction at $t = 3t_d$, it is completely absorbed, i.e., $V_{1s}^- = -1.25$ V travels both towards the source (where it is completely absorbed) and the load (where $\Gamma_L(V_{1s}^-) = -1.25$ V reflects back since $\Gamma_L = +1$). This process continues on as shown in the bounce diagram in Figure 2.47.

(b) For pulse excitation, we can use superposition to find the load voltage, as was done in Example 2.6 and Problem 2.9. For this, we note that the termination of the pulse is equivalent to excitation with a negative step applied at $t = 4$ ns, so that we have

$$V_{\text{pulse}}(t) = V_{\text{step}}(t) - V_{\text{step}}(t - 4 \text{ ns})$$

The superposition and the resultant pulse response are shown in Figure 2.48.

2.42 Capacitive load excited by two sources.

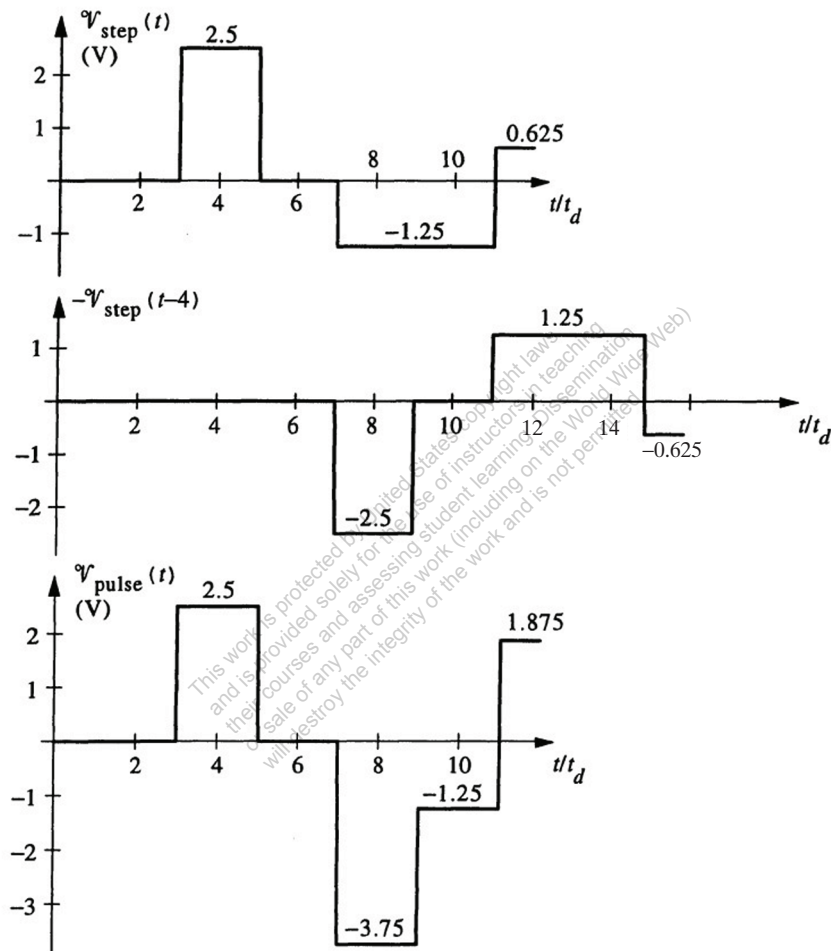


Figure 2.48 Figure for Problem 2.41. Load-end voltage pulse response obtained as the superposition of the step response to a negative step applied at $t = 4$ ns.

The effects of the two sources can be determined using the superposition principle. First, we only consider the step voltage source on the left and treat the voltage source on the right as a short circuit. At $t = 0$, this source causes an incident voltage wave of amplitude $\mathcal{V}_1^+ = 2.5$ V to be launched at the source end of the 100Ω line on the left. This voltage wave reaches the junction at $t = 500$ ps, when $\mathcal{V}_1^- = \Gamma_{j1}\mathcal{V}_1^+$ reflects back and $\mathcal{V}_1^{+*} = (1 + \Gamma_{j1})\mathcal{V}_1^+$ is transmitted into the other two lines. Since

$$\Gamma_{j1} = \frac{(100 \parallel 50) - 100}{(100 \parallel 50) + 100} = -0.5$$

we have $\mathcal{V}_1^{+*} = +1.25$ V. The voltage \mathcal{V}_1^{+*} reaches the capacitor at $t = 1$ ns and starts charging it up according to

$$\mathcal{V}_{C1}(t) = u(t - 1 \text{ ns})[K_1 + K_2 e^{-(t-1 \text{ ns})/\tau}]$$

Initially the capacitor is uncharged and acts like a short circuit, and after a long time it behaves like an open circuit.

$$\rightarrow \mathcal{V}_{C1}(1 \text{ ns}) = K_1 + K_2 = 0 \text{ and } \mathcal{V}_{C1}(\infty) = K_1 = 2\mathcal{V}_1^{+*} = 2.5 \text{ V}$$

$$\rightarrow \mathcal{V}_{C1}(t) = 2.5u(t - 1 \text{ ns})[1 - e^{-(t-1 \text{ ns})/(0.5 \text{ ns})}] \text{ V}$$

where the time constant τ is found from $\tau = (50\Omega)(10 \text{ pF}) = 0.5$ ns. The voltage wave reflected from the capacitor is completely absorbed by the two 100Ω lines at the junction at $t = 1.5$ ns and then by the two sources at $t = 2$ ns and $t = 2.5$ ns respectively. Next, we consider the negative step voltage source on the right only (i.e., replace the voltage source on the left with a short circuit). The capacitor voltage $\mathcal{V}_{C2}(t)$ due to this source is a scaled (by -1) and delayed (by 0.5 ns) version of $\mathcal{V}_{C1}(t)$, i.e., the total capacitor voltage due to both sources follows as

$$\mathcal{V}_C(t) = 2.5\{u(t - 1 \text{ ns})[1 - e^{-(t-1 \text{ ns})/(0.5 \text{ ns})}] - u(t - 1.5 \text{ ns})[1 - e^{-(t-1.5 \text{ ns})/(0.5 \text{ ns})}]\} \text{ V}$$

Figure 2.49 shows the sketch of $\mathcal{V}_C(t)$ versus t .

2.43 Two sources.

Before $t = 0$, since steady state applies, the step source on the left hand side is OFF (i.e., short circuit) and the step source on the right hand side is ON and the line is fully charged to

$$\mathcal{V}_{s1}(0^-) = \mathcal{V}_{s2}(0^-) = +\frac{V_0}{2}$$

due to the source on the right hand side. At $t = 0$, the step source on the left turns ON and launches a voltage wave of amplitude

$$\mathcal{V}_{1L}^+ = +\frac{V_0}{2}$$

from the left hand side and the source on the right turns OFF, which we interpret as a voltage wave of amplitude

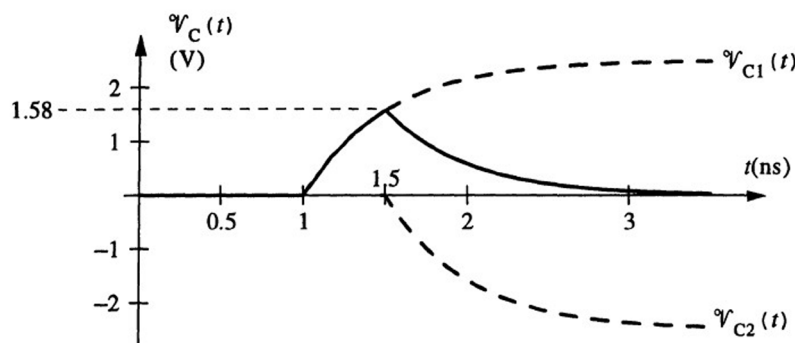


Figure 2.49 Figure for Problem 2.42. The capacitor voltage $V_C(t)$ versus t .

$$V_{IR}^- = -\frac{V_0}{2}$$

being launched from the right hand side. When both V_{IL}^+ and V_{IR}^- reach the junction between the three lines at $t = t_d$, a voltage wave of amplitude

$$V_{IL}^- = \Gamma_j V_{IL}^+ + (1 + \Gamma_j) V_{IR}^- = \left(\frac{-1}{3}\right) \left(+\frac{V_0}{2}\right) + \left(1 - \frac{1}{3}\right) \left(-\frac{V_0}{2}\right) = -\frac{V_0}{2}$$

is launched on the left line going toward the step source (which is OFF) on the left hand side and a voltage wave of amplitude

$$V_{IR}^+ = \Gamma_j V_{IR}^- + (1 + \Gamma_j) V_{IL}^+ = +\frac{V_0}{2}$$

is launched on the right line going toward the step source (which is ON) on the right hand side. The voltages transmitted onto the stub from both sides at $t = t_d$ add up to

$$V_{stub}^+ = (1 + \Gamma_j) \underbrace{(V_{IL}^+ + V_{IR}^-)}_{=0} = 0$$

i.e., as a result of this interval cancellation, no net voltage disturbance is launched onto the stub. Both V_{IL}^- and V_{IR}^+ are completely absorbed at their destinations at $t = 2t_d$ and no further reflections occur. The source-end voltages V_{s1} and V_{s2} versus t are sketched in Figure 2.50.

2.44 RG 8 coaxial line.

Using the velocity factor (i.e., $v_p/c = 0.66$) and the student's measurements of the diameter of the inner conductor (i.e., $2a \simeq 2$ mm) and the outer diameter of the dielectric (i.e., $2b \simeq 7.5$ mm) along with the expressions provided in Table 2.2, the line parameters for the RG 8 coaxial line can be found as

$$L = 0.2 \ln \left(\frac{b}{a} \right) = 0.2 \ln \left(\frac{7.5}{2} \right) \simeq 0.264 \mu\text{H}\cdot\text{m}^{-1} \simeq 80.6 \text{ nH}\cdot\text{ft}^{-1}$$

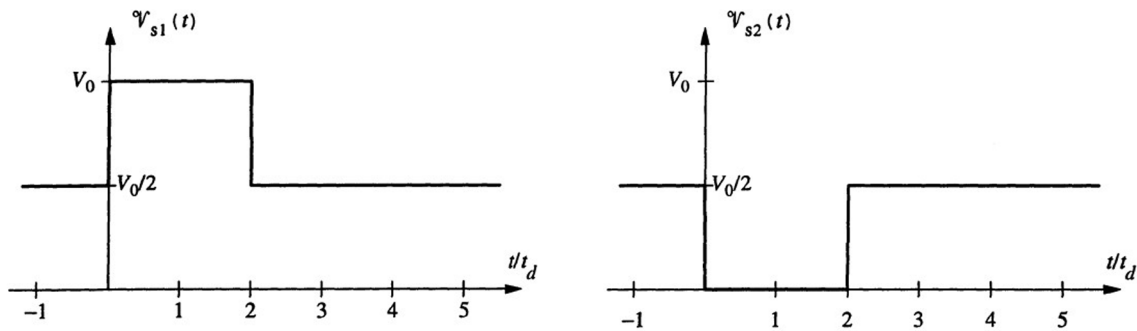


Figure 2.50 Figure for Problem 2.43. The voltages V_{s1} and V_{s2} versus t .

$$C = \left(\frac{c^2}{v_p^2} \right) \frac{55.6}{\ln(b/a)} = \frac{55.6}{(0.66)^2 \ln(7.5/2)} \simeq 96.6 \text{ pF}\cdot\text{m}^{-1} \simeq 29.4 \text{ pF}\cdot\text{ft}^{-1}$$

$$R = \frac{4.15 \times 10^{-8} (a+b) \sqrt{f}}{ab} = \frac{4.15 \times 10^{-8} (3.75+1) \sqrt{10^8}}{(3.75)(1)(10^{-3})} \simeq 0.526 \Omega\cdot\text{m}^{-1} \simeq 0.160 \Omega\cdot\text{ft}^{-1}$$

and

$$G \simeq \frac{1.58 \times 10^{-5}}{\ln(7.5/2)} \simeq 1.195 \times 10^{-5} \text{ S}\cdot\text{m}^{-1} \simeq 3.64 \times 10^{-6} \text{ S}\cdot\text{ft}^{-1}$$

respectively. The characteristic impedance of the line can be calculated as

$$Z_0 = \left(\frac{v_p}{c} \right) 60 \ln \left(\frac{b}{a} \right) = (0.66)(60) \ln \left(\frac{7.5}{2} \right) \simeq 52.3 \Omega$$

We thus find that both Z_0 and C values are verified because their values calculated above are quite close to the values provided in the Radio Shack product catalog.

2.45 Two-wire line.

Using the ratio

$$\frac{d}{2a} = \frac{21}{1.2} = 17.5$$

along with the expressions provided in Table 2.2 at 200 MHz, we have

$$L = 0.4 \ln \left(17.5 + \sqrt{(17.5)^2 - 1} \right) \simeq 1.42 \mu\text{H}\cdot\text{m}^{-1}$$

$$C = \frac{27.8}{\ln \left(17.5 + \sqrt{(17.5)^2 - 1} \right)} \simeq 7.82 \text{ pF}\cdot\text{m}^{-1}$$

$$R = \frac{8.3 \times 10^{-8} \sqrt{2 \times 10^8}}{6 \times 10^{-4}} \simeq 1.96 \Omega\text{-m}^{-1}$$

and $G = 0$ respectively. Using Table 2.2, the characteristic impedance can also found as

$$Z_0 = 120 \ln \left(17.5 + \sqrt{(17.5)^2 - 1} \right) \simeq 426.5 \Omega$$

This work is protected by United States copyright laws and is provided solely for the use of instructors in teaching their courses and assessing student learning. Dissemination or sale of any part of this work (including on the World Wide Web) will destroy the integrity of the work and is not permitted.